Title	Study on the growth responses of larch species raised under elevated ozone, nitrogen loading, and saline soil
Author(s)	菅井, 徹人
Citation	北海道大学. 博士(農学) 甲第14204号
Issue Date	2020-09-25
DOI	10.14943/doctoral.k14204
Doc URL	http://hdl.handle.net/2115/79559
Type	theses (doctoral)
File Information	Tetsuto_Sugai.pdf

Study on the growth responses of larch species raised under elevated ozone, nitrogen loading, and saline soil

オゾン暴露、窒素付加、及び塩類土壌下におけるカラマツ属樹種の成長応答に関する研究

北海道大学　大学院農学院

共生基盤学専攻　博士後期課程

菅井徹人

CONTENTS

Chapter 1: General introduction

Sustainable forest management considering for the rapid environmental changes have recently been focused (Aitken et al. 2013, Keenan 2015, Marchi et al. 2018, Isabel et al. 2020). The cover of forest in global terrestrial land is approximately 30% (FAO 2015). The demand of timber product has been increasing since 2010 worldwide (Fig.1-1, FAOSTAT 2016). As the trend from the last decades, the land area of artificial managed forest has been increasing to approximately 0.3 billion ha. This is a consequence of the world economic demand, implying that the provisioning services of forests and further afforestation will be needed, while the other ecological services; regulating services, cultural services, and supporting services are also essential for our life. So far, various approaches have been developed to sustainably manage forest ecological functions even under changing environments (Hahn and Knoke 2010, Keenan 2015, Breed et al. 2019).

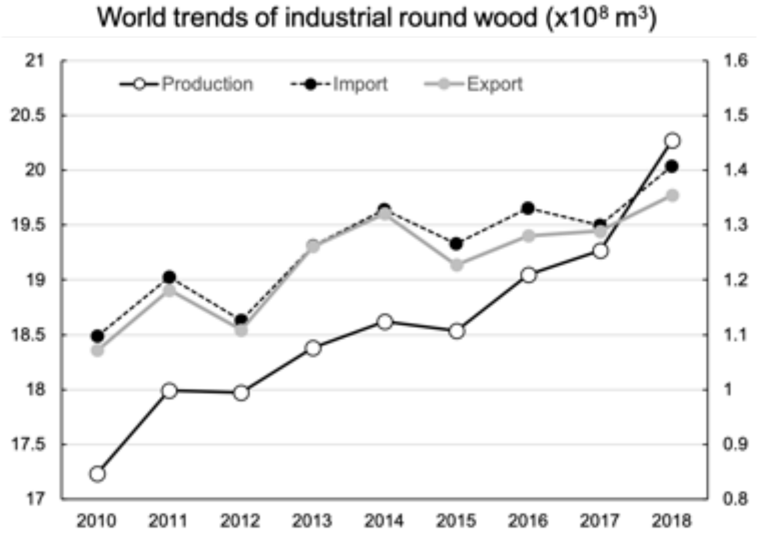

Fig. 1-1 Annual changes in global round wood production (White), import (Black), and export (Gray). Data source was referred from FAOSTAT.

Anthropogenic activities have induced the rapid environmental changes. The impacts of air pollution on forest ecosystem have still occurred worldwide (Agathokleous et al. 2016, Sicard et al. 2016), especially at Asia (Zhu et al. 2020). Since industrial evolution, the concentrations of ground-level ozone (Mills et al. 2018), and the amount of reactive nitrogen (N) deposition (Liu et al. 2013, Binkley and Högberg 2016) have rapidly been increasing in northern hemisphere, especially in northeast Asia (Koike et al. 2013). Further, it has been concerned that global climate change directly/indirectly induces the severe air pollutions and environmental degradations; such as soil salinization due to change in the pattern of rainfall and high temperature in worldwide (Fiore et al. 2015, Polle et al. 2019).

On the other hands, the afforestation for the ecosystem rehabilitation has been extensively studied in the degraded environment (Singh et al. 2012, Halwatura et al. 2015, Polle and Chen 2015, Polle et al. 2019, Kijowska-Oberc et al. 2020). In fact, most lands worldwide are not adequate for cropping system due to the naturally unfavorable pedo-climatic condition and/or incorrect land-uses (Wicke et al. 2011, Bui 2013, Setia et al. 2013, Farooq et al. 2018). Nevertheless, the world population has been increasing, indicating the increment of global food demand (UN 2019). Thus, it is essential to achieve the best balance of productions between refocuses, e.g. crop, timber, and fuel (Yue et al. 2020) as well as to recover the degraded land by greening (Azam et al. 2012, Polle and Chen 2015, Polle et al. 2019).

Afforestation and greening under changing environments require the normative foundations based on the forest ecological foresight. They have both objectives; production and conservation that have often conflicted each other (Yoshida 2010), where the optimal balance of them still remain to elucidate (Batavia and Nelson 2016). However, the current environmental changes have already leached the level enough to forest declines et several regions (e.g. Brodribb et al. 2020), requiring the urgent shift worldwide from the previous mono-culture systems to alternative forest management (Nelson et al. 2016, Jandl et al. 2019). While it just passively occurred rather than decisions of forestry policy (Thom et al. 2016), novel styles are emerging for confirming production based on the adaptation strategies to changing environment (e.g. Aitken and Whitlock 2013, Jandl et al. 2019), where the forest diversity has been seriously considered in terms of planted species as well as in forest structures.

Here, I focus on larch trees (*Larix* sp.) as a promising species for sustainable forest management. In Northeast Asia and European countries, there have commonly been high expectation for larch as an afforestation species due to several superior traits (Asada and Sato 1981, Kita et al. 2009, Ryu et al. 2009, Pâques et al. 2013, Mason and Zhu 2014). The managed forest in Northeast Asia has been gradually dominated by larch plantation (Yu et al. 2011, Peng et al. 2018) while the economic interests in Europe are relatively biased at mountain regions (Pâques et al. 2013). In fact, the greening practices have been extensively carting out as the policy project; Grain for Green from 1999 (Zhang et al. 2000), where larch has been employed as alternative species for reforestation. However, there are still challenges ahead regarding the poor quality and low productivity of many larch plantations due to the environmental changes and its degradation (Lie et al. 1998, Mason and Zhu 2014, Peng et al. 2018) as well as highly concern for air pollution impacts (Kita et al. 2018).

This study has investigated the growth responses of larch species under several environmental stresses; elevated ozone (O_3) exposure, N loading, and saline soil, which are most serious factor of changing environments in Northeast Asian regions. In the first part of general introduction, the significances of studying characteristics of larch trees are summarized. In next parts, the recent advances and future challenges regarding these environmental stresses are mentioned. Finally, the interests and objectives of this study are described with the structure schema.

Eco-physiological characteristics of Larch

Larch trees (*Larix* sp.) widely distribute in northern Eurasian continent, cold temperate-zone (Fig.1-2, Gower and Richard 1990). It has been reported that the larch forests occupy over 40 % of the total carbon growing stock in Eurasian boreal forest

(Myneni et al. 2001). As a deciduous conifer species, the distribution of larches includes permafrost regions (Abaimov 2010). Larch is one of light demanding species, which can invade infertile soil condition as like bare land after harvesting, landslide, and permafrost regions in Siberia ad Far East Russia (Asada and Sato 1981, Osawa et al. 2010). Due to its continuous distribution and non-barriers of reproduction, the traits transition, hybridization and introgression have widely occurred between larch species in the northeast Asian population (Semerikov et al. 2007, Polezhaeva et al. 2010). It has been reported the high genetic varieties of *Larix* sp. (Abaimov 2010, Polezhaeva et al.2010) as like *L. gmelinii* var. olgensis, *L. gmelinii* var. japonica, *L. cajanderi*, and *L. kamtschtica* (Farjon 1990). Among them, *L. gmelinii* var. japonica distributes at the eastern edge of the range of *L. gmelinii* complex, including Sakhalin Island and Kurile Island (Ishizuka et al. 2017). Besides, *L. kaempferi* distributes Japanese main land, showing the significantly difference of phylogenic relationships with *L. gmelinii* (Shiraishi et al. 1996).

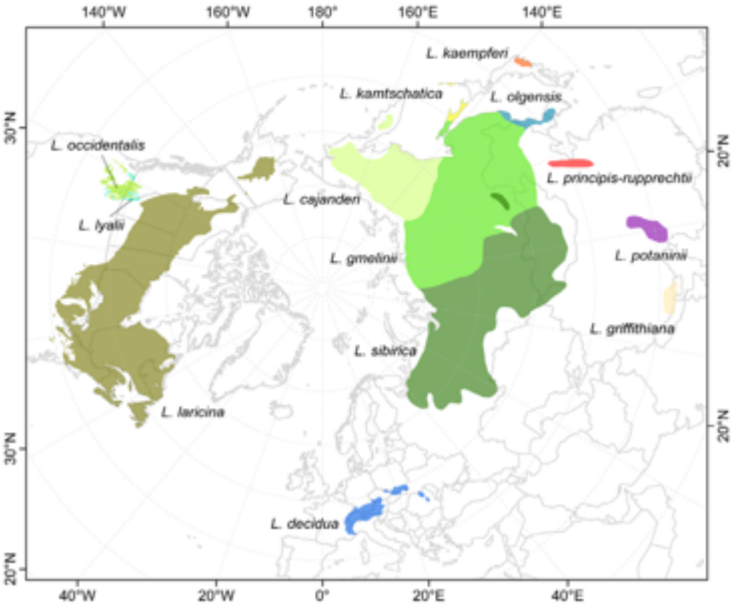

Fig. 1-2 Current distribution of larch (*Larix* taxa.) in northern hemisphere (Mamet et al. 2018).

As one of the dominant species of boreal forests in Northeast Asian regions, larches have two needle types, i.e. short and long shoot, for different roles in the seasonal photosynthetic activities (Clausen and Kozlowski 1967). Unique photosynthetic characteristics of larches, a light-demanding species, can be shown in higher photosynthetic rate and net assimilation rate than most other conifer species (Larcher 1969, Gowin et al. 1980). It is noteworthy that the photosynthetic physiology of Japanese larch (*L. kaempferi*) has similar to C_4 plants (Fry and Phillips 1976) based on its physiological traits, e.g. the phosphoenol pyruvate and Ribulose-bis-phosphate carboxylase activities, initial products of $^{14}CO_2$. Previous studies, however, have disproven the possibility of Japanese larch as C_4 plants in terms of $\delta^{13}C$ values and initial ^{14}C-labeled products of photosynthesis (Rechards and Teeri 1982) although they did not show the gas exchange rate in the same literature. Several studies have also reported that the photosynthetic rate of Japanese larch is commonly saturated under the light and temperature condition as like other *Larix* and normal C_3 plant (Crane et al. 1983); i.e. approximately 1000 $\mu mol\ m^{-2}\ s^{-1}$ and 25 °C. Due to the expected adaptive strategies of larch under cold temperate-zone, the possibility of C_4 characteristics of larches had not been supported from ecological views. In that way, the comparing of physiological responses to environmental stresses between *Larix* spp. is an effective strategy for better understanding of how the same genera adaptive the local environments of each species and its changes (e.g. Nagamitsu et al. 2014, Babushkina et al. 2016). Indeed, it has been reported that the distribution of *Larix* sp. would be responsive to climate change (Mamet et al. 2018), which provides the prediction that the population of southern Siberian boreal forest would disappear in future. The knowledge of adaptive strategies of larches, thereby, could contribute to reveal the future dynamics of *Larix* in Eurasian boreal forests, which would finally improve the prediction accuracy of ecological services under changing environments.

The numerous studies have investigated the superior traits of larch species as the high advantages for forestry, which were induced by wide plantation, hybridization and trans-migration (Matyssek 1987, Kurahashi 1988, Jansen and Geburek 2016, George et al. 2017, Marchal et al. 2017). In particular, Japanese larch is a great promising species for plantation not only in Japan but also in Europe (Pâques 1989, Gower and Richard 1990, Ryu et al. 2009). In China, where planted forests dominated 61,7 million ha, larch trees have been commonly planted in Northeast regions. To rapidly promote economic productivity of forestry with soil conservation, larch plantation has been addressed since 1950s (Zhang et al. 2000,). Although the secondary afforestation have been performed with improving the species diversity, serious problems have remained to solved in larch plantation as like soil degradation, low productivity, and a poor regeneration processes (Mason and Zhu 2014). Besides, in Northern part of Japan, larches have been introduced as afforestation species since they can survive, rapidly growth and tolerate to cold temperature rather than other traditional planting species (Asada and Sato 1981, Kurahashi 1988). Several types of hybrid larches have been developed to overcome the biotic/abiotic damages, e.g. grazing, wind, snow (Pâques 1989, Kita et al. 2018). Among them, hybrid larch F_1 (*Larix gmelinii* car. *japonica* x *Larix kaempferi*) is a great promising species for afforestation due to several superior traits e.g. initial growth rate, tolerance to grazing by red-back vole and shoots blight disease, timber quality (Kita et al. 2009). Indeed, the future plan of larch plantation in Hokkaido has decided the re-planting area as 5,900 ha in 2036 (Hokkaido 2017), where hybrid larch F_1 is also selected as one of afforestation species.

Ozone risks and future challenge for tree species

Ground-level ozone (O_3) is one of most serious air pollutants (Mills et al. 2018). The increment of O_3 concentration has been increasing since industrial evolution (Fowler et al. 2008), especially in Asia (Fig.1-3, Yamaji et al. 2006, Akimoto et al. 2015). The current O_3 concentration has already be enough to suppress the productivity and health of forest ecosystems in Europe (Paoletti 2006, Sicard et al. 2016), United states (Manning 1989, Chappelka and Samuelson 1998, Ainsworth et al. 2020), China (Feng et al. 2015, Li et al. 2017), India (Oksanen et al. 2013), and Japan (Koike et al. 2013, Watanabe et al.

2017).

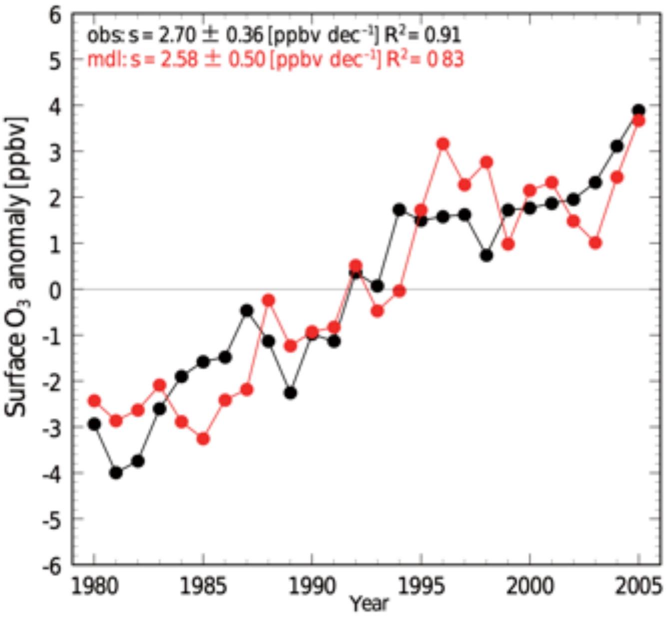

Fig. 1-3 Change in annual mean concentration of ground level O_3 in Japan, which were monitored (Black) or calculated by a chemistry climate model. (Nagashima et al. 2017).

Effects of elevated O_3 on forest ecosystem have been serious concern in northeast Asia. High level of ground-level O_3 has been monitored in Japan even under the low level of precursor (Hatakeyama 2017). Possible causes are related to the transport of O_3 and its precursors from China. The concentration of ground-level O_3 in China has been increasing from 2005 (Verstraeten et al. 2015). The annual average of daily maximum O_3 concentration may be 60 ppb at central cities in China (Chen et al. 2015). The extreme high level of air pollutants in China has been rapidly caused under the economic developments, industrialization and urbanization with over-consumption in fossil fuel.

Plant responses to O_3 have been reported the stomatal closure and its sluggishness occur (Paoletti and Grulke 2010, Hoshika et al. 2020), resulting suppression of gas exchange rate. Further, the oxidative stresses induced by the absorbed O_3 via stomata inhibit photosynthetic activities with the reduction of carboxylation and electron transport rate (Matyssek and Sandermann 2003, Li et al. 2017). As a common plant's defense mechanism, anti-oxidant systems are developed (Grulke and Heath 2020) since oxidative stresses are caused by conventional environmental factors as like drought, lower temperature, salinity as well as O_3 exposure. Previous meta-analyses have synthesized the negative O_3 impacts on biomass and gas exchange of trees based on the data set from temperate to boreal forest (Wittig et al. 2009, Li et al. 2017). Results suggested that O_3 sensitivity significantly varies depending on the functional groups as well as tree species (Li et al. 2017), especially a high variation in the O_3 sensitivity between evergreen and deciduous as well as broad-leaves and needle-leaves. To reveal a consistent pattern regarding O_3 sensitivity variation, details of physiological mechanism have been investigated from molecular to a whole-plant scale, including underground (Pell et al. 1997, Cho et al. 2011, Matyssek et al. 2012, Vainonen and Kangasjärvi 2015, Agathokleous et al. 2016).

Effects of N loading and changing ozone sensitivity

The amount of N deposition has been increased by approximately four-fold over the last century because of the anthropogenic activities, e.g. over fossil fuel consumption, livestock and artificial fertilization (Hatakeyama 2017). Future increment of N deposition has been predicted as the double from the current level in 2050 (Galloway et al. 2004, Bouwman et al. 2013). The extreme increment has recently occurred in Asia, especially in China (Fig.1-4, Liu et al. 2013) and India (Gurjar et al. 2016) due to the current social activities, the rapid industrial development, and changes in lifestyles including the increment in the number of automobiles used. Elevated N deposition has negatively influenced forest ecosystems with soil acidification and loss of biodiversity (Aber et al. 1989, Bleeker 2011, Liu et al. 2011, Tian et al. 2018).

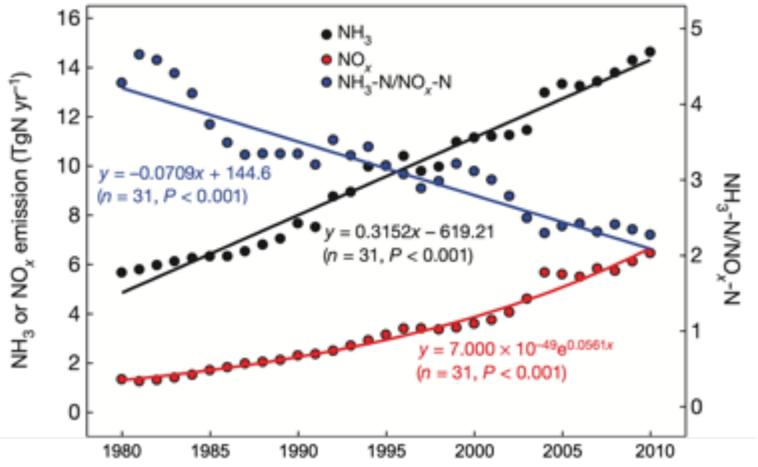

Fig. 1-4 Annual trends in the emission of NH_3 and NO_x and the ratios of NH_3-N to NO_x-N emission in China (Liu et al. 2013, the figure was partially modified).

Nitrogen (N) is one element of essential nutrients regulating plant growth (e.g. Marchner 2011), especially in boreal regions (Högberg et al. 2017). Thereby, N deposition can stimulate and promote tree growth and the productivity of forest ecosystem to some extent. Increased growth under N deposition, however, concurs the plastic changes in phenotypes of tree species (Zhang et al. 2018), which has been concerned as the reduction to other environmental stresses, e.g. chilling, drought, and insect herbivory. Excess N deposition causes forest declines when N input over the N sink capacity of forests, finally reducing the ecosystem productivity and functions (Aber et al. 1995, Bleeker 2011).

As mentioned above, numerous studies have reported that reduction of N deposition should be required based on the demonstrated results of N loading. However, the responses to N deposition show the high variability due to the tree species, N form (e.g. NH_4, NO_3), the amount of N loading from several to hundred kg N ha^{-1} yr^{-1}, the applied periods from weeks to years, and so on (Binkley and Högberg 2016, Högberg et al. 2017). Indeed, it has been reported the contamination of N deposition occurred with the effects of ground-level O_3 (Mill et al. 2016, Hunova et al. 2019), which are produced by photochemical reactions with reactive N pollutants. Namely, the air pollution of reactive N simultaneously occurs ground-level O_3, resulting in the serious concern in the combined effects of N deposition and elevated O_3 (Takemoto 2001, Watanabe et al. 2017).

Given the nutritional functions of N depositions, a reasonable assumption has risen as following; whether N loading would offset the O_3 effects on tree species (Utriainen and Holopainen 2001). Conversely, given the negative impacts of excess N deposition, there is another question; whether N loading would increase O_3 susceptibility (Pell et al. 1995). Namely, N deposition may change the O_3 sensitivity whereas its pattern has still been under investigated (Yamaguchi et al. 2010, Watanabe et al. 2017, Feng et al. 2019). In fact, there are obvious contrasting changes of O_3 susceptibility between representative temperate and sub-boreal tree species, i.e. beech and larch (Watanabe et al. 2017). However, the mitigation effects of N loading on changes of O_3 susceptibility are still under investigated, where the view of plant nutritional study would be needed for understanding of physiological mechanisms as well as optimizing of planted regions of tree seedlings.

Saline soil and its impacts on tree species

Saline soil occurs by salt accumulation in soils with a high evaporating relative to precipitation and a low salt leaching out, especially in the soil group of Solonetz and Solonchak (Bui 2013). Soil salinization also occurs by anthropogenic land degradations (Setia et al. 2013, Litalien and Zeeb 2020). Thus, saline soil distributes not only in semi-arid and arid zones as a natural soil salinization, but also irrigated lands due to the secondary salinization. The world land affected by salt is estimated as totally 1128 Mha (Fig.1-5, Wicke et al. 2011), where soil types are characterized by high concentration of NaCl, Na_2SO_4, Na_2CO_3, $NaHCO_3$, and so on. Furthermore, the increments of saline soil have been serious concerned under climate changes (Polle and Chen 2015), e.g. over-irrigation, changes of precipitation and evaporation patterns.

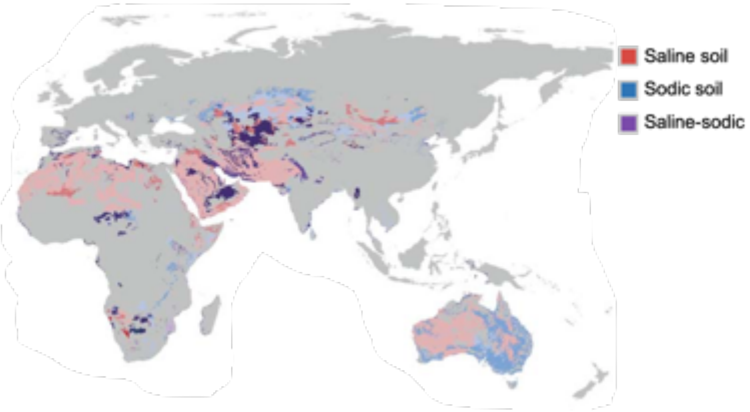

Fig. 1-5 Salinized soil map in Eurasian continent and its around, including Australia (Wicke et al. 2011, the figure was partially modified).

Salinity effects cause growth suppression of plants with plastic changes in morphological and metabolic traits (Lambers 2013, van Zelm et al. 2020). Impacts of salinity are mainly composed with both osmotic and ion toxic stresses of sodium (Na) ion, independently affecting plant developments and physiological activities. While there are spatial and temporal variations in salinity stresses, recent studies have reported that the rapid signals and developmental responses occurs both in roots and shoots (Galvan-Ampudia et al. 2013, Rewald et al. 2013). Plants have developed the various adaptive mechanisms to cope with salt stresses (Lambers 2013, Chen et al. 2017, Isayenkov and Maathuis 2019, Zhao et al. 2020), for example, (i) the accumulation or exclusion of selective ions; (ii) the regulation of uptake and transport from root to shoots; (iii) ion compartmentalization in a plant body; (iv) compatible solutes synthesis; (v) photosynthetic pathway changes; (vi) membrane structure changes; (vii) induction of hormones and anti-oxidative enzymes. Although the responses to salinity vary depending on the degree and exposure time of stress, and species, numerous studies have indicated that salt tolerance is widely recognized across many plants (Munns and Tester 2008, Farooq et al. 2018, van Zelm et al. 2020), where species can be categorized into glycophytes and halophytes, including woody species (Ball 1988, Allen 1994, Polle and Chen 2015).

A number of reviews have reported on various mechanisms of salinity impacts on trees and how they can be used as the ecological repairing (Ball 1988, Allen 1994, Kozloeski 1997, Bell 1999, Cimato et al. 2010, Polle and Chen 2015). The main background for the study of tree resistance was due to anthropogenic environmental degradation, for example, planting trees in arid areas (Mao et al. 2016), maintenance of coastal forests (Zhang et al. 2020), planting of urban roadside forests (Renalt 2005), and forest management near oil fields (Min et al. 2018). On the other hand, it has also been reported that high salt tolerance is often observed in non-native plants, and the use of the tolerance mechanism is expected to contribute to ecosystem restoration (e.g. Glenn et al. 2005). Even if considering the environmental repairing just through these introduced species, it is necessary to carefully manage the impact on the original ecosystem and its functions (Azam et al. 2012). So far, salt tolerance as the adaptive characteristics has been reported in woody species as well as herbs (Munns and Tester 2008), for example, mangroves (Ball 1988, Parida and jha 2010; Li et al 2020), eucalyptus (Farrell 1996, Niknam 2000) and poplars (Chen and Polle 2010).

However, the following questions remain to be elucidated; why there are diverse in physiological mechanisms and how they are evolutionally related to adaptation to saline soils. Progresses of these ecophysiological studies could give insights for managing strategies in harmony with environment, which eventually could achieve the sustainable resource uses (Polle and Chen 2015).

Because a given tolerance are often incompatible with other (Niinemets and Valladares 2006), the usefulness of trait selection under changing environment needs to be elucidated from multiple perspectives. Studying the distribution of plants as a sessile organism can help to understand how they adapt to the environment in which they are growing (e.g. Lamber 2013). In this sense, the geographic relationship between plant distribution and saline soil is expected to provide a better understanding of their adaptive significance in assessing tree tolerance (Bui 2013). Given that saline soil distributes northeast Asian regions (Zhang et al. 2010, Wicke et al. 2011), salt tolerance could be expected in larches.

Indeed, it has been reported that Siberian larch showed relative moderate salt tolerance within conifer species (Ogle and John 2010) although the interspecific difference of larches is still under investigated. The knowledge of salt tolerance in larches is also important for future Chinese reforestation. The forest policy in China has selected larches as afforestation species for ecological rehabilitation since 1999 (Zhang et al. 2000). It is needed to investigate the salt tolerance of larches, as alternative afforestation species to major greening trees (e.g. *Populus* sp., *Tamarix* sp.) in terms of the conservation in biodiversity of planting forests in northeast Asia (Xu 2011, Ren et al. 2015).

The viewpoints of this study

As a promising afforestation species, larches are widely planted in northern hemisphere (Asada and Sato 1987, Pâques et al. 2013, Mason and Zhu 2014). Previously, several critical reviews have suggested the guideline of larch forest managements under changing environment (Ryu et al. 2009, Kita et al. 2018). It is a central proposition in plant ecology to evaluate environmental responses of a sessility organism, which represents the species distribution and population (Lambers 2013). More specifically, effects of environmental chemicals, i.e. air pollutants, generated from anthropogenic activities have been studied in ecotoxicology (Saitanis and Agathokleous 2019). For estimating the critical levels to productivity in primary industries, the modeling of responses to toxic factors has been under improved since the stress responses are variable due to the contamination of several other factors. Given that the afforestation would be performed outside, more realistic effects need to be investigated. Even without the contaminated environmental condition, the inter-, intraspecific differences would occur in environmental responses due to the genetic variations, where the genotypic response capacity to environmental stimuli is known as reaction norm (West-Eberhard 2003). Better understandings of environmental response, thereby, requires both assessments of the internal response variability based on the inter-, intraspecific differences as well as the external environmental contaminations, which enable to predict the plants' plastic responses to changing environments (Nicotra et al. 2010, Arnold et al. 2019) and achieve suitable genetic resources for forestry use (Aitken and Whitlock 2013).

Based on the mention as above, there are still lacks in understanding of the environmental susceptibility in larches considering for the future afforestation assessment. First, I focused that the assessment of species-specific O_3 risks by evaluating the response capacity since the plastic response could be variable between parents and hybrid species (Resco de Dios et al. 2016, Hoshika et al. 2020) as well as different species (Li et al. 2017). Further, as pollutant concentrations are globally increasing with high uncertainty, it is urgently desirable to proceed with risk assessment from a more realistic response to concentrations. However, the number of cases only in the presence or absence of O_3 was dominated in previous studies, resulting in conventional manipulation experiments for evaluating of the response to expected future high or realistically unlikely concentrations of O_3.

Second, I concerned a combined effect of environmental factors in the actual field environment. There is serious concern that ground-level O_3 and nitrogen deposition have simultaneously affected on forest ecosystem (Watanabe et al. 2017). Furthermore, previous studies have reported that combined effects of ground-level O_3 and N deposition are different from single effects of them (Feng et al. 2019). These reports have suggested that the species-specific responsiveness to O_3 can be altered by N deposition. However, there is still controversial view on whether there is any inter-species difference in the plastic changes to species-specific environments, and if not, whether changes in responsiveness would converge on the same consequences. Given the changing environment at the continent, i.e. China, the combined effect of salt stress and elevated O_3 should be concerned as well as N deposition. Nevertheless, research cases are very few and limited to cases that assume the Mediterranean coast and urban environments.

The risk assessment for forest ecosystem should be performed under soil salinization (Polle and Chen 2015) as well as air pollution impacts. However, the ecological significance of salt tolerance may have been overlooked in woody species (Bui 2013).

Considering for the environmental repairing at Northeast Asia (Mason and Zhu 2014), I finally elucidated whether larch species have a potential for remediation of the degraded environment. Since stress tolerance itself is an expected adaptive trait, there is an ecological significance to reveal the interspecies differences in salt tolerance in larch species and its changes induced by hybridization, which could provide better understandings of larch distribution in Northeast Asia regions as well as sustainable forest management under changing environment.

Objectives, hypotheses, and structure

Here, the main theme of my study is to clarify the susceptibility of larches to the environmental stresses for reforestation in northeast Asian regions (Fig.1-6). In Chapter 2, effects of ground-level O_3 were investigated on the major afforestation species in boreal forest; Sakhalin fir, Japanese larch and hybrid larch F_1. Given the improved growth rate in hybrid larch, I assumed that impacts of elevated O_3 were significant on Japanese larch. In Chapter 3, the pattern of changes in O_3 sensitivity under N loading or salt loading was compared between larch species. When comparing with Japanese larch and hybrid larch F_1, there are contrasting hypothesizes; the mitigated O_3 sensitivity under N loading would be commonly observed in both larches, or O_3 sensitivity of hybrid larch F_1 would be increased by N loading. In Chapter 4, the interspecific differences in salt tolerance were investigated compared between Dahurian larch, Japanese larch, and hybrid larch F_1. By elucidating the following hypothesis, in Chapter 5, I discuss that (i) the possible relationship between the superior phenotypes by the hybridization and its potential reactivity to environment, and (ii) how much of the expected adaptive characteristics could represent the response to environmental stresses that are not yet adapted. Finally, I propose the novel assessment and guideline for future larch afforestation based on eco-physiological insights.

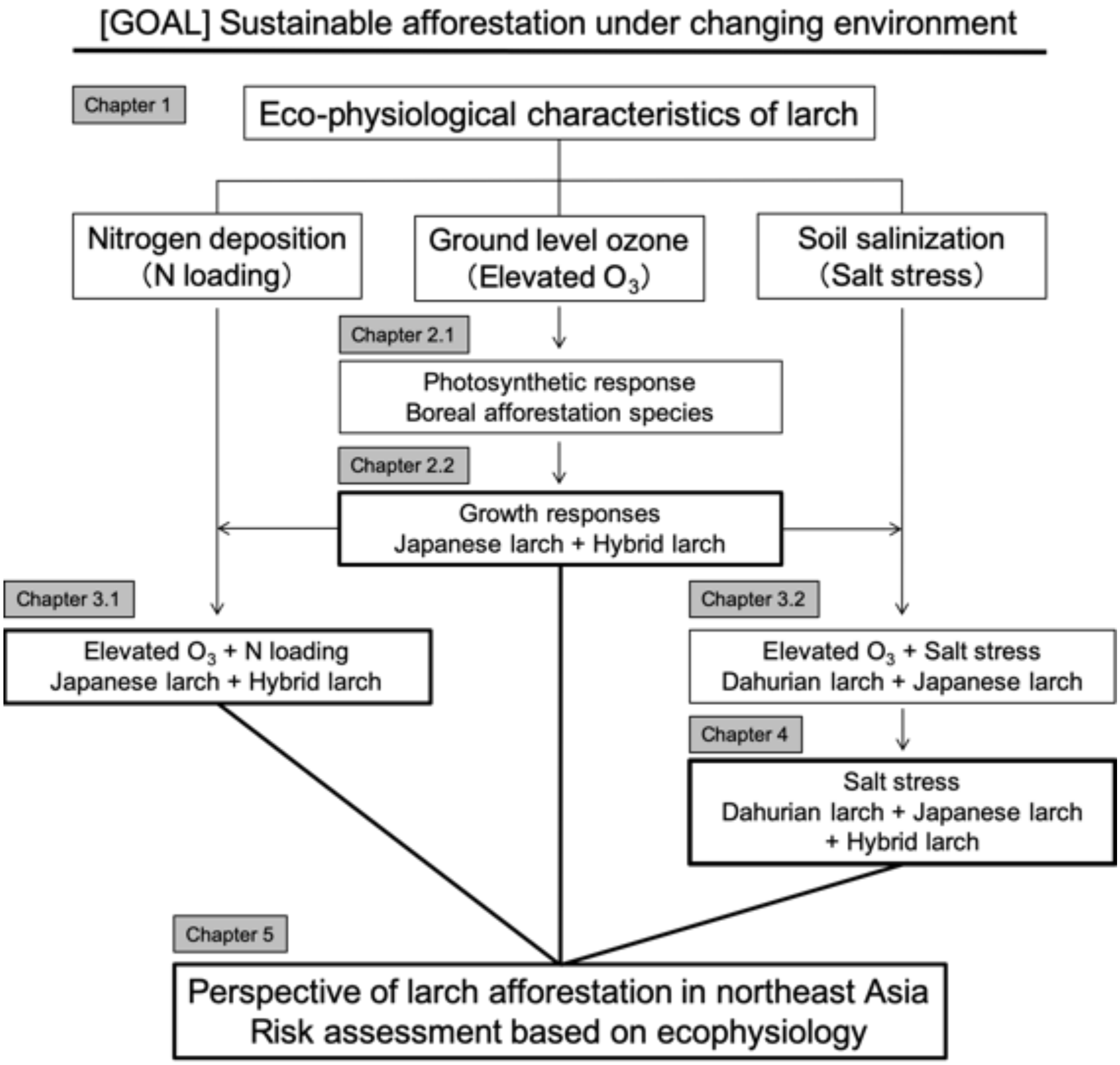

Fig. 1-6 Study scheme representing the research strategy and contents in the present thesis.

Chapter 2

Chapter 2-1: Interspecific difference in O_3 responses between afforestation species of boreal forests

INTRODUCTION

Ground-level ozone (O_3) concentrations have been increasing in Northeast Asia over the last several decades (Akimoto 2017). Ozone reduces growth, suppresses photosynthesis, decreases the allocation of photosynthates to the roots, accelerates leaf senescence, and causes a nutritional imbalance in woody species in temperate forests in Northeast Asia (e.g., Koike et al. 2012, Agathokleous et al. 2015, 2017, Kitao et al. 2017, Shi et al. 2017, Sugai et al. 2018).

Previous studies have evaluated several leaf functional traits, which could explain O_3 sensitivity in woody species (Bussotti 2008; Zhang et al. 2012; Li et al. 2016; Feng et al. 2018). Among them, leaf mass area (LMA) is strongly associated with the O_3 sensitivity of photosynthesis (e.g., Hayes et al. 2007, Bussotti 2008, Li et al. 2016, 2017). Compared with other indices of O_3 sensitivity, such as stomatal conductance, biogenic volatile organic compound emissions by leaves, LMA is regarded as the most critical index because it is a functional trait that is relatively easy to obtain (Li et al. 2016; Feng et al. 2018). It has also been reported that the thickness of the parenchyma cell layer is highly correlated with antioxidant capacity such as ascorbic acid equivalent antioxidant capacity (Matyseek et al. 2007, 2008). Relatively few studies have compared O_3 sensitivity between deciduous and evergreen trees based on LMA, particularly in conifer species (Mortensen 1994, Wieser and Havranek 1996, Watanabe et al. 2006, Weigt et al. 2012).

Another functional trait, leaf N content, could explain interspecific differences in the sensitivity of photosynthesis to O_3 in conifer tree species despite leaf N often being strongly positively correlated with LMA (Niinemets 1999, Kitaoka and Koike 2005). Leaf

N content has a strong correlation with photosynthetic capacity including carboxylation capacity and electron transport rate (Hikosaka et al. 2004). A meta-analysis revealed that the mass-based relationship between photosynthesis and leaf N was always stronger than the area-based relationship (Wright et al. 2004). In addition, deciduous and evergreen conifers are thought to have specific usages of needle N content, for example, photosynthetic N use efficiency, leaf N cycling, and storage pools (Small 1972, Reich et al. 1995, Temple et al. 1995; Hikosaka 2004, Takashima et al. 2004, Bussotti 2008, Weigt et al. 2012). Particularly, N demand and turnover in deciduous trees are generally higher than in evergreen trees (e.g. Matyssek 1986). Considering such interspecific differences, I investigated whether leaf N content could explain the variation in O_3 sensitivity of photosynthesis between deciduous and evergreen conifers.

I focused on Japanese larch (*Larix kaempferi*), a deciduous conifer, and Sakhalin fir (*Abies sachalinensis*), an evergreen conifer, because the species are ecologically and economically important in northern Japan (Kita et al. 2009, Goto et al. 2011), where O_3 tends to be elevated from spring to early summer (Koike et al. 2013, Hatakeyama 2017). Japanese larch is a light-demanding pioneer species and has a high photosynthetic capacity (Ryu et al. 2009). In addition, Japanese larch is a deciduous species that recycles N from the needles to non-photosynthetic organs during leaf senescence (Dong-Gyu et al. 2015). Conversely, Sakhalin fir has a lower photosynthetic capacity and does exhibit high shade tolerance, which implies that it utilizes low levels of light, such as those available on the forest floor, more efficiently (Noguchi et al. 2003). In addition, because the fir retains its evergreen needles for 5–10 years or more, depending on the light condition, it can allocate N to needles, with N being continually recycled in some years until the light environment will improve (Millard and Proe 1992, Noguchi et al. 2003, Weigt et al. 2012).

In the present study, I compared growth and physiology between Japanese larch and Sakhalin fir seedlings in response to elevated O_3. I hypothesized that the negative impacts of O_3 on larch would be significant, whereas those on fir would not be significant due to the higher needle N demand and turnover (Matyssek 1986). I also assessed whether needle N could be used as an indicator of the O_3 sensitivity of photosynthesis in larch and fir seedlings by considering how O_3-induced leaf senescence varies between deciduous and evergreen conifers.

MATERIAL AND METHODS

Study site and plant materials

The experiment was conducted at the Sapporo Experimental Forest of Hokkaido University in northern Japan (43°04′N, 141°20′E, 15 m above sea level). Two-year-old Japanese larch seedlings were grown from seeds at the nursery of the Hokkaido Research Organization (HRO), Forestry Research Department, Forest Products Research Institute at Bibai near Sapporo. Eight-year-old Sakhalin fir seedlings were obtained from the nursery of the Hokkaido Research Center of Forestry and Forest Products Research Institute (FFPRI), Sapporo, Japan.

The larch and fir seedlings were transplanted into 7-L pots on May 3, 2016, before the buds unfolded. Most of the soil was removed from around the roots of the seedlings prior to transplantation to adjust the edaphic conditions, and the pots contained well-weathered volcanic ash soil (Kanuma and Akadama soils, 1:1 v/v). Once the seedlings had completely rooted in the pots, 200 ml of commercial liquid fertilizer (1:1000, v/v, HYPONEX; Japan; N = 72.4 [mg l^{-1}], P = 284 [mg l^{-1}], K = 94.2 [mg l^{-1}]) was applied at 1 to 2-week intervals as basal dressing to prevent soil desiccation and nutrient imbalance.

Experimental design

Each seedling was exposed to O_3 in an open-top chamber (OTC; 1.2 × 1.2 × 1.2 m) with a steel frame. Each OTC was surrounded by polyvinyl chloride (PVC) film (Noh-bi Co Ltd., Sapporo, Japan), which could transmit 88% sunlight and blocked UVB and UVC radiation. Two O_3 treatments were used in the experiments: non-filtered air that represented the ambient O_3 concentration (AOZ; see below) and non-filtered air enriched with O_3 (EOZ). The target concentration of O_3 in the EOZ treatment was 60 nmol(O_3) mol^{-1} because it is the environmental standard value for the photochemical oxidant in Japan (Ministry of the Environment of Japan; http://www.env.go.jp/kijun/taiki.html). Each treatment had four replicates for each of the species in separate OTCs, with four seedlings in each of the 16 OTCs (64 seedlings in total).

The OTC system was operated by Hokkaido Branch office of DALTON Co. Ltd. (Sapporo, Japan). The target O_3 concentration was monitored using two devices: an O_3 monitor (2B Technologies, CO, USA) and an O_3 monitoring system (Ebara, Tokyo, Japan). In the AOZ treatment, ambient air was added to the OTCs, whereas in the EOZ treatment, the target level was attained by adding O_3 using a generator (Model PZ-1 C; Kofloc, Kyoto, Japan), which employed the pressure swing adsorption method to condense oxygen gas and use it as O_3 gas. The O_3 generation method produces only a minimal amount of NOx gas. A proportional integrative differential control algorithm was used to maintain the desired concentration. The O_3 treatments were applied to the seedlings from June 1 to Sept. 3, 2016, between 06:00–18:00 h Japan Standard Time (JST). The O_3 concentrations that were achieved each month from June to Aug. were 32.9 ± 1.49, 26.9 ± 1.76, and 28.3 ± 1.50 nmol(O_3) mol^{-1} respectively, in the AOZ treatment, and 64.2 ± 2.31, 62.2 ± 1.68, and 61.1 ± 1.85 nmol(O_3) mol^{-1} respectively, in the EOZ treatment. The temperature and light conditions were monitored at 5-min intervals throughout the experimental period using a HOBO Pendant data logger (UA-002-64; Onset Computer, Co., MA, USA) that was placed in the center of each OTC above the canopy of the plants.

Leaf gas exchange

Gas exchange measurements were obtained from the needles of all seedlings on Aug. 30, 2016. Because the effects of O_3 depend on the amount that has been absorbed (Wieser *et al.* 2013, Kitao *et al.* 2017), it is critical that same-age needles are used when comparing O_3 responses among different foliage types. Therefore, I measured the responses of current-year needles to O_3. The gas exchange rates were measured using an open gas exchange system (LI-6400; Li-Cor Inc., NE, USA) between 05:00–14:00 JST. During measurement, leaf temperature was maintained at 25 ± 0.5°C, water vapor deficit in the leaf chamber was approximately 1.2 ± 0.3 kPa, and photosynthetic photon flux density was approximately 1,500 μmol m^{-2} s^{-1}. To determine the net CO_2 assimilation rate per intercellular CO_2 concentration (A/Ci) curve, A was determined at 10 levels of C_i (C_a: 60–1,600 μmol(CO_2) mol^{-1}). The curve was then used to determine A, the transpiration rate, and stomatal conductance at 380 μmol(CO_2) mol^{-1} C_a (P_N and g_s, respectively). The A/Ci curve was also used to calculate the maximum net photosynthetic rate at 1600 μmol(CO_2) mol^{-1} C_a (P_{Nmax}), the maximum rate of carboxylation (V_{cmax}), and the maximum rate of electron transport (J_{max}) using an individual leaf photosynthetic model (Farquhar *et al.* 1980, Long and Bernacchi 2003). The A/Ci curve was analyzed using values of Rubisco Michaelis constants for CO_2 (K_c) and O_2 (K_o), and CO_2 compensation point in the absence of dark respiration (Γ^*), according to Bernacchi *et al.* (2001).

Once the photosynthetic measurements had been obtained, the needles were scanned and the projection areas of the needles were measured converted into a needle area index using the image analysis software ImageJ (National Institutes of Health, Bethesda, Maryland, USA; Schneider *et al.* 2012).

Leaf elements and photosynthetic N use efficiency

The needles that were used for gas exchange measurements were collected for further analyses of their N and carbon (C) contents per unit mass and area (N_{mass}, C_{mass}, and N_{area}, respectively) and their LMA. Once the needle areas had been measured, the needles were dried at 70°C for at least 3 days until they reached a constant dry mass and were then weighed. N_{mass} and C_{mass} were measured using a NC analyzer (VarioEL III; Elementar, Japan). N_{area} was then used to calculate the photosynthetic N use efficiency (NUE [μmol(CO_2) mgN^{-1} s^{-1}]) using the following equation (Koike *et al.* 2012):

$$NUE = \frac{P_N}{N_{area}}$$

Growth

The height and stem basal diameter (2 cm from the stem base) of each seedling were measured on May 28 and Aug. 29, 2016 using a measuring tape (1 mm gradient) and

Vernier calipers (Mitsutoyo, Kanagawa, Japan). The diameter was taken as the average of two crosswise measurements at the base of the stem. The larch seedlings had an initial mean stem diameter of 5.76 ± 0.32 mm in the AOZ treatment group and 5.79 ± 0.06 mm in the EOZ treatment group, and an initial mean height of 27.2 ± 0.15 cm in the AOZ treatment group and 27.0 ± 0.40 cm in the EOZ treatment group. The fir seedlings had an initial mean (± SE) stem diameter of 10.3 ± 0.25 mm in the AOZ treatment group and 9.59 ± 0.27 mm in the EOZ treatment group, and an initial mean height of 37.1 ± 1.02 cm in the AOZ treatment group and 36.7 ± 0.87 cm in the EOZ treatment group. Size growth in stem diameter and height were calculated by subtracting the initial size value in May from the final size value in August.

Statistical analyses

All statistical analyses were carried out in R version 3.4.3 (R Core Team 2017). Photosynthetic processes at the leaf scale in the two species were compared using a generalized linear mixed model (GLMM) using the package lmerTest. The model included O_3 treatment, species, and their interaction as explanatory variables. When a significant interaction effect was detected, Tukey's multiple comparison tests were conducted using the package multcomp. GLMM analysis was also used to determine how photosynthesis rate and stomatal conductance were correlated with LMA and needle N using the package lmerTest. I compared the performance of each model in predicting photosynthetic responses in each species to O_3 using Akaike's information criterion (AIC; Akaike 1974). I also used GLMM to evaluate the relationship between photosynthetic parameters, with the influence of leaf traits as the dependent variable and the different species as independent variables. Data from each replicate were averaged, giving four values per species for each treatment (*n* = 4).

RESULT

Physiological responses to O_3

Responses of the photosynthetic parameters and needle characteristics of each species to EOZ are summarized in Table 2-1-1. There were significant interspecific differences in all the photosynthetic parameters (except J_{max}, P=0.09), regardless of the O_3 treatment. Multiple comparison tests revealed that Sakhalin fir had significantly lower P_N and P_{Nmax} values than the larch under AOZ (P<0.05), whereas there were no differences in the two parameters between the two species under EOZ. In addition, all the photosynthetic parameters except g_s were significantly inhibited under EOZ in both species (P<0.001).

Table 2-1-1 Photosynthetic and leaf characteristics of the current-year needles of Japanese larch (*Larix kaempferi*) and Sakhalin fir (*Abies sachalinensis*).

All values are means ± SE (n = 4) for the ambient (AOZ) and elevated (EOZ) ozone treatments. *, P<0.05; **, P<0.01; ***, P<0.001, n.s, not significant (GLMM). Different letters within a row indicate significant differences between species (Tukey's multiple comparison test). P_N, net photosynthetic rate at 380 μmol(CO_2) mol^{-1} and light saturation per unit leaf area; g_s, stomatal conductance per unit leaf area; P_{Nmax}, net photosynthetic rate at 1500μmol(CO_2) mol^{-1} and light saturation per unit leaf area; J_{max}, maximum electron transport rate; V_{cmax}, maximum rate of carboxylation; N_{mass}, nitrogen content per unit leaf mass; C_{mass}, carbon content per unit leaf mass; N_{area}, nitrogen content per unit leaf area; LMA, leaf mass per area; NUE, nitrogen use efficiency.

	Japanese larch		Sakhalin fir		
	AOZ	EOZ	AOZ	EOZ	O_3
P_N [μmol(CO_2) m^{-2}s^{-1}]	6.74 ± 0.25^a	3.59 ± 0.10^c	4.57 ± 0.23^b	3.38 ± 0.17^c	***
g_s [mol(H_2O) m^{-2}s^{-1}]	0.10 ± 0.01	0.07 ± 0.01	0.08 ± 0.01	0.06 ± 0.01	n.s.
P_{Nmax} [μmol(CO_2) m^{-2}s^{-1}]	19.0 ± 0.68^a	11.7 ± 0.33^c	14.4 ± 0.53^b	10.3 ± 0.34^c	***
V_{cmax} [μmol m^{-2}s^{-1}]	60.9 ± 3.36^a	33.3 ± 2.66^{bc}	44.6 ± 4.48^b	28.2 ± 1.86^c	***
J_{max} [μmol m^{-2}s^{-1}]	123 ± 6.50	72.4 ± 3.00	106 ± 11.6	64.3 ± 4.00	***
N_{mass} [mgN g^{-1}]	22.9 ± 0.61^a	16.1 ± 0.78^b	15.5 ± 0.65^b	16.7 ± 0.48^b	***
C_{mass} [mgC g^{-1}]	488 ± 1.06^c	484 ± 2.29^c	533 ± 1.66^b	545 ± 0.61^a	n.s.
N_{area} [gN m^{-2}]	1.98 ± 0.09^{ab}	1.62 ± 0.14^b	1.87 ± 0.12^{ab}	2.34 ± 1.61^a	*
LMA [g m^{-2}]	85.0 ± 1.28	100 ± 4.81	121 ± 4.85	141 ± 5.38	*
NUE [μmol gN^{-1}s^{-1}]	3.59 ± 0.13	2.85 ± 0.21	2.53 ± 0.08	1.45 ± 0.09	***

LMA was significantly higher in the fir than in the larch regardless of the O_3 treatment (P<0.001). However, LMA was also significantly higher under EOZ than under AOZ (P<0.05). The effects of O_3 on N_{area} varied between species (P<0.05) with multiple comparison tests showing that N_{area} was higher in the fir than in the larch under EOZ

($P<0.05$). Although area-based differences were not clear in the larch, N_{mass} was significantly lower under EOZ than under AOZ ($P<0.05$). However, changes in both needle N parameters were observed in fir under EOZ in the opposite direction, although they were not significant. In addition, a significant, albeit only slight, increase in C_{mass} was observed in the fir under EOZ.

Correlation analysis

Correlations between LMA and P_N, g_s and correlations between N_{area} and P_N, g_s are presented in Fig. 2-1-1. P_N was more significantly correlated with LMA than with N_{area} ($P<0.01$), with larch having a stronger negative correlation between P_N and LMA than fir (Table 2-1-2). There was also a strong negative correlation between g_s and LMA in both species, with larch again exhibiting the strongest relationship. By contrast, the correlation between P_N and N_{area} varied between species ($P<0.01$), with a significant positive correlation being observed for larch ($P<0.05$) and a negative relationship being observed for fir ($P=0.09$). There was no significant correlation between g_s and N_{area} in either species.

Correlations between N_{mass} and P_{Nm}, and g_{sm} and NUE are shown in Fig. 2-1-2. P_{Nm} was significantly correlated with N_{mass} ($P<0.05$), whereas the correlation between P_{Nm} and N_{mass} was strongest among all models for both species ($R^2=0.76$). The model with the lowest AIC also indicated that the mass-based relationship could explain the O_3 sensitivity of photosynthesis in each species, despite the correlation not being particularly strong in the fir. The correlation between g_{sm} and N_{mass} was not significant, whereas the relationship varied between species ($P<0.05$). The correlation between NUE and N_{mass} also varied between species ($P<0.05$) with the GLMM analysis revealing that the larch had a stronger positive correlation between NUE and N_{mass} than the fir. In addition, Sakhalin fir had a negative correlation between the two parameters ($P<0.05$).

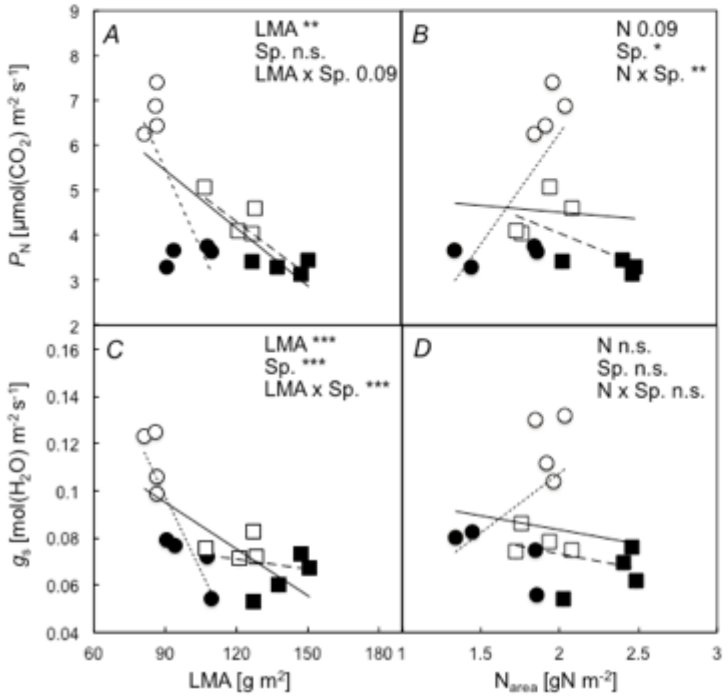

Fig. 2-1-1 Are-based correlation analysis between photosynthetic parameters. Relationships between the net photosynthesis rate per unit leaf area at ambient CO$_2$, i.e., 380 µmol(CO$_2$) mol^{-1} (P_N) and the leaf mass per area (LMA) (*A*), P_N and the leaf nitrogen per unit area (N$_{area}$) (*B*), the stomatal conductance at ambient CO$_2$ (g_s) and LMA (*C*), and g_s and N$_{area}$ (*D*). Significance: n.s, P>0.05; *, P<0.05; **, P<0.01; ***, P<0.001. Circle and square stands denote Japanese larch (*Larix kaempferi*) and Sakhalin fir (*Abies sachalinensis*), respectively. Open and solid symbols mean ambient (AOZ) and elevated (EOZ) ozone levels, respectively. The relationships between the parameters are indicated by fine dotted lines for Japanese larch, heavy dotted lines for Sakhalin fir, and solid lines for both species.

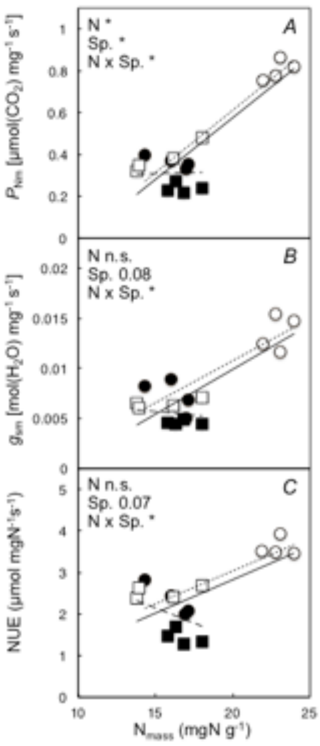

Fig. 2-1-2 Mass-based correlation analysis between photosynthetic parameters. Relationships between the net photosynthesis rate per unit leaf mass at ambient CO$_2$, i.e., 380 µmol(CO$_2$) mol^{-1} (P_{Nm}) and leaf nitrogen per unit mass (N_{mass}) (*A*), the stomatal conductance per unit leaf mass at ambient CO$_2$ (g_{sm}) and N_{mass} (*B*), and the photosynthetic nitrogen use efficiency (NUE) and N_{mass} (*C*) in the current-year needles of Japanese larch (*Larix kaempferi*) and Sakhalin fir (*Abies sachalinensis*) at ambient (AOZ) and elevated (EOZ) ozone levels. The relationships between the parameters are indicated by fine dotted lines for Japanese larch, heavy dotted lines for Sakhalin fir, and solid lines for both species.

Growth response

No significant growth inhibition was observed in either species (Table 2-1-3). Moreover, there were no statistical significances in the differences in height and diameter growth within species ($P>0.05$).

Table 2-1-2 Summary of the generalized linear mixed models (GLMM).

The relationship between area-based and mass-based photosynthetic parameters and morphological and nutritional factors in Japanese larch (*Larix kaempferi*) and Sakhalin fir (*Abies sachalinensis*). AIC, Akaike's information criterion; P_N, net photosynthetic rate at 380 µmol(CO_2) mol^{-1} and light saturation per unit leaf area; g_s, stomatal conductance per unit leaf area; P_{Nm}, net photosynthetic rate at 380 µmol(CO_2) mol^{-1} and light saturation per unit leaf area; g_{sm}, stomatal conductance per unit leaf mass; NUE, nitrogen use efficiency; LMA, leaf mass per area; N_{area}, nitrogen content per unit leaf area; N_{mass}, nitrogen content per unit leaf mass.

Model	Adj. R^2	P	AIC
Both conifer species			
$P_N = -0.04$ LMA $+ 9.30$	0.4766	0.003	61.35
$P_N = -0.30\ N_{area} + 5.11$	0.0044	0.806	61.79
$P_{Nm} = 0.06\ N_{mass} - 0.60$	0.7647	<0.001	–5.61
$g_s = -0.001$ LMA $+ 0.15$	0.4864	0.003	–56.02
$g_s = -0.01\ N_{area} + 0.10$	0.0262	0.549	–55.62
$g_{sm} = 0.001\ N_{mass} - 0.01$	0.6575	<0.001	–115.46
NUE $= 0.16\ N_{mass} - 0.39$	0.4232	0.006	43.34
Japanese larch			
$P_N = -0.12$ LMA $+ 16.0$	0.5123	0.003	36.89
$P_N = 4.94\ N_{area} - 3.63$	0.5146	0.045	29.38
$P_{Nm} = 0.06\ N_{mass} - 0.62$	0.9005	<0.001	1.17
$g_s = -0.002$ LMA $+ 0.31$	0.7660	0.004	–18.59
$g_s = 0.05\ N_{area} + 0.01$	0.2130	0.250	–18.34
$g_{sm} = 0.001\ N_{mass} - 0.01$	0.7105	0.009	–41.75
NUE $= 0.17\ N_{mass} - 0.39$	0.6663	0.013	21.77
Sakhalin fir			
$P_N = -0.04$ LMA $+ 9.08$	0.6728	0.013	24.13
$P_N = -1.42\ N_{area} + 6.90$	0.4029	0.091	20.06
$P_{Nm} = 0.002\ N_{mass} + 0.283$	0.0010	0.941	2.16
$g_s = -0.0002$ LMA $+ 0.09$	0.0454	0.607	–21.35
$g_s = -0.01\ N_{area} + 0.10$	0.1533	0.337	–29.78
$g_{sm} = -0.0001\ N_{mass} + 0.01$	0.0484	0.601	–51.56
NUE $= -0.15\ N_{mass} + 4.33$	0.1517	0.013	23.83

Table 2-1-3 Size growth (Sg) of a stem diameter and height under ambient (AOZ) and elevated (EOZ) ozone levels.

All values are means ± SE (n = 4). n.s, not significant (Student's t-test).

	Japanese larch			Sakhalin fir		
Sg	AOZ	EOZ	T value	AOZ	EOZ	T value
Height [cm]	6.57 ± 0.41	4.93 ± 1.06	$1.44^{n.s}$	7.29 ± 0.21	6.96 ± 0.54	$0.57^{n.s}$
Stem diameter [mm]	1.43 ± 0.20	1.33 ± 0.22	$0.35^{n.s}$	1.06 ± 0.25	0.88 ± 0.22	$0.74^{n.s}$

DISCUSSION

In the present study, I compared the physiological and growth responses of Japanese larch and Sakhalin fir seedlings to EOZ. At the leaf scale, significant reductions in photosynthesis under EOZ were observed in both species. However, responses of needle N content to O_3 differed between the two investigated species. A significant reduction in N_{mass} under EOZ was observed in Japanese larch ($P<0.05$; Table 2-1-2), whereas it was not in observed Sakhalin fir. However, N_{mass} of the studied fir was slightly increased by O_3 although the difference was not significant. Leaf N has a strong correlation with photosynthetic capacity because a large fraction of leaf N content is invested in photosynthetic apparatus (Hikosaka *et al.* 2004). The O_3 responses of photosynthesis in Japanese larch were illustrated by needle N contents, which is a result that is consistent with those of previous reports (Watanabe *et al.* 2006, Koike *et al.* 2012; Wang *et al.* 2015; Sugai *et al.* 2018). Previous studies have also reported that P_N in Japanese larch was significantly decreased by EOZ, although needle N content also declined but the difference was not significant. An effect of O_3 has also been observed in the form of reduction of N allocation to protein in leaves (Yamaguchi *et al.* 2007; Yamaguchi *et al.* 2011), particularly to photosynthetic apparatus (Shang *et al.* 2018). Based on the results of previous studies, an O_3 effect could have suppressed N allocation to photosynthetic apparatus in Japanese larch in the present study.

Needle N content in Sakhalin fir was slightly increased by O_3 although the increase was not significant. The increase in leaf N concentration under elevated O_3 conditions has also been observed in other evergreen tree species, such as ponderosa pine (*Pinus ponderosa*, Beyers *et al.* 1992, Temple *et al.* 1995), loblolly pine (*Pinus taeda*, Mandercheid *et al.* 1992), and camphor laurel (*Phoebe bournei*, Cao *et al.* 2016). A potential mechanism of the increase in leaf N concentration, according to the above studies, is that O_3 increased N availability by increasing protein turnover rate in the senescence-accelerated leaves under EOZ. I hypothesize that the slight N increment in the fir under study fir is attributable to O_3-induced N turnover from aged needles, although I did not investigate age dependent N dynamics in Sakhalin fir.

The responses of the needle N contents to EOZ were different between the species, whereas the NUE responses exhibited similar decreases. The results suggest that the mechanism of NUE reduction could be different between the two investigated species. NUE (P_N/N$_{area}$) reduction in larch reflected the reduction in P_N relatively more accurately than in N$_{area}$ (reduction rates were 46.7% and 18.2%, respectively, Table 2-1-2). In fir, however, NUE were more accurate in reflecting the reduction in N$_{area}$. Although there was no significant difference between the two species, the extent of NUE reduction was relatively higher in the fir than in the larch. The contrasting responses to O_3 may be associated with the species-specific utilization of needle N. Larch, which has a deciduous leaf habit, exhibits a higher photosynthetic capacity and recycles N in needles before shedding, whereas evergreen conifers such as Sakhalin fir generally maintain needle N for relatively long periods (Millard and Proe 1992, Matsuda *et al.* 2002, Weigt *et al.* 2012). Evergreen conifer species also have lower NUE values to facilitate adaptation to resource poor environments (Reich *et al.* 1992; 1995) and they could drive sites toward resource poor conditions by producing litter that does not easily decompose (Reich *et al.* 1992). Effects of O_3, therefore, could have negative effects on fir not only by decreasing NUE but also by introducing N-rich conditions through the increase of needle N contents. Additional long-term studies that focus on the impacts of O_3 on species composition and the ecological N cycle are required.

Photosynthetic parameters, including N$_{mass}$ in both species, were significantly correlated with needle N. The lowest AIC values indicated that N$_{mass}$ was the optimal index for explaining photosynthetic parameters in both species. I also observed that photosynthetic parameters had a higher correlation with N$_{mass}$ than N$_{area}$. The result indicates the overall relationship between photosynthesis and needle N varies depending on the needle N unit. Hereafter, I discuss why N$_{mass}$ could explain the O_3 sensitivity of photosynthesis in conifers with different leaf habits with greater accuracy. N$_{mass}$ has the higher correlation with photosynthesis regardless of species (Wright *et al.* 2004; Hikosaka *et al.* 2004). The correlations between photosynthesis and N$_{area}$, however, vary depending on species (Field and Mooney 1986, Peterson 1999, Larcher 2003, Matyssek *et al.* 2005).

In addition, generally, photosynthesis rate has a negative correlation with LMA regardless irrespective of plant species (Field and Mooney 1986).

The present results also supported the hypothesis because the correlation between area-based photosynthesis rate and LMA were negative in both species. Because P_{Nm} = P_{N}/LMA and $\mathrm{N}_{\mathrm{mass}}$ = $\mathrm{N}_{\mathrm{area}}$/LMA, higher NUE values in species result in high P_{Nm} and $\mathrm{N}_{\mathrm{mass}}$ values, whereas lower NUE values in species result in low P_{Nm} and $\mathrm{N}_{\mathrm{mass}}$ values. Consequently, the relationship between P_{Nm} and $\mathrm{N}_{\mathrm{mass}}$ has a higher correlation regardless of species (Hikosaka 2004). In the present study, P_{Nm} had a higher correlation with $\mathrm{N}_{\mathrm{mass}}$ in all treatments, implying that $\mathrm{N}_{\mathrm{mass}}$ was more effective in explaining the O_3 sensitivity of photosynthesis in both species. Based on the interactive effects of $\mathrm{N}_{\mathrm{mass}}$ and species, I established that P_{Nm} and g_{sm} were clearly independent of $\mathrm{N}_{\mathrm{mass}}$ in the fir. The result could imply that both parameters were significantly more robust to EOZ in the fir than in the larch. This could have been due to the relatively lower sensitivity to O_3 in evergreen trees (Li *et al.* 2016, 2017). It has previously been reported that there is no relationship between LMA, the apoplastic fraction, and ascorbic acid, which plays a key role in O_3 flux in chloroplasts (Niinements 1999, Li *et al.* 2016). However, there may be other differences at the molecular scale based on antioxidant capacity, stomatal regulation systems, and leaf internal structures (Feng *et al.* 2018, Shang *et al.* 2018). Further studies are required to determine the specific mechanism underlying the robustness of mass-based photosynthetic parameters in the fir even under O_3 exposure.

Chapter 2-2: Interspecific difference in O_3 responses between Japanese larch and hybrid larch F_1

INTRODUCTION

Larch (*Larix* sp.) is distributed broadly in the northeast Eurasian continent and northern America where permafrost occurs (Gower and Richards 1990, Osawa et al. 2010). Larches contribute significantly to fixing CO_2 in Eurasia continent and are promising for man-made forests (Ryu et al. 2009). Japanese larch [*L. kaempferi* (Lamb.) Carr.] has been widely planted in northeast Asia and introduced to central Europe from the 1930s (Matyssek and Schulze 1987, Ryu et al. 2009) due to its high growth rate, survival in xeric infertile soil condition, etc. (Qu 2016). To overcome some weak points (shoot blight disease and vole grazing), a hybrid larch F_1 (*L. gmelinii* var. *japonica* × *L. kaempferi*) has been developed and has many advantages: higher initial growth rate, resistance to biological stresses, and high specific gravity of a stem (Kita et al. 2009, Ryu et al. 2009). The high growth rate in larches may contribute to greater CO_2 fixation but also to higher uptake of gaseous pollutant.

Ground-level O_3 concentrations have significantly increased over the past decades, especially in northeast Eurasian region (Akimoto et al. 2015, Feng et al. 2015, Verstraeten et al. 2015). Further increase has been predicted in the future (Ainsworth et al. 2012, Chatani et al. 2014). Overall, O_3 mixing ratios in the Northern Hemisphere are nowadays doubled as compared to the preindustrial period ones (Hartmann et al. 2013). Although precursor substances are decreasing in some areas or regions, O_3 concentrations remain at high mixing ratios due to transport of O_3 or its precursor molecules at regional or trans-boundary level (Akimoto et al. 2015, Kalabokas et al. 2015, Sicard et al. 2016).

Ozone is a strong oxidant that severely affects vegetation (Paoletti et al. 2006, Agathokleous et al. 2016, 2017). Ozone enters plant tissues via stomata and generates the production of reactive oxygen species (ROS); thus, forcing plants to undergo a stress-response process which often leads to suppressed photosynthetic capacity due to degradation of chlorophyll (Chl) and enzymes, and inhibition of growth and biomass accumulation (e.g., Ainsworth et al. 2012, Agathokleous et al. 2016). However, the plant response to O_3 varies among species (Yamaguchi et al. 2011, Koike et al. 2013, Feng et al. 2015) due to variability in stomatal response, carbon allocation patterns, and defense ability to detoxify radical oxygen species (Matyssek et al. 2007, Paoletti et al. 2008, Manninen et al. 2009).

Hormesis is a biological phenomenon occurring in exposure-response studies, where low exposures to an agent stimulate the performance of an organism and high exposures inhibit its performance, therefore generating a biphasic exposure-response relationship (e.g. Calabrese 2015). Hormesis can be observed for biological and physiological processes in a cell or an organism, and has received increasing attention (Cedergreen et al. 2007, Calabrese 2013, 2015). Hormesis can be generalized as to stressors and organisms (e.g., plants, animals, bacteria), both qualitative and quantitative (Calabrese 2013, 2014, Agathokleous 2018a).

Although the effects of O_3 on plants have been extensively studied over the past decades (Feng et al. 2015, Agathokleous et al. 2016), the hypothesis that O_3 induces hormesis in plants, i.e., potential biphasic response in the full exposure-response continuum, has never been tested. Only a few studies provided evidence suggesting that low O_3 exposures may have stimulatory effects on plants (Eamus et al. 1990, Flowers et al. 2007, Vázquez-Ybarra et al. 2015). Whether O_3 induces hormesis, it requires further examination, especially, because the physiological response of plants to O_3 is influenced by various factors (e.g., Ainsworth and Long 2005, Grantz et al. 2006).

The aim of this study was to test if chronic O_3 exposure induces hormetic responses in Japanese larch and its hybrid, which differ in their competitive capacity, and if there are differences in their responses. For this purpose, seedlings of the two larches were exposed to four O_3 treatments, ranging from approximately 10 to 60 nmol mol^{-1}, during two consecutive growing seasons. The two taxa were selected because of prior evidence for their response to O_3 (Koike et al. 2012, Dong-Gyu et al. 2015, Agathokleous et al. 2017). Based on these prior studies, I hypothesized that elevated O_3 exposures may inhibit the growth over time. I further predicted that low O_3 (i.e. approximately 30 nmol mol^{-1}), which widely occurs in the Northern Hemisphere nowadays, might cause stimulatory effects on larches, compared to exposures similar to preindustrial concentrations (i.e. approximately 10 nmol mol^{-1}). I discussed plausible understanding of O_3-induced hormesis in photosynthesis of larches in relation to potential competitive capacity for light and space because stress effects are driven by competition or tolerance, according to the primary strategies of plants (Grime 1977).

MATERIAL AND METHODS

Study site, plant materials, and experimental design

The experiment was conducted in the open-top chambers (OTCs) of Hokkaido University, located at Sapporo Experimental Forest of Hokkaido University in northern Japan (43°04' N, 141°20' E, 15 m a. s. l.). The experimental site was selected because of low background O_3 mixing ratios (Hoshika et al. 2013) compared to elevated O_3 mixing ratios commonly occurring in the Northern Hemisphere nowadays (e.g., Feng et al. 2015, Sicard et al. 2016). The main meteorological conditions at the experimental area can be found in Agathokleous et al. (2016, 2017).

Two-year-old seedlings of Japanese larch (*Larix kaempferi*) and its hybrid larch F_1 (*L. gmelinii* var. *japonica* × *L. kaempferi*) were directly planted in the ground of OTCs (brown forest soil, classified as Dystric Cambisols) in middle of May 2013. The initial stem diameter of seedlings was 2.30 ± 0.04 mm for Japanese larch (JL) and 2.11 ± 0.04 mm for hybrid larch (HL), and the seedling height was 13.81 ± 0.24 and 17.94 ± 0.47 cm for JL and HL, respectively. After planting, 200 ml of liquid balanced fertilizer (1:1000, v/v, N:P: K = 6:10:5, Hyponex Japan Corp., Ltd., Japan) was applied to each seedling as soil drench.

In this experiment, four O_3 treatments were used: (a) a charcoal-filtered air treatment

(CF) to imitate the preindustrial mixing ratio; (b) a non-filtered air treatment (NF) representing low O_3 mixing ratios which occur nowadays; (c) a non-filtered air enriched with additional O_3 to reach a target O_3 mixing ratio of 40 nmol mol^{-1} (NF40); and (d) a non-filtered air enriched with additional O_3 to reach a target O_3 mixing ratio of 60 nmol mol^{-1} (NF60) simulating future elevated O_3 mixing ratios. The NF60 was set as environmental standard value for the photochemical oxidant of Japan (Ministry of the Environment in Japan 1996; http://www.env.go.jp/kijun/taiki.html). Each O_3 treatment was replicated four times, making a total of sixteen OTCs with four seedlings per larch variety in each OTC (128 seedlings in total), on a split-plot completely randomized design. The size of each OTC was 1.2 × 1.2 × 1.2 m in the first growing season and then extended to 2.2 m early in the second growing season due to an increased plant size. Each OTC was constructed as a steel frame (shaping an empty cube), which was parametrically surrounded by a polyvinyl chloride film (Noh-bi, Japan) with an 88% sunlight transmittance (blocking only UVB). For the CF treatment, charcoal-filtered air was added in the OTCs whereas for the NF treatment ambient air was added to the OTCs. For the NF40 and NF60 treatments, additional O_3 was added to reach the target concentration by using a generator (Model PZ-1 C, Kofloc, Japan), which employs the pressure-swing-adsorption method for condensing the concentration of oxygen gas and using it as an O_3 gas material. This O_3 generation method produces just a tiny amount of NO_x gas and is environmentally clean. A proportional-integrative-differential control algorithm was used to maintain the desired O_3 mixing ratio. The targeted O_3 mixing ratio was regulated by an O_3 monitor (2B Tech, CO, USA) and Ebara O_3-monitoring system (Ebara, Japan). The OTCs system was operated by Hokkaido Branch office of DALTON Co. Ltd. (Sapporo, Japan). The O_3 treatment lasted from 17 June to 29 October 2013 and from 18 June to 15 September 2014, during the daylight hours (06:00–18:00 h, Japan Standard Time). The achieved O_3 mixing ratio were following; 12.9 ± 0.56 (CF), 31.7 ± 1.53 (NF), 40.1 ± 0.99 (NF40), and 61.4 ± 1.68 (NF60) nmol(O_3) mol^{-1} in 2013, and 12.4 ± 0.35 (CF), 29.9 ± 1.61 (NF), 39.4 ± 1.03 (NF40), and 62.5 ± 1.95 (NF60) nmol(O_3) mol^{-1} in 2014, respectively. The values of mixing ratios accumulated over the threshold of 40 nmol mol^{-1} (AOT40, Fuhrer et al. 1997) for the four O_3 treatments over the treatment periods of the years 2013 and 2014 were following; 0.827 (CF), 4.864 (NF), 10.671 (NF40), and 35.645 (NF60) μmol(O_3) mol^{-1} h in 2013, and 0.846 (CF), 5.106 (NF), 8.776 (NF40), and 37.634 (NF60) μmol(O_3) mol^{-1} h in 2014, respectively.

The temperature and light conditions were monitored using a HOBO pendant data logger (UA-002-64, Onset Computer, Co., USA) placed in the center of an OTC chamber, above the canopy of the plants; the OTC was in the middle of the OTC rows. One observation was recorded in a 5-min interval during August–October, in both years. The average daily temperature for the period of 06:00–18:00 was 20.53 ± 0.09 and 20.16 ± 0.14 °C for 2013 and 2014, respectively, and the average daily PPFD was 24.15 ± 0.51 and 28.86 ± 0.56 mol m^{-2} s^{-1} for 2013 and 2014, respectively.

Data collection

Growth and dry matter production: The height and stem basal diameter (2 cm from stem base) of each seedling were measured on 17 June, 1 August, 6 September, and 6 October in 2013 and on 15 June and 20 September in 2014, using measuring tapes (1 mm gradient) and Vernier calipers (Mitsutoyo, Japan). The diameter was taken as the average of two crosswise measurements at the stem base. Since the sampling was not destructive, the relative growth rate (RGR) over a certain time interval was calculated for each plant using the classical approach (Hoffmann and Poorter 2002) based on the following equation;

$$RGR = \frac{Ln(Pj) - Ln(Pi)}{Tj - Ti}$$

where Pj is the parameter value for height and diameter at a certain time point, Pi is the value at the preceding time point, and tj and ti is the time, when each measurement was conducted in days. RGR is of particular importance when comparing growth between taxa and over a variety of environmental conditions (Whitehead and Myerscough 1962). The actual height gain was also calculated for each plant by subtracting the baseline height (17 June 2013) from the final height (20 September 2014), as an indicator of competition for light.

The 128 seedlings were harvested on 11 November 2014 by digging out the root system, and separated into foliage, branches, stem, and roots. The root system was gently washed with tap water to remove the soil particles. The samples were oven-dried at 70 °C until constant dry mass and then weighed using a digital balance.

In early September 2014, gas exchange measurements were taken from mature long shoot needles of 122 seedlings. Measurements could not be taken from six seedlings (two hybrid larches and four Japanese larches) whose needles were severely injured by NF60 treatment. Sun-lit mature needles were randomly selected from the upper position of the crown. The gas exchange rates were measured using an open gas exchange system (LI-6400, Li-Cor Inc., Lincoln, USA). The net photosynthetic rate (P_N), transpiration rate (E), and stomatal conductance (g_s) were determined at 380 μmol CO_2 mol^{-1}, 60 ± 5% relative air humidity, and PPFD of 1500 μmol m^{-2} s^{-1}, as it has been previously described (Koike et al. 2012). The leaf temperature was maintained at 25 °C. From the curve of net CO_2 assimilation rate vs. intercellular CO_2 concentration, P_{Nmax}, V_{cmax}, and J_{max} were calculated using an individual leaf photosynthetic model (Farquhar et al. 1980, Long and Bernacchi 2003). The water-use efficiency (WUE) was also calculated as the ratio of PN to E.

After photosynthetic measurements, the measured needles were scanned, and the measured needle area was calculated using the image analysis software ImageJ (U. S. National Institutes of Health, Bethesda, USA, Schneider et al. 2012). The needles used for gas-exchange measurements were collected for further analysis of Chl, C, and N contents. For Chl measurements, dimethyl sulfoxide (DMSO) was used to extract the Chl from the fresh needles (Shinano et al. 1996). Then, the extracts were spectrophotometrically measured (100-50, Hitachi, Japan), and Chl contents were estimated as described by Shinano et al. (1996). For analysis of N and C content, the needles were dried at 70 °C for at least 3 d until constant dry mass and then weighed. Nitrogen and C content in those needles were measured by a NC analyzer (Elementar, VarioEL III, Japan).

Data analysis

For all the response variables, the data were averaged per experimental unit (block), thus, resulting in four values per O_3 treatment (one per OTC) per larch taxon for data analysis. For a better fitting to the Gaussian distribution, the data of each response variable were transformed with a Box-Cox transformation (Box and Cox 1964), as described by Agathokleous et al. (2016). The data of each response variable (except height RGR and diameter RGR) were analyzed by general linear model (GLM) randomized by block, taxa, and O_3 were the predictors.

The height RGR and diameter RGR data were analyzed by repeated GLM models with between-subjects factors the taxa and O_3 and within-subjects factor the time, which was carrying five levels. For significant factors with more than two levels, the single-step multiple comparison test of Tukey's honest significance difference (HSD) was followed. The defined level of significance for all the statistical tests was $\alpha = 0.05$.

Simple linear regression analysis was conducted (n = 32) between pairs of Chl a, Chl b or Chl (a+b) vs. P_{Nmax}, V_{cmax} or J_{max} (taxa and O_3 treatments pooled). The same analysis (n = 16) was also conducted between the whole-plant dry matter and $P_N$max, $V_c$max, and Jmax, respectively, of Japanese larch (O_3 treatments pooled). MS EXCEL 2010 (Microsoft ©) and STATISTICA v. 10 (StatSoft Inc. ©) software were used for data processing and statistics.

RESULTS

Growth and dry matter

NF60 significantly inhibited the RGR of plant height (Table 2-2-1) and stem basal diameter (Table 2-2-2) in both larches independently from time. Independently from taxa and O_3, RGR of height and diameter was increasing up to the second time period, decreasing from the third time period onwards to the fifth time period when it increased again. Taxa and the interaction O_3 × taxa were insignificant, but the interaction taxa ×

time was significant for the RGR of plant height and stem basal diameter. HL had greater height RGR over the first (226%) and second (128%) time periods, but lower over the third time period (45%) than that of JL in 2013; both larches had statistically indifferent height RGR over the fourth and fifth time periods in 2014 (grand means, Table 2-2-1). HL had also greater or lower diameter RGR over the first or third time periods, respectively, than that of JL; HL and JL had statistically indifferent diameter RGR over the second, fourth, and fifth time periods (grand means, Table 2-2-2). The interaction of O_3 × taxa × time was significant for height RGR (Table 1), but insignificant for diameter RGR (Table 2-2-2). In CF and NF40, HL had greater height RGR over the first and second time periods, lower over the third time period and indifferent over the fourth and fifth time periods, compared with JL (Table 2-2-1). In NF and NF60, HL had higher height RGR over the first time period, lower over the third time period, and indifferent over the second, fourth, and fifth time periods, compared to JL.

Plants after NF60 had significantly lower height gain than plants treated by CF, NF, and NF40, independently from taxa (Fig. 2-2-1F). HL had greater plant height than that of JL, independently from O_3 treatment. The interaction O_3 × taxa were insignificant.

Ozone treatments significantly affected the dry matter production of needles, branches, stem, roots, and of total plant (Fig. 2-2-1). HL had significantly lower needle dry matter (Fig. 2-2-1A) and greater stem dry matter (Fig. 1B) than that of JL, but branch (Fig. 2-2-1D), roots (Fig. 2-2-1E), and whole-plant dry matter (Fig. 2-2-1C) were not statistically different. The taxa performance varied significantly among O_3 treatments (O_3 × taxa) in dry matter of needles, branch, stem, and whole plant (Fig. 2-2-1). HL had greater dry matter production of needles, branch, stem, and whole plant in CF treatment. However, HL had lower dry matter of needles than that of JL (Fig. 2-2-1A), but not statistically different dry matter of branch, stem, and whole plant after the NF treatment. HL did not have also statistically different dry matter of needles, branch, stem, and whole plant from JL in NF40 and NF60 treatments (Fig. 2-2-1A–D).

Dry matter of needles, branch, stem, and whole plant were reduced by NF, NF40, and

NF60 treatments in HL, albeit it was not statistically significant for the stem. There was a decrease in the dry matter of needles, branch, stem, and whole plant of JL in NF60 treatment, whereas there was an increase in NF, compared with CF control, which was statistically insignificant.

Table 2-2-1 Time course (mean ± SE) of relative growth rate (RGR) of plant height. Data were Japanese larch and hybrid larch F_1 plants exposed to charcoal-filtered air (CF), nonfiltered air (NF), NF enriched with O_3 to reach 40 nmol mol^{-1} (NF40) or NF enriched with O_3 to reach 60 nmol mol^{-1} (NF60). Different *uppercase letters* above time points or O_3 treatments show statistically significant difference between time points or O_3 treatments (within Time or O_3). Different *uppercase letters* above values of Time grand means of the two larches show statistically significant differences within the interaction taxa × time. Different *lowercase letters* above values show statistically significant differences within the interaction O_3 × taxa × time. Differences are marked according to HSD test. Each single mean is the average of four values, whereas each grand mean is the average of 16 values.

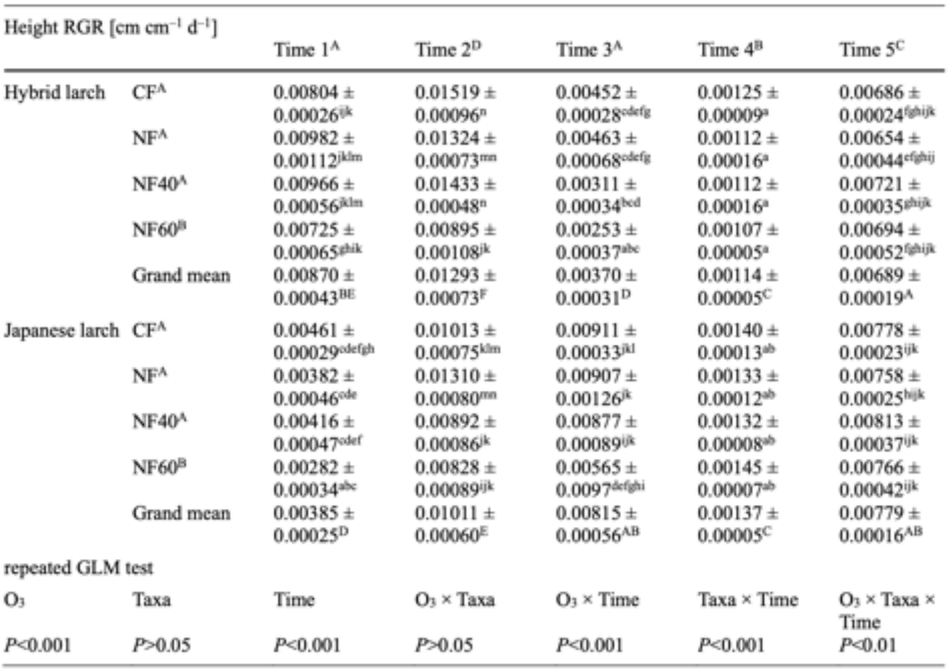

Height RGR [cm cm^{-1} d^{-1}]		Time 1^{A}	Time 2^{D}	Time 3^{A}	Time 4^{B}	Time 5^{C}
Hybrid larch	CF^{A}	0.00804 ± 0.00026^{ijk}	0.01519 ± 0.00096^{n}	0.00452 ± 0.00028^{cdefg}	0.00125 ± 0.00009^{a}	0.00686 ± 0.00024^{fghijk}
	NF^{A}	0.00982 ± 0.00112^{jklm}	0.01324 ± 0.00073^{mn}	0.00463 ± 0.00068^{cdefg}	0.00112 ± 0.00016^{a}	0.00654 ± 0.00044^{efghij}
	NF40^{A}	0.00966 ± 0.00056^{jklm}	0.01433 ± 0.00048^{n}	0.00311 ± 0.00034^{bcd}	0.00112 ± 0.00016^{a}	0.00721 ± 0.00035^{ghijk}
	NF60^{B}	0.00725 ± 0.00065^{ghik}	0.00895 ± 0.00108^{jk}	0.00253 ± 0.00037^{abc}	0.00107 ± 0.00005^{a}	0.00694 ± 0.00052^{fghijk}
	Grand mean	0.00870 ± 0.00043^{BE}	0.01293 ± 0.00073^{F}	0.00370 ± 0.00031^{D}	0.00114 ± 0.00005^{C}	0.00689 ± 0.00019^{A}
Japanese larch	CF^{A}	0.00461 ± 0.00029^{cdefgh}	0.01013 ± 0.00075^{klm}	0.00911 ± 0.00033^{jkl}	0.00140 ± 0.00013^{ab}	0.00778 ± 0.00023^{ijk}
	NF^{A}	0.00382 ± 0.00046^{cde}	0.01310 ± 0.00080^{mn}	0.00907 ± 0.00126^{jk}	0.00133 ± 0.00012^{ab}	0.00758 ± 0.00025^{hijk}
	NF40^{A}	0.00416 ± 0.00047^{cdef}	0.00892 ± 0.00086^{jk}	0.00877 ± 0.00089^{ijk}	0.00132 ± 0.00008^{ab}	0.00813 ± 0.00037^{ijk}
	NF60^{B}	0.00282 ± 0.00034^{abc}	0.00828 ± 0.00089^{ijk}	0.00565 ± 0.0097^{defghi}	0.00145 ± 0.00007^{ab}	0.00766 ± 0.00042^{ijk}
	Grand mean	0.00385 ± 0.00025^{D}	0.01011 ± 0.00060^{E}	0.00815 ± 0.00056^{AB}	0.00137 ± 0.00005^{C}	0.00779 ± 0.00016^{AB}

repeated GLM test

O_3	Taxa	Time	O_3 × Taxa	O_3 × Time	Taxa × Time	O_3 × Taxa × Time
$P<0.001$	$P>0.05$	$P<0.001$	$P>0.05$	$P<0.001$	$P<0.001$	$P<0.01$

Table 2-2-2 Time course (mean ± SE) of RGR of stem basal diameter.

Data were Japanese larch and hybrid larch F_1 plants exposed to charcoal-filtered air (CF), nonfiltered air (NF), NF enriched with O_3 to reach 40 nmol mol^{-1} (NF40) or NF enriched with O_3 to reach 60 nmol mol^{-1} (NF60). Different *uppercase letters* above time points or O_3 treatments show statistically significant difference between time points or O_3 treatments (within Time or O_3). Different *uppercase letters* above values of Time grand means of the two larches show statistically significant differences within the interaction taxa × time. Differences are marked according to HSD test. Each single mean is the average of four values, whereas each grand mean is the average of 16 values.

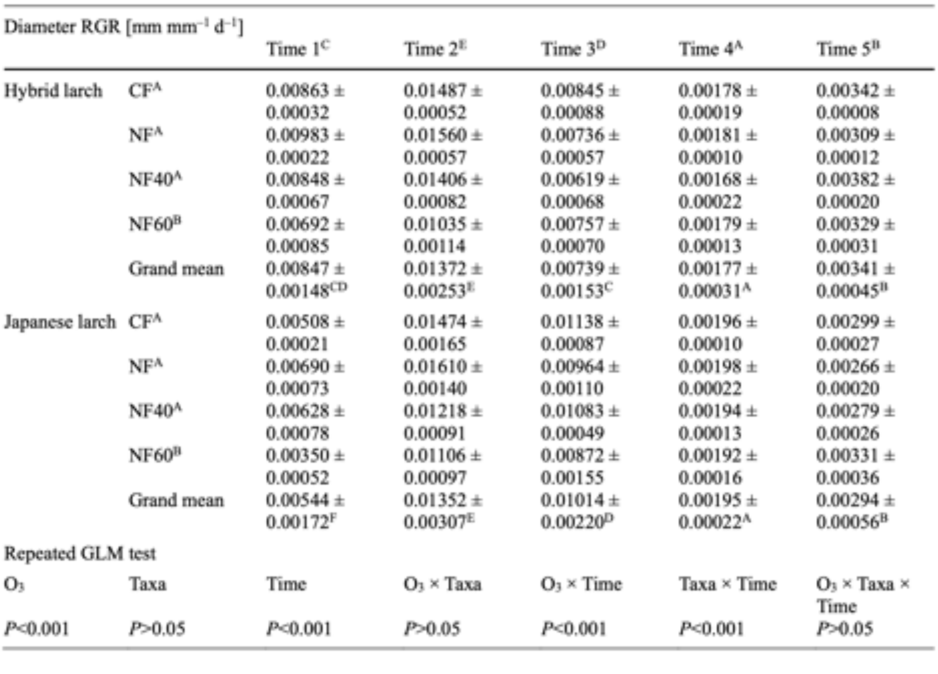

Diameter RGR [mm mm^{-1} d^{-1}]		Time 1^{C}	Time 2^{E}	Time 3^{D}	Time 4^{A}	Time 5^{B}
Hybrid larch	CF^{A}	0.00863 ± 0.00032	0.01487 ± 0.00052	0.00845 ± 0.00088	0.00178 ± 0.00019	0.00342 ± 0.00008
	NF^{A}	0.00983 ± 0.00022	0.01560 ± 0.00057	0.00736 ± 0.00057	0.00181 ± 0.00010	0.00309 ± 0.00012
	NF40^{A}	0.00848 ± 0.00067	0.01406 ± 0.00082	0.00619 ± 0.00068	0.00168 ± 0.00022	0.00382 ± 0.00020
	NF60^{B}	0.00692 ± 0.00085	0.01035 ± 0.00114	0.00757 ± 0.00070	0.00179 ± 0.00013	0.00329 ± 0.00031
	Grand mean	0.00847 ± 0.00148^{CD}	0.01372 ± 0.00253^{E}	0.00739 ± 0.00153^{C}	0.00177 ± 0.00031^{A}	0.00341 ± 0.00045^{B}
Japanese larch	CF^{A}	0.00508 ± 0.00021	0.01474 ± 0.00165	0.01138 ± 0.00087	0.00196 ± 0.00010	0.00299 ± 0.00027
	NF^{A}	0.00690 ± 0.00073	0.01610 ± 0.00140	0.00964 ± 0.00110	0.00198 ± 0.00022	0.00266 ± 0.00020
	NF40^{A}	0.00628 ± 0.00078	0.01218 ± 0.00091	0.01083 ± 0.00049	0.00194 ± 0.00013	0.00279 ± 0.00026
	NF60^{B}	0.00350 ± 0.00052	0.01106 ± 0.00097	0.00872 ± 0.00155	0.00192 ± 0.00016	0.00331 ± 0.00036
	Grand mean	0.00544 ± 0.00172^{F}	0.01352 ± 0.00307^{E}	0.01014 ± 0.00220^{D}	0.00195 ± 0.00022^{A}	0.00294 ± 0.00056^{B}
Repeated GLM test						
O_3	Taxa	Time	O_3 × Taxa	O_3 × Time	Taxa × Time	O_3 × Taxa × Time
$P<0.001$	$P>0.05$	$P<0.001$	$P>0.05$	$P<0.001$	$P<0.001$	$P>0.05$

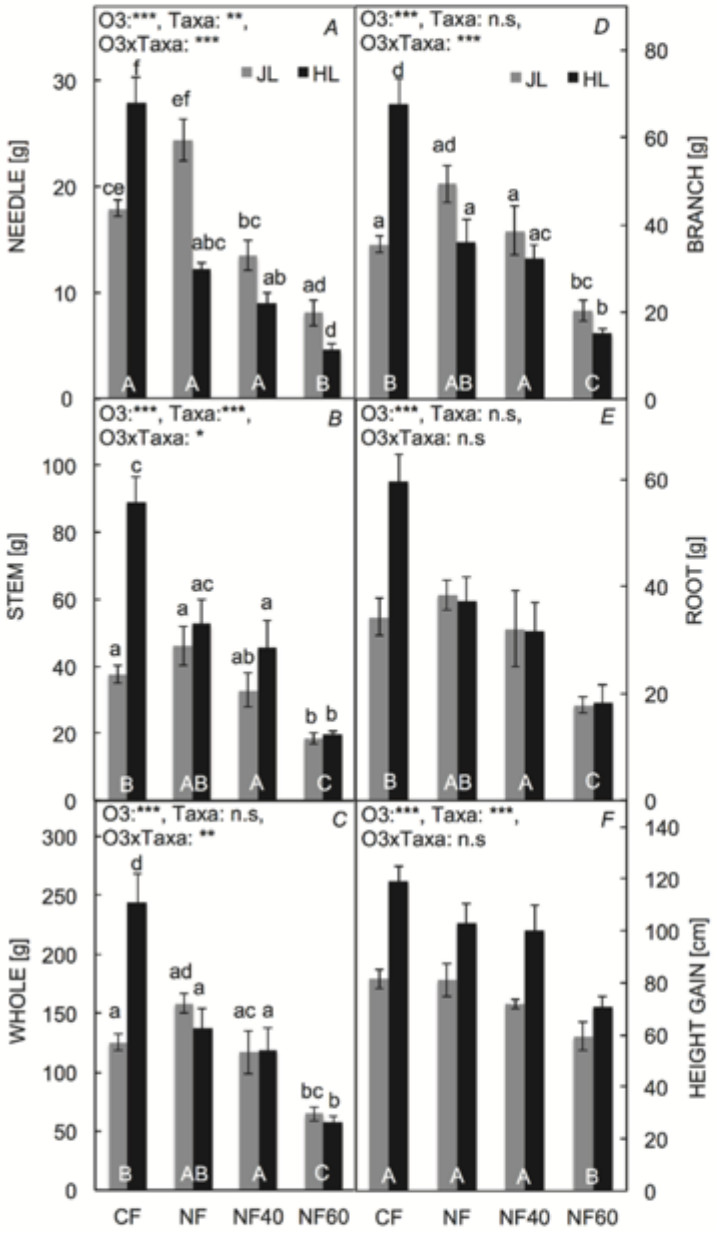

Fig. 2-2-1 Responses of dry mass at a whole plant level to elevated O_3.

Mean values ± SE ($n = 4$) of dry matters and height gain of Japanese larch (JL) and hybrid larch F_1 (HL) exposed to charcoal-filtered air (CF), nonfiltered air (NF), NF enriched with O_3 to reach 40 nmol mol^{-1} (NF40) or NF enriched with O_3 to reach 60 nmol mol^{-1} (NF60). Asterisks indicate GLM significant effects at $P<0.05$ (*), $P<0.01$ (**), and $P<0.001$ (***), whereas "n.s" indicates insignificant GLM effects ($P>0.05$). Different *uppercase letters* A, B, and C show statistically significant differences between the O_3

treatments (taxa pooled). Different *lowercase letters* above the means show statistically significant differences within the interaction O_3 × taxa. Differences are marked according to HSD test.

Leaf gas-exchange

Ozone was significant predictor in all gas-exchange parameters (P_N, g_s, E, V_{cmax}, J_{max}, and P_{Nmax}) for both HL and JL (Fig. 2-2-2). The NF treatment did not statistically differ from CF treatment in P_N, gs, and E (Fig. 2-2-2A, B, D); however, the NF treatment resulted in greater V_{cmax}, J_{max}, and P_{Nmax} (Fig. 2-2-2C, E, F), compared with CF, for both HL and JL. The NF40 treatment suppressed P_N and g_s, but not E, V_{cmax}, J_{max}, and P_{Nmax}, compared with CF. Similarly, the NF60 treatment suppressed all the gas- exchange parameters except J_{max} (Fig. 2-2-2C), compared with CF.

HL showed lower P_N, gs, and E than that of JL (Fig. 2-2-2A, B, D); V_{cmax}, J_{max}, and P_{Nmax} did not significantly differ between taxa (Fig. 2-2-2C, E, F). The interaction of O_3 × taxa was significant for P_N, g_s, and E, while insignificant for V_{cmax}, J_{max}, and P_{Nmax}. Regarding P_N, the only significant difference between larches within each O_3 condition was a greater mean of JL than HL in NF60 (Fig. 2-2-2A). However, while HL had not statistically different g_s between O_3 treatments, JL showed lower g_s in NF40 and NF60 compared with CF (Fig. 2-2-2D). Similarly, NF, NF40, and NF60 treatments did not significantly alter E of HL compared with CF, but NF40 and NF60 suppressed E of JL (Fig. 2-2-2B). WUE did not differ between taxa or between O_3 treatments, and the interaction O_3 × taxa were also insignificant (Fig. 2-2-3D). Regression analysis revealed a significant linear correlation, across all the treatments, of the whole-plant dry matter with P_{Nmax} ($R^2 = 0.608$), V_{cmax} ($R^2 = 0.727$), and J_{max} ($R^2 = 0.706$), respectively, in JL.

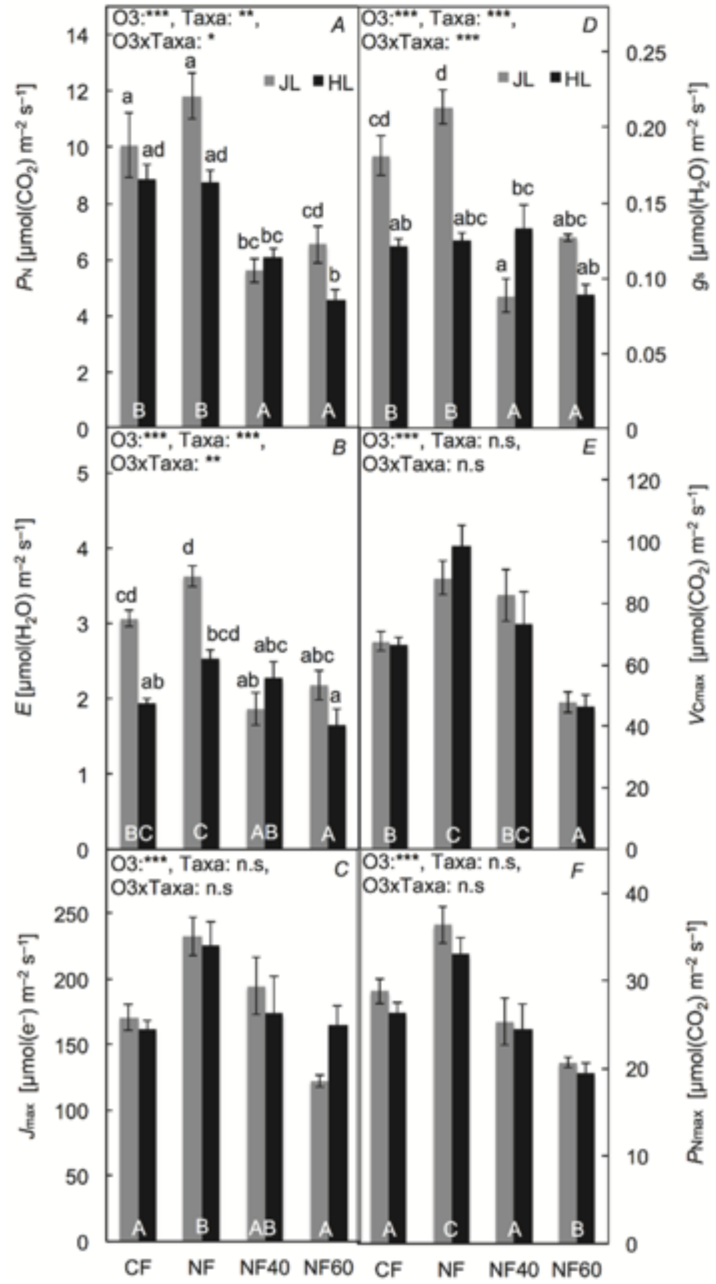

Fig. 2-2-2 Responses of photosynthetic parameters to elevated O_3.

Mean values ± SE (*n* = 4) of gas-exchange parameters of JL and HL exposed to charcoal-filtered air (CF), nonfiltered air (NF), NF enriched with O_3 to reach 40 nmol mol^{-1} (NF40) or NF enriched with O_3 to reach 60 nmol mol^{-1} (NF60).

Leaf Chl and nutrients

Ozone was significant predictor in all the contents [N, Chl a, Chl b, and Chl (a+b)], except C (Fig. 2-2-3). In comparison with CF, reductions were observed in the N content at NF40 and NF60 (Fig. 2-2-3A) and in the contents of Chl a, Chl b, and Chl (a+b) at NF60 (Fig. 2-2-3C, E, F). HL had greater contents of C, Chl a, Chl b, and Chl (a+b) than that of JL, whereas the N content did not differ between larches (Fig. 2-2-3A). The interaction O_3 × taxa were significant only in the N content, which it was reduced by NF60 in HL and by NF40 and NF60 in JL, compared with CF.

However, HL had 30% more Chl (a+b) in NF and NF40 than that in CF, and thus statistically insignificant; JL did not appear to have such a difference between CF and NF or NF40 (Fig. 2-2-3F). Chl contents could effectively predict scores ($P < 0.05$) on P_{Nmax}, J_{max}, and V_{cmax} (Table 2-2-3). Chl a had a large correlation magnitude with P_{Nmax} and a very large correlation magnitude with J_{max} and V_{cmax}. Chl b and Chl (a+b) always had a large correlation magnitude with P_{Nmax}, J_{max}, and V_{cmax}.

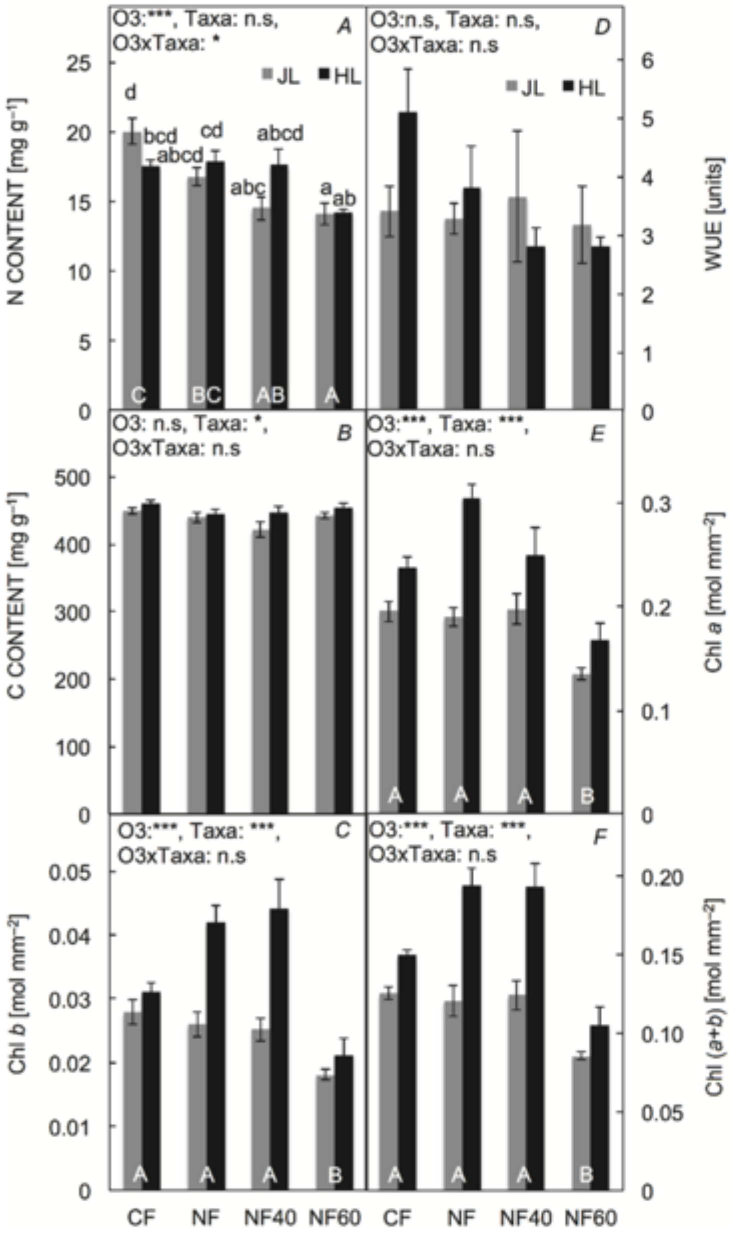

Fig. 2-2-3 Responses of leaf chlorophyll, N, and C contents to elevated O_3.

Mean values ± SE ($n = 4$) of nitrogen (N), carbon (C), chlorophyll (Chl) *a*, Chl *b*, and Chl (*a*+*b*) contents and water-use efficiency (WUE) of JL and HL exposed to charcoal-filtered air (CF), nonfiltered air (NF), NF enriched with O_3 to reach 40 nmol mol^{-1} (NF40) or NF enriched with O_3 to reach 60 nmol mol^{-1} (NF60).

DISCUSSION

Hormesis was clearly observed in P_{Nmax}, J_{max}, and V_{cmax}, and the quantitative characteristics of hormesis were similar for both larches. Hormesis may occur after a direct O_3-induced stimulation or through overcompensation after an O_3-induced disruption in homeostasis (Calabrese 2014, 2015; Agathokleous 2018b). Plant stress in NF, as pictured by P P_{Nmax}, J_{max}, and V_{cmax}, indicates disruption in the homeostasis, an unstable equilibrium in the physiological functioning (Agathokleous 2017, 2018b).

Growth of Japanese larch and its hybrid was inhibited at NF60 but not at NF40 and NF. In NF60, O_3 stress was high enough to inhibit the competitive capacity of HL to the point that plant height was similar between HL and JL, consequently creating a similar light environment for both larches. Previous experiments also revealed a growth inhibition of both larches at approximately 60 nmol mol^{-1} (Dong-Gyu et al. 2015, Agathokleous et al. 2017). The sensitivity of *Larix* spp. to elevated O_3 has been widely shown (Yamaguchi et al. 2011, Koike et al. 2012; Agathokleous et al. 2017). This sensitivity may relate to leaf habit as deciduous trees are considered to have higher O_3 sensitivity than evergreen trees (Paoletti 2006, Calatayud et al. 2010). Both larches shared a similar response to O_3 as shown by plant height and stem basal diameter, in agreement with earlier findings in a free air O_3-enrichment system (Agathokleous et al. 2017). However, greater initial height RGR of HL indicated higher competitiveness for light resources over the JL. This superiority of HL in height RGR lasted until autumn of the first growing season. In contrast to stem growth, height growth is one of the desirable characteristics of this hybrid, which outperforms Japanese larch (Kurinobu 2005). Insignificant interaction of O_3 × taxa in height RGR and height gain suggests that HL had an overall greater height than JL, indicating sustained heterosis and competitiveness of HL across O_3 treatments, as shown before (Agathokleous et al. 2017). Overall, the results of height RGR and height gain suggest that HL had a faster initial growth which contributed in the continuous superiority in height over JL.

HL outperformed JL in dry matter production at CF. HL had 149% greater WUE than that of JL in CF, albeit the difference was statistically insignificant, which may explain the dry matter superiority of HL in CF. Despite the superiority of HL to JL in height gain, HL appeared to have greater O_3-induced reductions in dry matter than that of JL. HL had greater Chl contents than that of JL across O_3 treatments, likely because of greater amount of light reaching the foliage, as HL grew taller than JL. Needle dry matter of JL was greater than that of HL in NF, but not in NF40 treatment. There are two potential explanations for the greater needle dry matter in JL compared to HL in NF: (1) accelerated leaf senescence in HL due to O_3 stress, a typical result of damaged Rubisco (Pell et al. 1994, Yendrek et al. 2013, Kitao et al. 2016); and (2) a difference in the period and timing of needle senescence and in the needle structure between the larches: needles usually fall faster in *L. gmelinii* than in *L. kaempferi* (e.g., Ryu et al. 2009).

Photosynthesis was not limited by stomatal closure in NF, showing no activation of an O_3-avoidance mechanism. Rubisco activity was, nonetheless, up-regulated by NF as indicated by an increase in P_{Nmax}, J_{max}, and V_{cmax} in both taxa. This up-regulation in P_{Nmax} ($R^2 = 0.126$), V_{cmax} ($R^2 = 0.178$), and J_{max} ($R^2 = 0.026$) was not related to the measured N content in needles. It was, however, related to the Chl contents and, especially Chl a content, which was more effective than Chl b and Chl (a+b) in predicting the outcome of P_{Nmax}, J_{max}, and V_{cmax}. The up-regulation in P_{Nmax}, J_{max}, and V_{cmax} may suggest better performance of Rubisco, which is responsible for converting atmospheric CO_2. To our knowledge, this was the first evidence for up-regulation of physiological performance in Rubisco by low O_3 mixing ratios. The effects may also relate to the antioxidant activity, which affects the photosynthetic apparatus (Flowers et al. 2007). The inhibition of J_{max} and V_{cmax} were observed at NF60 in both larches, which might result in the decreased N content in NF60 compared to CF. The O_3 effects on photosynthetic reactions are defined by the amount of absorbed O_3 dose (Paoletti and Manning 2007).

The greater g_s in JL than that in HL in NF may suggest higher O_3 intake dose in JL. Hence, it can be postulated that the HL showed similar stress as JL, even if the O_3 intake dose in HL was lower than that in JL. Stress under NF seemed to lead to suppressed biomass productivity in HL but not in JL, a phenomenon, which was not upon a higher O_3 intake dose in HL than in JL. Although statistically insignificant, the greater plant dry matter of JL at NF (+126%), compared to CF, agreed with greater P_{Nmax} (+126%), V_{cmax} (+130%), and J_{max} (+136%). This was supported by the regression analysis, which showed that responses of whole-plant dry matter were associated with responses of P_{Nmax}, J_{max}, and V_{cmax}. Long-term experiments may be needed to depict the consequences of hormesis in productivity, because trees usually possess relatively high plasticity (e.g., Küppers 1989).

Stimulation in gas-exchange traits by NF did not affect biomass at the whole plant level in JL. These observations suggest that stimulation of physiological functions, which occurs below the no observed adverse effect level in hormetic exposure-response relationships, do not necessarily lead to benefits to the productivity at whole-plant level. Despite the physiological O_3-induced stimulation, it seems that HL could not sustain its productivity through plastic response to low O_3 exposures whereas JL could do so. It should be mentioned that potential failure of plants to re-establish the disruption in the homeostasis in the appropriate time period could cause severe injuries. With reference to the C-S-R diagram of plant strategies (Grime 1977), when the larches were grown under low-exposure stress (i.e. NF), HL seems to have a competitive strategy in this productive and relatively undisturbed vegetation, whereas JL seems to show a stress-tolerant strategy. The allocation of resources towards competitive capacity in HL along with the O_3 stress led to restricted productivity (i.e., less dry matter) in NF. In contrast, JL maintained the productivity in NF through stress-tolerant strategy. Such findings have been also reported by Liancourt et al. (2005) where the species competitive capacity was inverse to stress tolerance, via a trade-off between them.

Chapter 3

Chapter 3-1: Effects of N loading on O_3 sensitivity of Japanese larch and hybrid larch F_1

INTRODUCTION

Larch (*Larix* sp.) species are widely distributed in Northeast Asia and have been planted for timber production and ecosystem rehabilitation (Abaimov et al. 2000; Zhang et al. 2000). In addition to the native Japanese larch (*Larix kaempferi*), a hybrid larch F_1 (*L. gmelinii* var. *japonica* x *L. kaempferi*), which is more tolerant to stress and exhibits higher photosynthetic performance, has also been developed (Kita et al. 2009). However, increasing concentrations of ground-level ozone (O_3) (Akimoto 2017) and nitrogen (N) deposition (Galloway et al. 2004; Liu et al. 2013; Yamaguchi et al. 2014) are raising concern, particularly in Northeast Asian forests (Yamaji et al. 2008, Koike et al. 2013). Concentrations of such air pollutants are projected to continue increasing in future (Nagashima et al. 2010, Ainsworth et al. 2012, Izuta 2017). Therefore, there is a need to evaluate the responses of the *Larix* spp. to elevated O_3 and N deposition (Ryu et al. 2009, Koike et al. 2012).

Ozone is a toxic pollutant that inhibits numerous physiological functions such as photosynthesis and it eventually causes a decrease in growth, particularly belowground growth (Li et al. 2016, Shi et al. 2016, Wang et al. 2016, Agathokleous et al. 2016, Sugai et al. 2018). Conversely, N loading may promote the growth of trees when soil N limits growth, such as in a boreal forest (Vitousek et al. 2002). However, excess N loading could also have negative effects on tree growth (Aber et al. 1989, Ryu et al. 2009, Wang et al. 2018). Although numerous studies have reported the combined effects of elevated O_3 and N deposition, they have primarily concluded that N loading might not affect or increase the sensitivity of woody species to O_3 (e.g., Nakaji and Izuta 2001, Yamaguchi et al. 2011, Izuta et al. 2017). Regarding larch species, contrary to previous reports, Watanabe et al. (2006) reported that N loading could mitigate the negative impacts of O_3 on Japanese larch seedlings. However, a recent study reported that N loading could not mitigate the negative impacts of O_3 on hybrid larch F_1 (Dong-Gyu et al. 2015). Consequently, researchers' views regarding the combined effects of N loading and O_3 on larch species are inconsistent. In addition, the physiological mechanisms of the effects on combined N loading and O_3 deposition remain still unclear (e.g., Mills et al. 2016, Izuta 2017).

The effects of N loading vary depending on the phosphorus (P) conditions in plants (e.g., Güsewell 2004, Elser et al. 2010). For instance, N loading promoted the growth of hybrid larch F_1 under high P conditions (Fujita et al. 2018). Indeed, the leaf N/P ratio could be a critical indicator of N or P limitation (Güsewell 2004) since N loading increases the N/P ratio in plants (e.g., Reich and Oleksyn 2004, Güsewell 2004, Elser et al. 2010). Conversely, one of the effects of O_3 is accelerated leaf senescence, resulting in imbalances in leaf nutrients (Uddling et al. 2006, Shi et al. 2016, Shi et al. 2017). However, few studies have reported leaf N and P reductions in larch species under elevated O_3 (Koike et al. 2012, Wang et al. 2015). The relationship between leaf N/P ratio and physiological activities under elevated O_3 and/or N loading remains relatively poorly understood (Beyears et al. 1992, Kainulainen et al. 2000, Utriainen and Holopainen 2001, Waillin et al. 2002, Wang et al. 2015). Considering that the senescence effect of O3 does not induce reductions in leaf P concentrations (Wang et al. 2015), a positive effect of N loading on hybrid larch F_1 and lower leaf N/P ratio may be observed (Fujita et al. 2018). Here, I expected that leaf N/P ratio could be a useful indicator of N and P limitation in the larches and facilitate comparison of their responses to N loading under elevated O_3.

The aim of the present study is to investigate the effect of N loading on the responses of Japanese larch and hybrid larch F_1 seedlings to O_3. The present hypothesis is N loading could mitigate the negative impacts of O_3 on larch seedlings. To assess the hypothesis, I investigated the relationship between physiological and nutritional responses based on correlation tests.

MATERIAL AND METHODS

Experimental design

This experiment was conducted at Sapporo Experimental Forest, Hokkaido University, Japan (43°04'N, 141°20'E; 15 m above sea level). Weather data from 2015 to 2016 were recorded at a meteorological station in Sapporo (Japan Meteorological Agency, 2016). The monthly average values of metrological data from May 2015 to September 2016 were: mean monthly average air temperature: 12.31°C; maximum temperature: 23.53°C; minimum temperature: 3.41°C; total precipitation: 106.8 mm; and total sunshine duration: 162.1 h, respectively. Japanese larch (*Larix kaempferi*) is tolerant to harsh conditions such as low temperature and infertile soils although it is sensitive to grazing damage from red-backed voles. To overcome such limitations, hybrid larch F_1 (*L. gmelinii* var. *japonica* x *L. kaempferi*) was developed (Kita et al. 2009). These two species of larch seedlings were grown for one year from seeds at a nursery at Hokkaido Research Organization, Forestry Research Institute, Bibai. On May 12, 2015, all larch seedlings were transplanted to 7 L pots before leaf formation. The initial stem diameter and height were 2.21 ± 0.44 mm (mean ± se) and 16.56 ± 2.93 cm, respectively, for Japanese larch, and 2.45 ± 0.17 mm and 20.44 ± 1.39 cm, respectively, for hybrid larch F_1. Soil in the pots was chosen so as to mimic immature volcanic ash soil (Kanuma soil and Akadama soil, volume ratio 1:1). To prevent soil desiccation and nutrient imbalances, I applied 100 mL of commercial liquid fertilizer (HYPONEX; Japan, N = 72.4 mg l^{-1}, P = 284 mg l^{-1}, K = 94.2 mg l^{-1}) as a basal dressing after complete rooting. There, all pots initially received 5.5 kgN $ha^{-1}yr^{-1}$.

N loading treatments were applied at two-week-intervals using $(NH_4)_2SO_4$ dissolved in 500 ml tap water to simulate recent N deposition such as $PM_{2.5}$ (Particulate matter less than 2.5 μm in aerodynamic diameter; Hatakeyama 2011). N loading was set to 50 kg N ha^{-1} yr^{-1}, which are the estimated levels in 2050 (Galloway et al. 2004, Liu et al. 2013). The N amount included the initial liquid fertilization. N loading was performed on June

19, July 15, August 5 and 17 in 2015, and June 27, July 22, and August 1 and 17 in 2016, while avoiding rain days. To avoid drought conditions, control seedlings that were not N treated were irrigated with 500 ml tap water over a period similar to that of N loading. For pH and inorganic N concentration measurements, surface soil (<5 cm) was sampled from each pot on 29 August 2016.

To expose seedlings to ambient or elevated O_3, open-top cambers (OTCs; 1.2 x 1.2 x 1.2 m) framed using steel were used following complete rooting. A polyvinyl chloride film (Noh-bi Co Ltd., Sapporo, Japan), which transmits 88% sunlight (blocking only UV-B and UV-C), was used to cover the OTCs. Two O_3 concentration treatments were applied. The first consisted of a non-filtered air treatment representing low O_3 concentration, which occurs at ambient conditions, while the second was a non-filtered O_3-enriched air treatment. The target of the enriched O_3 concentration was 60 nmol mol^{-1}, which is the value for the environmental standard for photochemical oxidants in Japan (Japanese Ministry of the Environment 1996). The enriched O_3 concentration target was also set to assume predicted future O_3 concentrations in Asian countries (Yamaji et al. 2008, Ainsworth et al. 2012). O_3 treatments were carried out from June 19, 2015 to September 18, 2015 and from May 18, 2016 until August 29, 2016. O_3 was supplied using air pumps (APN-110K, IWAKI, Japan) from an electrical discharge O_3 generator (PZ-1B, Kofloc-Kojima, Japan) into the OTCs only during daylight hours (06:00–18:00, JST). Ambient air inside the OTCs was constantly driven to the atmosphere using over 24 hours and wind speeds at the openings to the surfaces of the OTCs were set to 0.1 m^3 per second. During the exposure periods, O_3 concentrations were continuously monitored (1-minute interval) with UV absorption O_3 analyzer (Model 202-EPA, 2B Technologies, CO, USA) and an O_3 monitoring system (EG-3000F, Ebara, Japan). An algorithm of proportional integrative differential system was applied to maintain the target O_3 concentrations. Table 3-1-1 presents the achieved O_3 concentration values and the value of accumulated exposure over the threshold of 40 nmol mol^{-1} (AOT40). During the non-exposure periods, O_3 generators were switched off and all the seedlings were maintained in the chamber except for the heavy snow seasons. The monitored O_3 concentrations and AOT40 in each treatment were summarized in Table 3-1-1.

Table 3-1-1 The mean value (standard error; SE, n = 4) of ozone concentration (nmol O_3 mol^{-1}) and AOT40 (mmol O_3 mol^{-1} h) in each month of the years 2015 and 2016.

		Ozone concentration				AOT 40			
Year	Month	Control	Elevated O_3 (O_3)	N loading (N)	O_3 x N	Control	O_3	N	O_3 x N
2015	July	29.1 ± 1.6	60.9 ± 1.4	25.6 ± 1.4	60.8 ± 1.4	1.00	6.89	0.92	6.88
	August	30.9 ± 1.3	64.1 ± 1.4	27.2 ± 1.2	64 ± 1.4	1.01	7.26	0.89	7.24
	September	35.1 ± 1.7	59.6 ± 2.2	30.9 ± 1.5	59.6 ± 2.1	1.14	6.75	1.01	6.74
2016	June	33.6 ± 1.5	64.3 ± 2.3	32.9 ± 1.4	64.2 ± 2.3	1.10	7.28	1.07	7.27
	July	27.4 ± 1.8	62.3 ± 1.7	26.9 ± 1.7	63.2 ± 1.6	0.89	7.05	0.88	7.16
	August	28.9 ± 1.5	61.2 ± 1.9	28.3 ± 1.5	61.1 ± 1.9	0.94	6.92	0.92	6.92

In total, there were 4 treatment: tap water + ambient O_3 (Control); tap water + elevated O_3 (O_3); N loading + ambient O_3 (N); and elevated O_3 x N loading (O_3 x N). All the treatments had four replicates, yielding 16 OTCs. OTC positions were set based on a completely randomized split-plot design. Four larch seedlings of each species were set in each chamber (64 seedlings of each species, 128 seedlings in total). All the seedlings were utilized throughout the experiments and the positions of seedlings within each OTC were regularly changed to prevent biased edge effects.

Leaf gas-exchange measurements

Gas-exchange measurements were conducted for all the seedlings in all the treatments between the 17 and 21 August 2016. An open gas-exchange system (LI-6400, Li-Cor Inc., Lincoln, NE, U.S.A.) was used to measure the gas-exchange parameters. For each seedling, approximately six fresh mature needles were selected from the non-shaded position of a branch and attached to the leaf clip chamber of a LI-6400. Measurements were conducted between 05:00 and 15:00, JST, and the leaf temperature was maintained at 25 ± 2 °C. The water vapor deficit in the leaf chamber was approximately 1.2 ± 0.3 kPa and the photosynthetic photon flux was approximately 1500 μmol m^{-2} s^{-1}. To plot curves of net CO_2 assimilation rate (A) versus intercellular CO_2 concentration (C_i), i.e., A/C_i curves; A was determined at ten C_i levels (C_a: 60–1600 μmol mol^{-1}). The net photosynthesis rate and stomatal conductance at 380 μmol mol^{-1} C_a (A_{380} and Gs_{380}, respectively) were determined from the A/C_i curves. In addition, using the individual leaf photosynthetic model, the curves were used to calculate the maximum net photosynthetic rate at 1600 µmol mol^{-1} C$_a$ (A_{max}), the maximum rate of carboxylation (V_{cmax}), and the maximum rate of electron transport (J_{max}) (Farquhar et al. 1980, Long and Bernacchi 2003). Values of Rubisco Michael's constants for CO$_2$ (K_c), O$_2$ (K_o) and CO$_2$ compensation points in the absence of dark respiration (Γ^*) were derived following analyses of the *A/Ci* curves as described by Bernacchi et al. (2001). After photosynthetic measurements, the measured needles were scanned and needle areas calculated using Image-J software (U. S. National Institutes of Health, Bethesda, Maryland, USA; Schneider et al. 2012).

Leaf nutrients and photosynthetic parameters

The needles used for gas-exchange measurements were used to conduct further analyses of leaf nitrogen content per mass (N) and leaf mass per area (LMA). The needles were dried at 70℃ for approximately 3 days until they achieved a constant dry mass and then weighed. Nutrient contents per needle area were calculated based on the obtained LMA value. N was measured using an NC analyzer (Elemntar, VarioEL III, Japan). In addition, approximately twenty fresh mature needles were selected on 29 August 2016 from the same non-shaded position as the photosynthetic measurement as much as possible. They were digested with HNO$_3$ and subjected to elemental analysis using inductively coupled plasma mass spectrometry (ELAN, DRC-e; PerkinElmer, Waltham, MA, U.S.A.), based on the method of Sha et al. (2012). Photosynthetic nitrogen-use efficiency (*PNUE*) and photosynthetic phosphorus use efficiency (*PPUE*) were calculated as follows:

$$PNUE\ (\mu molCO_2\ mgN^{-1}s^{-1}) = \frac{A_{380}}{N \times LMA}$$

$$PPUE\ (\mu molCO_2\ mgP^{-1}s^{-1}) = \frac{A_{380}}{P \times LMA}$$

Production and allocation of dry matter

In total, 128 seedlings were harvested on 29 August 2016 and then separated into foliage, branches, stems, and roots. The roots were gently washed with tap water to remove soil particles. The samples were oven-dried at 70°C until they achieved a constant dry mass and then weighed using a digital balance. Top shoot/root ratio (T/R_{ratio}) was calculated as follows:

$$T/R_{ratio}\ (g\ g^{-1}) = \frac{Needle\ + Branch + Stem}{Root}$$

Statistical analyses

The data were averaged per experimental unit (block) resulting in four values per treatment (n = 4). All parameters were analyzed for each species using a general–linear mixed model (GLMM) randomized by blocks. O_3 exposure, N loading treatments, and different species constituted the predictors. For significant interaction factors with more than two levels, the multiple comparison test of Tukey's honestly significant difference (HSD) was used. P = 0.05 was considered statistically significant. R software ver. 3.4.3 was used for data processing and statistics.

RESULTS

Dry mass

Ozone enrichment significantly decreased needle, branch, and stem dry mass in Japanese larch (Fig. 3-1-1, $P < 0.05$) whereas significant reductions attributable to O_3 were not observed in hybrid larch F_1. In Japanese larch, although N loading did not have significant effects, needle dry mass increased whereas stem dry mass slightly decreased due to N loading. However, in hybrid larch F_1, N loading increased needle, branch, and stem dry mass ($P < 0.05$).

Under N loading, O_3 did not decrease any dry mass in Japanese larch (Fig. 3-1-1, $P > 0.05$). O_3 slightly increased branch and stem dry mass in Japanese larch although there were no significant differences. In hybrid larch F_1, O_3 significantly decrease dry mass in under N loading in all the tested parts ($P < 0.05$) except in the branches (Fig. 3-1-1*C*). Notably, the branch dry mass responses to O_3 were contrasting in the two investigated species *Larix* spp. under N loading. Although there were no significant changes (Fig. 3-

1-1*C*), branch dry mass in Japanese larch increased whereas that in hybrid larch F_1 decreased following O_3 enrichment.

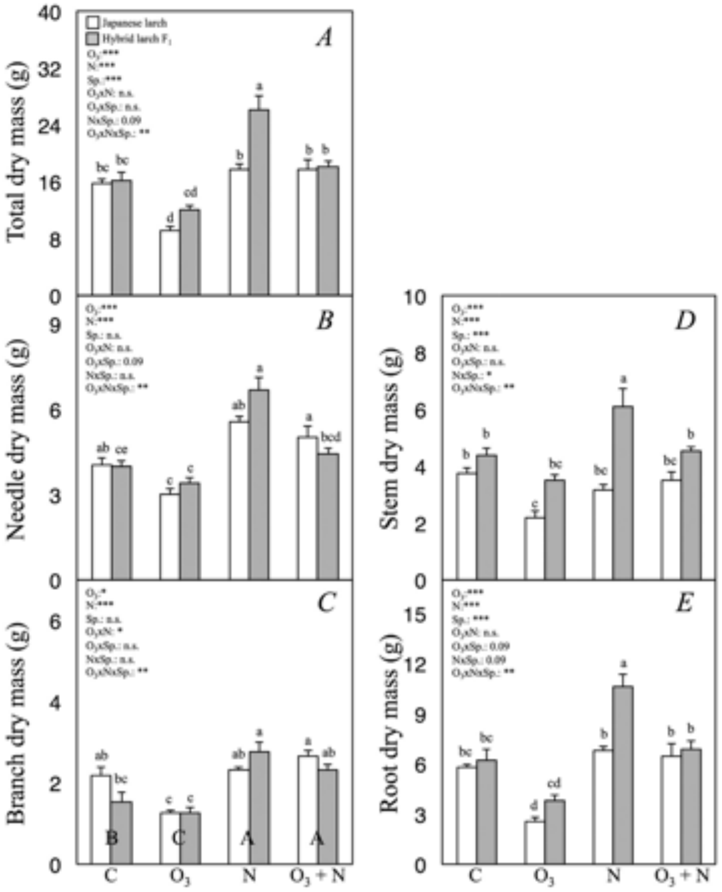

Fig. 3-1-1 Responses of dry mass at a whole plant level to O_3 and N loading.

The total dry mass (g), needle dry mass (g), branch dry mass (g), stem dry mass (g), and root biomass (g) of two larch species (white bar: Japanese larch; gray bar: Hybrid larch F_1) in each treatment (control: C, elevated ozone: O_3, nitrogen loading: N, ozone and nitrogen loading: O_3 + N). Each bar + error bar is the mean value and standard errors. GLMM analysis: ozone (O_3), N loading (N), species difference (Sp.), and these interactions, $^{*}P<0.05$, $^{**}P<0.01$, $^{***}P<0.001$, n.s. denotes non-significant values; Different lower-case letters denote significant differences between species and treatments (Tukey HSD test; P b 0.05), and different capital letters denote significant differences between treatments (species pooled).

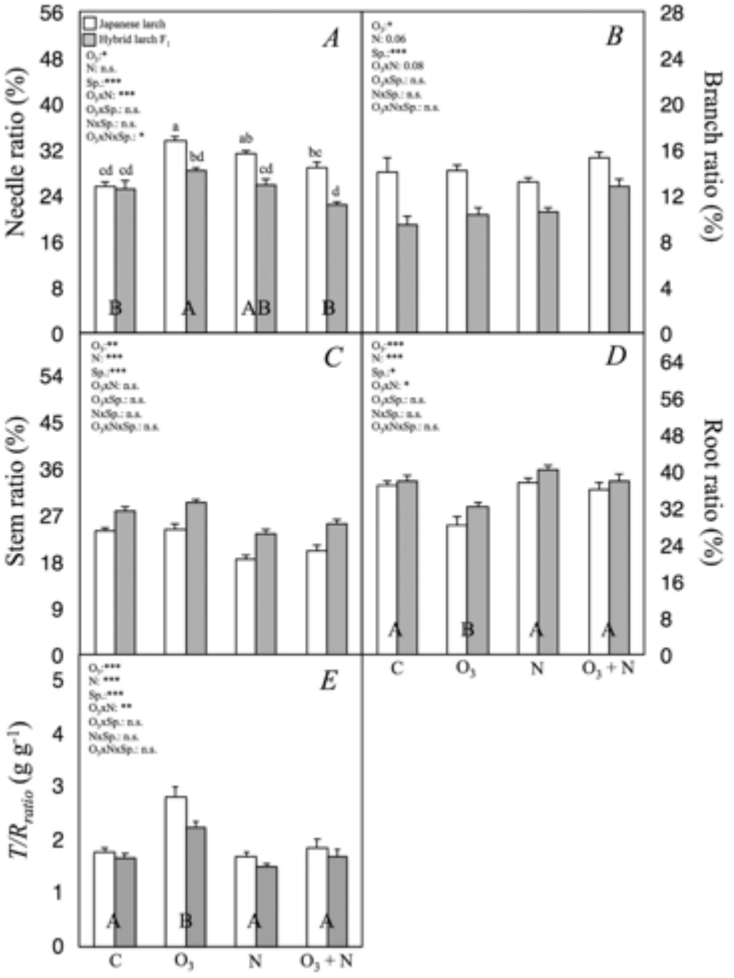

Fig. 3-1-2 Responses of dry mass allocation to O_3 and N loading.

Dry mass allocation (%) to needle, branch, stem, and root and top shoot/root ratio (T/R ratio, g g^{-1}) in two larch species (white bar: Japanese larch; gray bar: Hybrid larch F_1) for each treatment (control: C, elevated ozone: O_3, nitrogen loading: N, ozone and nitrogen loading: O_3 + N).

Dry mass allocation

Ozone decreased root proportions in the two *Larix* spp. whereas it increased the aboveground proportions (Fig. 3-1-2*D, E*). In Japanese larch, O_3 and N loading significantly increased the needle proportions (Fig. 3-1-2*A, D,* $P < 0.05$). Responses of the branches to N loading were contrasting between species although the degree was marginal. The needle proportions under N loading were decreased by O_3 in both *Larix* spp. although these were no significant changes. Regarding the differences between the species, the needle proportions under N loading were significantly higher in Japanese larch than in hybrid larch F_1 (Fig. 3-1-2*A, D,* $P < 0.05$). The differences between the species were maintained under elevated O_3 and N loading.

Photosynthetic activity

Ozone significantly decreased Gs_{380} and A_{max} in Japanese larch (Fig. 3-1-3*B*, *G*; $P < 0.05$). In Japanese larch, N loading did not increase any photosynthetic parameters except A_{380}. However, in hybrid larch F_1, N loading significantly increased A_{max} and J_{max} (Fig. 3-1-3*F, G*; $P < 0.05$). In addition, O_3 did not decrease any parameters except A_{380} in hybrid larch F_1. In both *Larix* spp., O_3 decreased A_{380} under N loading (Fig. 3-1-3*A*, $P < 0.05$). The effects of O_3 on *NUE*, *PUE*, and Vc_{max} were not significant while negative effects on species were observed.

Nutrient conditions of leaves

Table 3-1-2 presents the concentration of each nutrient element per needle mass, the LMA values, and the coefficients of correlation between leaf N and leaf N/P with A_{mass} and needle dry mass. As expected, O_3 did not decrease leaf P in both species. However, N loading significantly increased leaf P in the hybrid larch F_1 (Table 3-1-2). In addition, the O_3 and N loading combined increased nutrient element concentrations in hybrid larch F_1. In addition, leaf N/P under N loading in hybrid larch F_1 was decreased by O_3. Needle dry mass of both *Larix* spp. exhibited significant positive correlations with leaf N and leaf N/P.

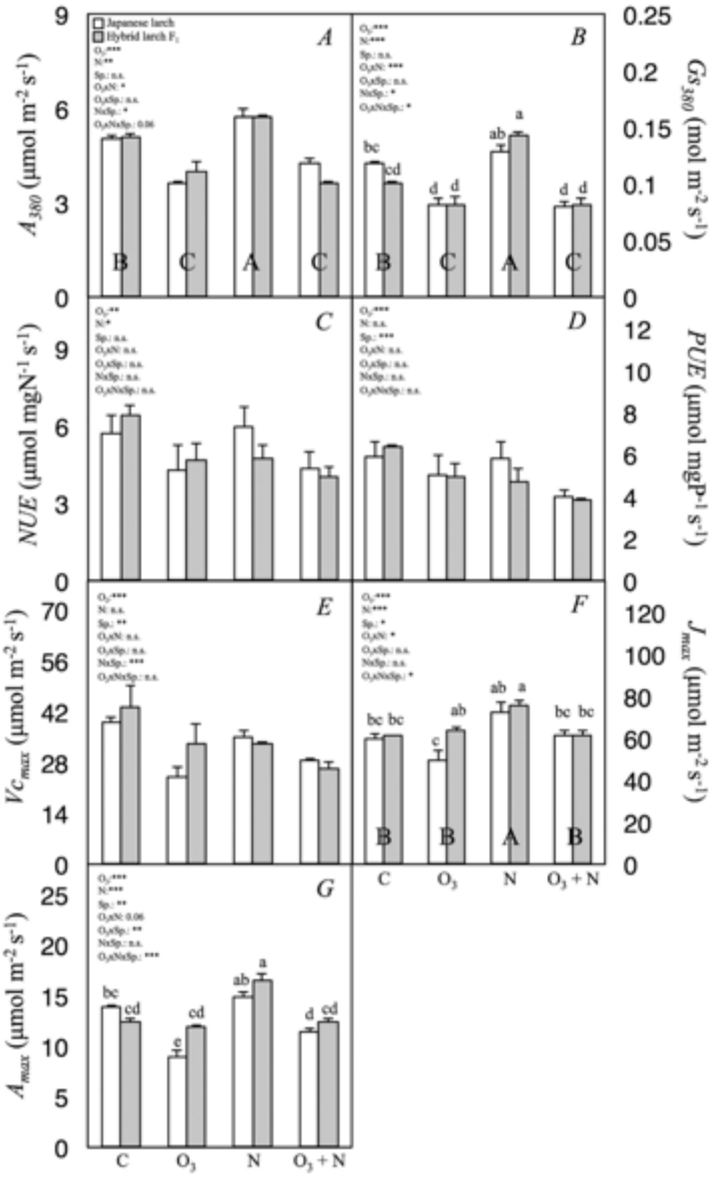

Fig. 3-1-3 Responses of photosynthetic parameters to O_3 and N loading.

The net photosynthesis rate at a CO_2 concentration of 380 ppm (A_{380}, μmol m^{-2} s^{-1}), stomatal conductance (Gs_{380}, mol m^{-2} s^{-1}), photosynthetic nitrogen-use efficiency (NUE, μmol mgN^{-1} s^{-1}), photosynthetic phosphorus use efficiency (PUE, μmol mgP^{-1} s^{-1}), maximum carboxylation rate (V_{cmax}, μmol m^{-2} s^{-1}), maximum electronic transport rate (J_{max}, μmol m^{-2} s^{-1}), and maximum photosynthetic rate (A_{max}, μmol m^{-2} s^{-1}) in two larch species (white bar: Japanese larch; gray bar: Hybrid larch F_1) for each treatment

Table 3-1-2 Summary of needle element responses O_3 and N loading.
concentrations (N, P, mg g^{-1}), N/P and leaf mass per area (LMA, g m^{-2}) in the Japanese larch and hybrid larch F_1 in each treatment (control: control, O_3: elevated ozone, N: nitrogen loading, O_3 + N: ozone and nitrogen loading), n = 4. Data indicate mean values (SE); GLMM analysis: ozone (O_3), N loading (N), species difference (Sp.), and these interactions. $^{*}P < 0.05$, $^{**}P < 0.01$, $^{***}P < 0.001$, n.s. denotes non-significant values; Different letters indicate significant differences (Tukey HSD test). Correlation coefficients between nutrients, photosynthesis, and needle dry mass were calculated using Pearson's correlation test, $^{*}P < 0.05$, $^{**}P < 0.01$, $^{***}P < 0.001$. No sign denotes non-significant values.

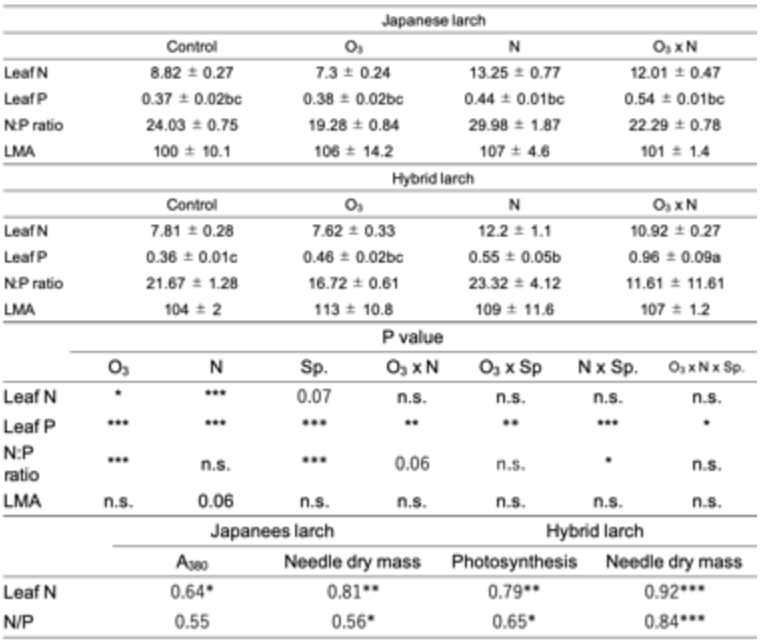

	Japanese larch			
	Control	O_3	N	O_3 x N
Leaf N	8.82 ± 0.27	7.3 ± 0.24	13.25 ± 0.77	12.01 ± 0.47
Leaf P	0.37 ± 0.02bc	0.38 ± 0.02bc	0.44 ± 0.01bc	0.54 ± 0.01bc
N:P ratio	24.03 ± 0.75	19.28 ± 0.84	29.98 ± 1.87	22.29 ± 0.78
LMA	100 ± 10.1	106 ± 14.2	107 ± 4.6	101 ± 1.4

	Hybrid larch			
	Control	O_3	N	O_3 x N
Leaf N	7.81 ± 0.28	7.62 ± 0.33	12.2 ± 1.1	10.92 ± 0.27
Leaf P	0.36 ± 0.01c	0.46 ± 0.02bc	0.55 ± 0.05b	0.96 ± 0.09a
N:P ratio	21.67 ± 1.28	16.72 ± 0.61	23.32 ± 4.12	11.61 ± 11.61
LMA	104 ± 2	113 ± 10.8	109 ± 11.6	107 ± 1.2

	P value						
	O_3	N	Sp.	O_3 x N	O_3 x Sp	N x Sp.	O_3 x N x Sp.
Leaf N	*	***	0.07	n.s.	n.s.	n.s.	n.s.
Leaf P	***	***	***	**	**	***	*
N:P ratio	***	n.s.	***	0.06	n.s.	*	n.s.
LMA	n.s.	0.06	n.s.	n.s.	n.s.	n.s.	n.s.

	Japanees larch		Hybrid larch	
	A_{380}	Needle dry mass	Photosynthesis	Needle dry mass
Leaf N	0.64*	0.81**	0.79**	0.92***
N/P	0.55	0.56*	0.65*	0.84***

DISCUSSION

Growth responses to the combined effect of O_3 and N loading varied between Japanese larch and hybrid larch F_1. O_3 enrichment did not result in a significant reduction in any dry mass in Japanese larch under N loading. The same type of response was also observed in the previous study (Watanabe et al. 2006; Dong-Gyu et al. 2015). Watanabe et al.

(2006) suggested that reducing O_3 sensitivity in Japanese larch with N loading was not related to the amount of O_3 absorbed through the stomata. In the present study, I observed no significant combined effect on Gs_{380} in Japanese larch, although O_3 decreased Gs_{380}. Such a stomatal response suggested that N loading did not alter the amount of O_3 absorbed, which is consistent with some previous findings (Watanabe et al. 2006).

In contrast, O_3 significantly reduced the total dry mass of hybrid larch F_1 under N loading. I observed a reduction in photosynthetic parameters following O_3 enrichment under N loading, as well as dry mass (Fig. 3-1-3). The results are consistent with those of a previous study that reported that NH_4NO_3 loading may not mitigate the negative impacts of O_3 on hybrid larch F_1 (Dong-Gyu et al. 2015). The results suggest that the responses to the combined effects of O_3 and N loading in the two *Larix* spp. are clone-specific. In addition, the results reinforce the argument that N loading could intensify the negative effects of O_3 on hybrid larch F_1 to some extent. Previous studies have suggested that excess N loading could simulate detoxification and repair activities against O_3 stress (Watanabe et al. 2006, Izuta 2017). However, Yamaguchi et al. (2010) reported that N loading did not change anti-oxidant capacities activated by O_3 such as acidic amino acids. As described, the mechanisms of changes in O_3 sensitivity attributable to N loading remain unclear (e.g., Mills et al. 2016). Hereafter, I discuss the contrasting responses in two *Larix* spp. to consider the potential mechanisms.

Hybrid larch F_1 could be affected more by the combined effects of O_3 and N loading (Fig. 3-1-1) potentially due to its higher growth response to N loading. This hypothesis could be supported by several previous studies (Pell et al. 1995, Matyssek et al. 1997, Maurer et al. 1997, Yamaguchi et al. 2010, Kinose et al. 2017). The seasonal responses of photosynthesis rates in Siebold's beech (*Fagus crenata*) were significantly decreased by O_3 only when the levels of liquid fertilizer were relatively high (Kinose et al. 2017). In European white birth clone (*Betula pendula*) seedlings, macro- and micro nutrient supply did not mitigate the negative impacts of O_3 (Maurer et al. 1997). Conversely, the degree of physiological inhibition by O_3 was significantly increased by nutrient supply.

In addition, total dry mass in *Fagus crenata* seedlings decreased due the combined effect of N loading and elevated O_3 because of a higher growth response to NH_4NO_3 loading (Yamaguchi et al. 2007). Pell et al. (1995) also reported that the negative effect of O_3 on *Populus tremuloides* increased with increase in N supply. Based on such reports, I postulate that the responses to O_3 could be more significant when plants have higher sensitivity to N loading. In addition, I should consider the degree of change in response to O_3 and sensitivity to N loading by comparing the contrasting responses in the larch species. In the next section, I focus on role of the effect of N loading in understanding the effect of N loading on O_3-induced changes such as increments in leaves.

N loading responses were particularly varied between the between two *Larix* spp. Soil inorganic N, particularly NO_3^- concentrations, in the N loading treatment in Japanese larch and its hybrid larch F_1 were 3.41 and 2.66 mg l^{-1}, respectively (Table 3-1-2). However, the growth responses of hybrid larch F_1 were higher under similar N treatment. Increment in total dry mass following N loading was higher in hybrid larch F_1 than in Japanese larch. Plant growth is largely regulated by the spatial distribution of leaves i.e., the quantity of leaves and photosynthetic capacity (e.g., Poorter 1989). I observed a positive effect of N loading on A_{380} in both *Larix* spp. (Fig. 3-1-3*A*). However, N loading did not increase the total dry mass in Japanese larch (Fig. 3-1-1*A*). The results are consistent with the previous report in Watanabe et al. (2006). In the present study, stem dry mass was not changed in Japanese larch whereas it was significantly increased by N loading in hybrid larch F_1. Notably, N loading increased only needle proportions in Japanese larch. Therefore, Japanese larch might have a relatively lower capacity for N utilization than hybrid larch F_1. Soil NO_3^- concentrations in control treatments in Japanese larch and hybrid larch F_1 species were 0.08 and 0.28 mg l^{-1}, respectively. These results could also suggest that the Japanese larch initially had a lower capacity for N absorption and/or utilization rate.

N loading significantly increased leaf P in hybrid larch F_1. The increment in leaf P certainly decreased N/P ratio in hybrid larch F_1. The results could suggest that N loading promotes P absorption and utilization. In addition, the P increment was significant under N loading and elevated O_3 (Table 3-1-2, $P < 0.05$). The result could indicate that relative N limitation may occur following O_3 enrichment even under N loading. Such key responses were not observed in Japanese larch, suggesting that the contradictory responses in the two larch species could be associated with physiological responses to changes in leaf nutrient contents, in particular under N loading.

Knowledge regarding leaf P content responses to O_3 remains relatively limited (e.g., Beyears et al. 1992, Kainulainen et al. 2000, Shi et al. 2017). Previous studies have reported no significant reductions, rather, slight increments of leaf P contents under elevated O_3 (e.g., Beyears et al. 1992, Kainulainen et al. 2000, Utriainen and Holopainen 2001, Waillin et al. 2002, Wang et al. 2015). In the present study, I also observed a slight increment in leaf P content under elevated O_3 in both *Larix* spp. The increment in P in the present study was significant in hybrid larch F_1 under N loading, particularly with elevated O_3 (Table 3-1-2, $P < 0.05$). Further studies are required to evaluate why leaf P increased in hybrid larch F_1. Potential mechanisms would be related to ectomycorrhizal fungi (ECM) infection ratio and species diversity of under elevated O_3 conditions (Wang et al. 2015). It is also critical consider the role of ECM symbioses since symbiotic ECM enhance nutrient conditions for the host plants as long as the host plants have the capacity to photosynthesize efficiently.

Demand for P could vary depending on N conditions. In Japanese larch, P demand is much greater than N demand (Li et al. 2016). Therefore, to investigate the leaf N and P balances, I evaluated leaf N/P ratio under elevated O_3 and N loading. In the present study, all leaf N/P values in in Japanese larch were >20 irrespective of treatments (Table 3-1-2). A leaf N/P ratio >20 is indicative of P limited biomass production (Güsewell 2004). Therefore, the results indicate that P could limit biomass production in Japanese larch. In addition, higher N/P, i.e., relative P deficiency, accelerates leaf senescence, which becomes a physiological limiting factor (Güsewell 2004, Killingbeck 2004). However, in the present study, N loading decreased *NUE* in hybrid larch F_1 (Fig. 3-1-3*C*, 6.40±0.39 to

4.71±0.56 μmol $\mathrm{mgN^{-1}\ s^{-1}}$ in the control and N loading treatment, respectively). Translocation of photosynthates in chloroplasts is inhibited by relative deficiency in inorganic phosphorous, i.e., higher leaf N/P constrains the carboxylation cycle (e.g., Sharkey 1985). Although I did not observe any significant inhibition of *PUE* in both species (Fig. 3-1-3*D*), a plausible explanation for the observed phenomenon could be an increase in sucrose synthesis via the Calvin cycle due to N loading. It would induce P limitations at the early stages of photosynthate translocation, which would also reduce *NUE* (Luo et al. 2014, Li et al. 2016).

Chapter 3-2: Effects of salt loading on O_3 sensitivity of Japanese larch and hybrid larch F_1

INTRODUCTION

Ground-level ozone (O_3) is the most harmful air pollutant to forest ecosystems on both local and global scales (Paoletti et al., 2007, 2010, Matyseek et al., 2012, Sicard and Dalstein-Richier 2015, Sicard et al., 2016). Ozone suppresses plant growth, accelerates leaf senescence, changes carbon allocation to roots, and induces nutritional imbalances in leaves (Matyseek et al., 2012, Agathokleous et al., 2015, Shi et al., 2017). Effects of elevated O_3 (eO_3) on forest ecosystems are a concern in northeast (NE) Asia (Koike et al., 2013, Akimoto et al., 2015). In China, the annual daily maximum O_3 concentration in some regions often reaches 60 nmol mol^{-1} (Gaudel et al., 2018). Recent studies have predicted that the annual mean change in surface O_3 concentrations in Asia will rise to approximately 8 nmol mol^{-1} by 2050 (Lee et al., 2015, Turnock et al., 2018). The current eO_3 level is high enough to suppress tree growth and degrade ecosystem health (Chen et al., 2015, Feng et al., 2015). Thus, the conservation of forests in China is an issue of increasing interest in regions that face multiple environmental stresses, such as eO_3, nitrogen deposition, and drought (Reilly et al., 2007, Fang et al., 2014, Hu et al., 2015, Yuan et al., 2016).

Several regions of China have begun reforestation because of the intensive thinning and harvesting that has persisted since the Grain for Green Project began in 1999 (Zhang et al., 2000, Feng et al., 2005, Xu 2011). However, in NE China, where forestry practices have been active, not all afforestation is well established cause to the soil salinization that occurs with low precipitation and high temperature (e.g., Feng et al., 2005, Sakai 2012). Saline soil occupies approximately 99,000 km^2 of China’s land area (Zhang et al., 2010, Xu 2011, Li et al., 2014). The frequency of extreme high temperatures in summer has been increasing in China over 60-fold since the 1950s (Sun et al., 2014). The relative drought conditions may increase the potential for salinization stresses (Polle and Chen 2015). Especially in NE China, soil salinization often occurs with low precipitation and high temperature (Ma and Fu 2006, Zhou et al., 2011, Sakai 2012). Excess salinity causes physiological and metabolic imbalance in plants via ionic stresses (Marschner 2012, Polle and Chen 2015, Wungrampha et al., 2018). The effects of salinity on plants have been investigated with sodium chloride (NaCl), which are known to cause ionic imbalance and inhibit mineral ion uptake of potassium (K) and calcium (Ca) (Gerosa et al., 2014, Guidi et al., 2016, Plesa et al., 2018). Since arid and semi-arid lands contain chlorides and carbonates of several minerals, including Na, Ca, and magnesium (Mg), the severe effects of alkaline salt accumulation on plants and trees have received increased attention (Yang et al., 2008, Liu and Shi 2010, Wang et al., 2013). For example, in the Songnen plain of Heilongjiang Province, 3.2 million ha are influenced by alkaline salt accumulation, and continues to expand by 20,000 ha per year (Wang et al., 2009). Thus, for forest conservation in NE China, I should investigate the combined stresses of eO_3 and salts on forest growth and health.

The combined effects of eO_3 and salt have largely been described in Mediterranean areas. For example, metabolic responses in pomegranate (*Punica granatum* L.) have indicated eco-physiological adaptation up to 50 mM NaCl stress but did not mitigate O_3-induced oxidative stresses (Calzone et al., 2019). Holm oaks (*Quercus ilex* L.) treated under 150 mM NaCl treatments did not show significant photosynthetic depression by eO_3 (Guidi et al., 2016). In addition, previous studies have reported that salt stresses mitigated negative effects of eO_3 via stomatal closure (Gerosa et al., 2014), and its effects were exacerbated under salt stresses (Calzone et al., 2019), or no interaction between eO_3 and salt stresses (Guidi et al., 2016). Thus, the views of the combined effects of eO_3 and salt stresses are still inconsistent.

Larch (*Larix* sp.) has a higher tolerance to harsh conditions and is widely planted throughout northern hemisphere (Gower and Richards, 1990, Zhang et al., 2000, Ryu et al., 2009, Mao et al., 2010). For examples, Dahurian larch (*Larix gmelinii*) has a higher expectation as an afforestation species in NE China (Zhang et al., 2000, Shi et al., 2010). Japanese larch (*L. kaempferi*, JL) has been planted in the Korean peninsula and northern Japan (Lee et al., 2004, Ryu et al., 2009). The current larch forests occupy over 40 % of the total carbon growing stock in Eurasian boreal forests, including NE China (Alexeyev et al., 2000, Wang et al., 2001). Based on the Chinese policy of replantation since 1999, increased afforestation has raised concerns regarding low species diversity in forests and poor ecological functions, such as material cycling and habitat provision (Xu and Wilkes 2004, Zhang et al., 2007). Thus, the effects of eO_3 and salt should be investigated on *Larix* sp. (Zhang et al., 2000, Chazdon 2008, Ryu et al., 2009) as well as exciting afforestation species, such as *Populus* sp.

The purpose of this study was to evaluate the effects of eO_3 and alkaline salt on Dahurian larch (DL) and Japanese larch (JL) seedlings. Koike et al. (2012) reported the O_3 suppressed photosynthesis rate of only DL but not of JL. While many studies have reported that O_3-induce inhibition can be determined by absorbed O_3 amount (Matyseek et al., 2004, Hu et al., 2015), there were no significant differences in stomatal conductance between DL and JL seedlings (Koike et al., 2012). These results indicate that O_3 sensitivity differences between these two species can be caused by non-stomatal factors, which may be evaluated through PSII photochemical systems (Gielen et al., 2006, Guidi et al., 2016) and the leaf nutritional status (e.g. Barnes et al., 1995, Shang et al., 2018). I expected that the inhibitions of eO_3 and salt could be evaluated via nutrient imbalance status. It was reported that the nutrient concentrations in plants, such as N and P, were increased by eO_3, which may be adaptive strategy against eO_3 (Cao et al., 2016, Shang et al., 2018). Besides, Larch may have specific salt tolerance to the K homeostasis (Renault 2005, Plesa et al., 2018). It was reported that NaCl treatment did not inhibit K absorption in larch saplings; rather, the saplings took up more K even with NaCl treatment compared to the control condition (Renault 2005, Plesa et al., 2018). K homeostasis is one of the salt tolerances and it has been considered as secondary importance in many published literatures (Tester and Davenport 2003, Marschner 2012). There are several other mechanisms to manage excess Na contents such as the exclusion of Na and osmotic regulation by compatible solutes (Flowers 2004, Munns et al., 2006). However, it has reported that the practical outcomes of these approaches were not effective on improving salt tolerance of plants under filed conditions (Shabala and Cuin 2007, Wang et al., 2013, Anschütz et al., 2014).

Increasing K contents could induce the homeostasis of photosynthesis and metabolic activity, and the osmotic adjustment (Volkov et al., 2003, Shabala and Cuin 2007). In fact, an optimal K status can be index for stress resistance when plants are exposed to abiotic stresses (Marschner 2012). It was reported that a K fertilization compensated the O_3 effects on potted Norway spruce (*Picea abies*) seedlings although there were genetic-specific responses (Keler and Matyssek 1990, Barnes et al., 1995), suggesting that the species with relatively higher K content may show insights for the O_3 tolerance. Furthermore, several studies have investigated the mineral homeostasis under eO_3 (Alcántara et al., 2006, Agathokleous et al., 2018b). These studies suggest that the homeostatic adjustment in element content of leaves can mitigate physiological inhibitions of eO_3 although they focused on the homeostasis of other mineral element such as iron and P.

Here, I firstly expected that (i) O_3 would suppress growth of DL but not of JL as Koike et al. (2012) reported. However, I hypothesized (ii) DL is more tolerant relative to JL since it is more adapted to salty soils due to its ecological distribution (Abaimov 2010, Mao et al., 2010, Mamet et al., 2019), where soil salinization often occurs (Shi et al., 2010, Zhou et al., 2011), and thus salt treatment would not inhibit K absorption in DL. This comparison of salt responses between the two larches may provide novel insights on the eco-physiology to understand how larch acquires the adaptive capacity to salt stress. Further, it has reported that the reduction of K content in salt-tolerant wheat was lower than in salt-sensitive wheat at combined effect of eO_3 and salt treatment (Zheng et al., 2014). Hence, given that DL can maintain higher K contents than JL under eO_3 and salt treatment, (iii) DL may show higher tolerance to the synergic effect than JL. Based on these results, I assessed the possibility of future candidate afforestation species in northeast Asian regions.

MATERIAL AND METHOD

Study site and Plant materials

Experiments were conducted at the experimental nursery of the Sapporo Experimental Forest, Hokkaido University in northern Japan (43° 04' N, 141° 20' E 15 m a. s. l.). Two-year-old Dahurian larch (*Larix gmelinii* var. *japonica*; DL) and Japanese larch (*Larix kaempferi*; JL) seedlings were cultivated from seeds in the nursery of the Hokkaido Forestry Research Organization (HRO), Forestry Research Institute in Bibai city near Sapporo. The seedlings were transplanted into 1-L pots (Height: 114 mm, top diameter: 135 mm, bottom diameter: 95 mm) in early May 2017 before buds opened. The initial stem diameter means ± standard deviations were 1.13 ± 0.23 mm for DL and 1.32 ± 0.31 mm for JL, and the height was 8.83 ± 1.35 cm for DL and 8.55 ± 1.73 cm for JL, respectively. Soils underneath the seedlings were removed just before transplantation, with well-weathered volcanic ash soil (Kanuma and Akadama soil, 1:1, v/v) used as cultivation soil in pots. To measure the original nutrient status of the soil, approximately 10 g of soil and 25 ml ultrapure water were mixed and shaken for 1 hour. The samples were poured through filter paper (110 mm mesh, ADVANTEC, Tokyo, Japan) and the filtrate was centrifuged at 2000 G for 20 minutes. The supernatant fluid was mixed with 61% nitric acid and adjusted for the concentration of 2% nitric acid. Mineral elements contents of K, Ca, Mg, and Na were measured by ICP-MS (ELAN, DRC-e; Perkin Elmer, Waltham, MA, USA). The Na adsorption rate of this soil medium was also measured. The three levels of NaCl dissolved in demineralized water were loaded on the pot soil, which contained approximately 1200 g of soil without seedlings, seven times for three weeks (110, 190, and 240 mmol Na in total). There were no leaks from the pot after each loading. After completing Na loading, the soil sample was obtained from the well-mixed and dried soil. Na content of the sample was measured by the same method described above. Na adsorption rate was calculated as the difference between total loaded Na and the water extracted Na amount.

Results of the original nutrient status and the Na adsorption rate were summarized in a supplemental data. Until treatments started, irrigation was manually carried out in the morning once every three or four days to avoid soil drying. Balanced liquid fertilizer (200 ml, 1/2000, v/v, HYPONEX, Japan; 36.2 mg N L^{-1}, 142 mg P L^{-1}, 47.1 mg K L^{-1}) was applied once every week to ensure nutrient balance (4 times in total).

Experimental design

Four treatments were totally established in this study: ambient O_3 and tap water irrigation as the control (aO_3+CW), elevated O_3 and control water irrigation (eO_3+CW), ambient O_3 and salt water irrigation (aO_3+SW), and elevated O_3 and salt water irrigation (eO_3+SW), respectively. All treatments were conducted from June 27 to September 25, 2017 before the winter season. The mean temperature was 19.6°C and precipitation was 127.38 mm during the experimental period. The open top chamber (OTC; 1.2 x 1.2 x 1.2 m) system was adopted to control the O_3 concentration levels in each treatment. Seedlings were grown in OTC surrounded by a polyvinyl chloride film (Noh-bi Co. Ltd., Sapporo, Japan), such that approximately 88% sunlight could be transmitted without UVB and UVC radiation. The O_3 concentration monitored is described in Table 3-2-1. More detailed descriptions of the methodology of the O_3 exposure system in OTCs were provided in Sugai et al., (2019).

Plants in the salt treatment were watered with 200 ml of saline water. Control plants were maintained by watering with 200 ml of tap water. The applications were performed at 3- or 4-day intervals for a total of 20 times. Mixed salt composed of alkaline salt ($NaHCO_3$) and neutral salt (NaCl) was used to imitate the realistic extant salt-alkaline soil condition of NE China (Ge and Li 1990, Sakai 2012). The two salts were mixed $NaHCO_3$: NaCl = 9:1 to make 20 mM Na^+ saline water. To prevent salt leaching, rainfall was excluded by plastic shelters over the top of the OTC only during rainy days. During the final experimental period when the seedlings were harvested, 10 g of fresh soil samples were taken from the surface and bottom soils in the pots of all treatments to measure soil pH. The depth of soil sampling was set at approximately 2 cm from both the surface and bottom. The soil was shaken for 1 hour, with 25 ml ion-exchanged water as soon as possible after sampling. The soil pH was measured by a portable pH meter (M-12, Horiba, Japan). The monitored manipulated conditions were summarized in Table 3-2-1. All treatments were replicated four times with 16 OTCs, with a split-plot completely randomized design with four seedlings in each OTC (totally 128 seedlings).

Table 3-2-1 Summary of the environmental condition in this experiment.

Mean concentration at ambient (AOZ) and elevated ozone (EOZ) for daytime (06:00–18:00) and over 24 hours in the OTC from June to September 2017, and pH in the surface and bottom soil (approximately 2 cm layer) of Dahurian larch (DL) and Japanese larch (JL) seedlings under all treatments: ambient O_3 and tap water irrigation (AOZ+CW) as the control, elevated O_3 and control water irrigation (EOZ+CW), ambient O_3 and salt water irrigation (AOZ+SW), and elevated O_3 and salt water irrigation (EOZ+SW) in September 2017. All values are means ± SE.

		O_3 concentration (nmol mol^{-1})	
		Daytime average	24-hr average
AOZ	June	43.99 ± 0.79	39.28 ± 0.62
	July	43.59 ± 0.82	36.99 ± 0.61
	August	40.09 ± 1.48	32.24 ± 0.94
	September	34.02 ± 1.00	27.11 ± 0.89
EOZ	June	71.91 ± 1.29	50.28 ± 1.39
	July	71.13 ± 1.12	47.38 ± 1.28
	August	70.64 ± 1.44	46.60 ± 1.62
	September	70.39 ± 1.19	46.17 ± 1.87
		Soil pH	
		Surface soil	Bottom soil
DL	AOZ+CW	6.37 ± 0.01	6.05 ± 0.03
	EOZ+CW	6.52 ± 0.04	6.08 ± 0.03
	AOZ+SW	7.96 ± 0.11	7.19 ± 0.01
	EOZ+SW	8.17 ± 0.13	6.93 ± 0.01
JL	AOZ+CW	6.37 ± 0.03	6.04 ± 0.04
	EOZ+CW	6.37 ± 0.02	6.11 ± 0.02
	AOZ+SW	7.92 ± 0.07	7.21 ± 0.07
	EOZ+SW	8.10 ± 0.02	7.29 ± 0.04

Growth, leaf mass area and total leaf area index

Total 64 seedlings for each species were harvested and washed with tap water. After washing, needles, branches, stems, and roots were separated. Each sample was oven dried at 70°C until a constant weight was achieved, and then weighed. Mature needle leaves were sampled at the same shoot position near the crown in each seedling at the end of September 2017. Part of the needle samples was used to measure the leaf mass per area (LMA) and the other part was used to measure the contents of several nutrient elements (see below). The projected area of fresh needles was measured by an image scanner (LIDE 200, Canon, Japan). After the projection measurement, the needle dry mass was measured by the same method as above. LMA was calculated as dry weight divided by the needle area projected.

As a species difference between two studied larches, the lower needle proportion of DL than JL has been reported (Harayama et al., 2013, Dong-Gyu et al., 2015). To evaluate these differences under eO_3 and salt stress, I calculated needle dry mass divided by total dry mass as the needle ratio. While larch species have both short and long needles (Gower and Richards 1990), the ratio of mature short needles dry mass is relatively lower than the mature long needles at a seedling stage (Powell 1988). Based on this characteristic, I estimated the leaf area at the whole plant level as an index of total leaf area (TLA) by LMA of mature needle leaves times needle dry mass per a seedling.

Maximal photochemical efficiency of photosystem II

The maximal photochemical efficiency of photosystem II (F_v/F_m) was measured with a portable fluorometer (PAM-2000, Walz, Effeltrich, Germany) in September 2017. The measurement was conducted after an overnight dark adaptation to evaluate the chronic photoinhibition (Krause et al., 1995, Kitao 2003). F_v/F_m was calculated with the following parameters and formula: F_0 for the steady state yields, F_m for the maximum yields measured under irradiance of approximately 5,000 μmol m^{-2} s^{-1} photon flux density for 1 s, and $F_v/F_m = (F_m – F_0) / F_m$ as defined by Schreiber et al. (1986).

Nutrition and chlorophyll contents in needles

Approximately 15 mg powder samples obtained from mature needles sampled at the end of September 2017 were weighed and used to measure nitrogen (N) content with a NC analyzer (Elementar, Vario EL III, Japan). Approximately 50 mg of powder samples were weighed and digested with 2 ml of 61% nitric acid (Kanto Chemical, Tokyo, Japan) at 110˚C for approximately 2 hours. A 0.5 ml solution of hydrogen peroxide was added, and the sample was heated continuously at 110°C for 20 minutes. After cooling to room temperature, 10 ml of 2% nitric acid were added. The concentration of K, Ca, Mg, and Na in these samples was measured by ICP-MS. Element contents were calculated as the dry weight unit and converted as the leaf area unit by LMA.

Samples were stored at −75°C after sampling and weighing. Needles were immersed in 2 ml dimethyl sulfoxide and incubated at 65°C in the dark to extract chlorophyll (Chl). Then, the extracts were measured with a spectrophotometer (Gen spec III, Hitachi, Tokyo, Japan) with two waves; 665 nm (A_{665}) and 648 nm (A_{648}). Chl-a and Chl-b contents were calculated according to Barnes et al., (1992) and Shinano et al., (1996). The total Chl (i.e., Chl a+b) and Chl a/b were also calculated. I also obtained ratio of total Chl/ needle N content (Chl/N) as an index of allocation in foliar nitrogen (Kitaoka and Koike 2004).

Statistical Analyses

Statistical analyses were conducted using R (R Core Team 2017). All the data of response variables were set as the four mean values per treatment, which were obtained from four seedlings per species in each chamber (n = 4). The effects of eO_3 and salt stress were determined by analysis of variance in each species (Two-way ANOVA). The relationships between needle Na and mineral element contents at all treatments in both species were analyzed using a generalized linear mix model (GLMM, n = 32). The random effect was set as the experimental unit. When species differences and their interactions were significant, correlation analysis was performed in each species (n = 16). Relationships between TLA and content of each element in needles were analyzed by the same GLMM. In each model, explanatory variables (= fixed effects) were set with each mineral element, species, and its interaction, whereas the response variables were the mean values at all treatments in both species. In all the linear analyses, the coefficient of determination (R^2), *P* value, and the *Akaike*'s information criterion were calculated (AIC, Akaike 1974). AIC is one of the most popular criteria for linear model identification and the optimal model is selected when AIC is minimized.

RESULTS

Response to elevated O_3 and salt stress

No significant effects of elevated O_3 (eO_3) were observed on the total dry mass of DL. I did not observe significant inhibition of O_3 on F_v/F_m between both larch species. However, O_3 significantly increased total dry mass and TLA of only JL ($P < 0.05$, Fig. 3-2-1). The mean value of total dry mass and TLA at eO_3 were approximately 23% and 34% higher than at the ambient O_3 condition, respectively. No significant effects of O_3 were observed in other biometric (i.e. needle ratio, LMA) and biochemical parameters (i.e. element contents and chlorophyll in needles, Table 3-2-2).

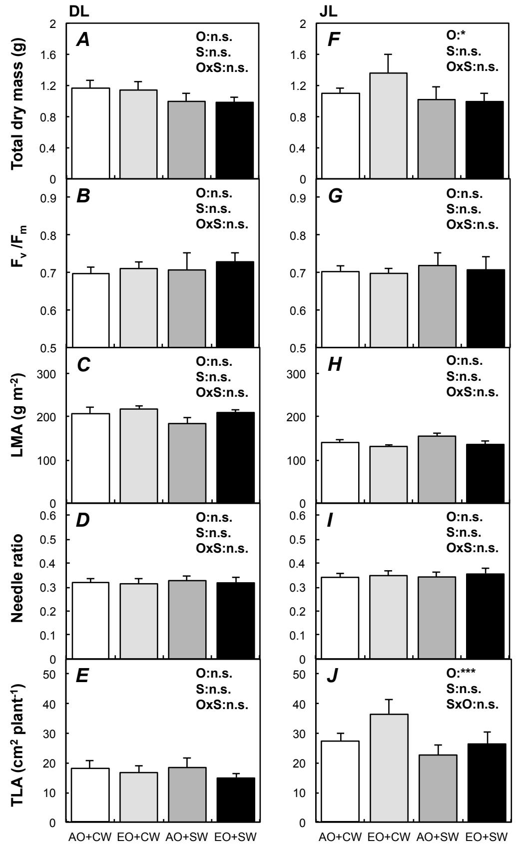

Fig. 3-2-1 Responses to salt treatment and elevated ozone (O_3) in Dahurian larch (DL, *Larix gmelinii*, A-E) and Japanese larch (JL, *Larix kaempferi*, F-J).

White bar means ambient ozone (O_3) and control tap water (AOZ+CW), light gray bar means elevated O_3 and control tap water (EOZ+CW), dark gray bar means ambient O_3 and salt water (AOZ+SW), and black bar means elevated O_3 and salt water (EOZ+SW). The explanatory variables were set as elevated O_3 (O), salt treatment (S), and its interaction (OxS). Results of Two-way ANOVA (n = 4) with statistically significant difference are shown as: ***; $P < 0.001$, *; $P < 0.05$, and n.s.; $P \geqq 0.05$.

Table 3-2-2 Summary of the biochemical needle traits.

Data were mineral element contents, total chlorophyll (Chl) contents, Chl a, Chl b, the ratio of Chl a/b, and the ratio of total Chl/ needle N contents in Dahurian larch (DL) and Japanese larch (JL) seedlings at all the treatments. All the values are shown as the mean ± SE with the results of two-way ANOVA (n = 4). Statistically significant differences are shown as: ***; $P < 0.001$, **; $P < 0.01$, *; $P < 0.05$, and n.s. ; $P \geqq 0.05$.

		Treatments				Two-w
cies	Factor	AOZ+CW	EOZ+CW	AOZ+SW	EOZ+SW	O$_3$
	Na (mg gDW^{-1})	0.64 ± 0.27	0.29 ± 0.10	3.13 ± 0.62	4.50 ± 1.21	n.s.
	K (mg gDW^{-1})	4.10 ± 0.42	4.97 ± 0.54	4.09 ± 0.51	4.84 ± 0.28	n.s.
	Ca (mg gDW^{-1})	2.61 ± 0.22	2.71 ± 0.18	2.16 ± 0.05	2.07 ± 0.16	n.s.
	Mg (mg gDW^{-1})	1.45 ± 0.06	1.54 ± 0.13	1.24 ± 0.05	1.22 ± 0.10	n.s.
	N (mg gDW^{-1})	1.38 ± 0.04	1.30 ± 0.06	1.57 ± 0.06	1.56 ± 0.12	n.s.
	Na (g m^{-2})	0.13 ± 0.06	0.06 ± 0.02	0.55 ± 0.07	0.95 ± 0.26	n.s.
	K (g m^{-2})	0.83 ± 0.05	1.09 ± 0.15	0.77 ± 0.13	1.01 ± 0.04	n.s.
	Ca (g m^{-2})	0.54 ± 0.05	0.59 ± 0.06	0.40 ± 0.04	0.44 ± 0.04	n.s.
	Mg (g m^{-2})	0.30 ± 0.02	0.34 ± 0.03	0.23 ± 0.03	0.25 ± 0.02	n.s.
	N (g m^{-2})	0.29 ± 0.02	0.28 ± 0.02	0.29 ± 0.03	0.33 ± 0.03	n.s.
	Total Chl (mg gFW^{-1})	8.75 ± 0.39	10.09 ± 1.10	9.24 ± 1.49	7.78 ± 0.97	n.s.
	Chl-a (mg gFW^{-1})	6.87 ± 0.29	7.83 ± 0.76	7.58 ± 1.25	6.18 ± 0.82	n.s.
	Chl-b (mg gFW^{-1})	1.88 ± 0.11	2.26 ± 0.36	1.67 ± 0.24	1.60 ± 0.15	n.s.
	Chl a/b	3.62 ± 0.16	3.60 ± 0.25	4.46 ± 0.18	3.78 ± 0.14	n.s.
	Chl/N (mg mgN^{-1})	6.32 ± 0.15	7.89 ± 1.05	5.93 ± 1.08	4.95 ± 0.30	n.s.
	Na (mg gDW^{-1})	0.28 ± 0.04	0.08 ± 0.02	3.82 ± 0.43	4.55 ± 0.49	n.s.
	K (mg gDW^{-1})	5.05 ± 0.46	5.23 ± 0.51	3.95 ± 0.41	4.63 ± 0.66	n.s.
	Ca (mg gDW^{-1})	3.01 ± 0.12	2.97 ± 0.22	1.89 ± 0.09	1.95 ± 0.05	n.s.
	Mg (mg gDW^{-1})	1.58 ± 0.02	1.60 ± 0.09	1.00 ± 0.06	1.12 ± 0.09	n.s.
	N (mg gDW^{-1})	1.25 ± 0.11	1.25 ± 0.11	1.45 ± 0.05	1.38 ± 0.10	n.s.
	Na (g m^{-2})	0.04 ± 0.01	0.01 ± 0.00	0.60 ± 0.09	0.61 ± 0.04	n.s.
	K (g m^{-2})	0.70 ± 0.06	0.69 ± 0.08	0.60 ± 0.05	0.64 ± 0.13	n.s.
	Ca (g m^{-2})	0.42 ± 0.02	0.39 ± 0.03	0.29 ± 0.03	0.27 ± 0.02	n.s.
	Mg (g m^{-2})	0.22 ± 0.01	0.21 ± 0.01	0.16 ± 0.02	0.15 ± 0.02	n.s.
	N (g m^{-2})	0.17 ± 0.01	0.16 ± 0.01	0.22 ± 0.01	0.19 ± 0.02	n.s.
	Total Chl (mg gFW^{-1})	8.41 ± 0.68	9.21 ± 0.99	7.64 ± 0.99	8.04 ± 1.49	n.s.
	Chl-a (mg gFW^{-1})	6.44 ± 0.53	7.11 ± 0.75	5.95 ± 0.77	6.32 ± 1.30	n.s.
	Chl-b (mg gFW^{-1})	1.97 ± 0.16	2.10 ± 0.24	1.69 ± 0.25	1.72 ± 0.20	n.s.

While salt stress had also no significant effects on all biometric and physiological parameters of the two species, several element contents in needles were significantly changed (Table 3-2-2). Needle Na contents were significantly increased under salt stresses in both larches. In the dry mass unit, needle Na content of DL with salt treatment was approximately eight times greater than in the salt-free condition ($P < 0.05$) whereas Na of JL with salt treatment was at least 13 times greater ($P < 0.001$). Salt stress increased Chl ratio only in DL, which showed an approximately 14% increase in average values ($P < 0.01$). In contrast, salt stress significantly reduced K, Ca, and Mg contents of JL. In the dry mass unit, the K, Ca, and Mg contents of DL decreased approximately 17% under salt treatment ($P < 0.05$), 36% ($P < 0.001$), and 34% ($P < 0.001$), respectively. In the needle area unit, however, the increment of N content was observed in only JL ($P < 0.05$).

Relationship between needle Na and other elements

The overall relationship between Na and K contents was not significant in the larch seedlings (Fig. 3-2-2). However, a significant relationship between Na and K contents was observed in JL ($R^2 = 0.2$, $P < 0.05$, AIC = 48.6) but not in DL ($R^2 = 0.02$, $P = 0.33$, AIC = 47.1). A significant relationship between Ca and Mg were observed in both larch species, as was a significant relationship between Na and Mg content (DL; $R^2 = 0.35$, $P < 0.01$, AIC = -10.22, JL; $R^2 = 0.23$, $P < 0.05$, AIC = -4.63). On the contrary, there were species differences in the relationship between Na and Ca content ($P < 0.05$, Fig. 3-2-3). The coefficient value of Na on Ca content was approximately 1.8 times higher in JL than DL (Table 3-2-3). All the relationships between Na and N contents in both and each larch species were not significant.

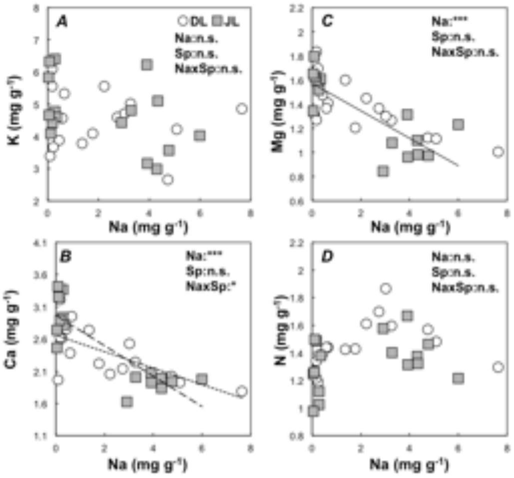

Fig. 3-2-2 Relationship between the needle Na content and other cation contents (K, Ca, Mg, and N).

Data were shown as mass-based unit (mg g^{-1}) in Dahurian larch (DL, white circle) and Japanese larch (JL, gray square) were analyzed by GLMM with statistically significant difference are shown as: ***; $P < 0.001$, *; $P < 0.05$, and n.s.; $P \geqq 0.05$. The explanatory variables were set as needle Na content (Na), species (Sp), and its interaction (NaxSp). The relationships between needle Na content and other element contents are shown as solid lines for both species, a fine dotted line for DL, and a heavy dotted line for JL.

Table 3-2-3 Results of relationship between cations.

The relationship between needle Na and other element contents in Dahurian larch (DL) and Japanese larch (JL) were analyzed by GLMM. All the values of element content were mass based unit (mg g^{-1}). R^2, the coefficient of determination; AIC, *Akaike*'s information criterion.

Model formula	R^2	P value	AIC
Both larch species			
K = -0.13 Na + 4.90	0.087	0.057	91.43
Ca = -0.18 Na + 2.81	0.586	< 0.001	24.14
Mg = -0.09 Na + 1.54	0.577	< 0.001	-17.68
N = 0.03 Na + 1.33	0.099	0.954	-13.01
DL			
K = -0.05 Na + 4.61	0.015	0.326	47.05
Ca = -0.13 Na + 2.66	0.467	< 0.01	11.61
Mg = -0.07 Na + 1.52	0.521	< 0.001	-10.22
N = 0.03 Na + 1.40	0.107	0.891	-6.17
JL			
K = -0.22 Na + 5.19	0.202	< 0.05	48.63
Ca = -0.24 Na + 2.97	0.723	< 0.001	13.59
Mg = -0.11 Na + 1.57	0.654	< 0.001	-4.63
N = 0.03 Na + 1.27	0.118	0.904	-4.79

Relationship between TLA and needle mineral elements

Table 3-2-3 shows the summary of model formulas to explain TLA by each element in needles. The best model to explain TLA of both larches determined by AIC was constructed with N ($R^2 = 0.54$, $P < 0.001$, AIC = 211). This significant relationship was also observed within each species (DL; $R^2 = 0.35$, $P < 0.01$, AIC = 94, JL; $R^2 = 0.23$, $P < 0.05$, AIC = 116) whereas the highest R^2 in model of DL was performed by K ($R^2 = 0.36$, $P < 0.01$, AIC = 94) although AIC was the same value with N (Fig. 3-2-3).

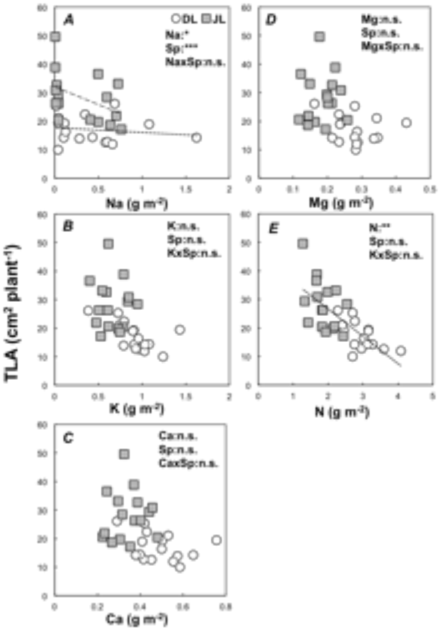

Fig. 3-2-3 Relationship between the total leaf area index (TLA, cm^2 plant^{-1}) and needle element contents (*i.e.*, Na, K, Ca, Mg, and N).

Data were shown as leaf area-based unit (g m^{-2}) in Dahurian larch (DL, white circle) and Japanese larch (JL, gray square) were analyzed by GLMM with statistically significant difference are shown as: ***; $P < 0.001$, **; $P < 0.01$, *; $P < 0.05$, and n.s.; $P \geqq 0.05$. The explanatory variables were set as each needle element content, species (Sp), and its interaction. The relationships between TLA and each element content are shown as solid lines for both species, a fine dotted line for DL, and a heavy dotted line for JL.

The second-best model of both larches was constructed with K ($R^2 = 0.28$, $P < 0.01$, AIC = 225) while the third models contained almost equal R^2 and AIC values (Ca; $R^2 = 0.20$, $P < 0.01$, AIC = 229, Mg; $R^2 = 0.20$, $P < 0.01$, AIC = 229). However, no significant relationships between TLA and K, Ca, and Mg content were observed in JL (Table 3-2-4).

Table 3-2-4 Relationship between TLA and cation contents.

Results of the generalized liner mixed models (GLMM) to describe the relationship between total leaf area (TLA, cm^2) and needle mineral element contents in Dahurian larch (DL) and Japanese larch (JL). All the values of element content were area-based unit (g m^{-2}).

Model formula	R^2	P value	AIC
Both larch species			
TLA = -7.31 Na + 25.3	0.097	< 0.05	232
TLA = -19.9 K + 38.5	0.278	< 0.01	225
TLA = -32.2 Ca + 36.0	0.196	< 0.01	229
TLA = -56.5 Mg + 35.8	0.204	< 0.01	229
TLA = -95.7 N + 45.8	0.535	< 0.001	211
DL			
TLA = -1.71 Na + 17.8	0.024	0.282	101
TLA = -12.5 K + 28.7	0.355	< 0.01	94
TLA = -13.5 Ca + 23.7	0.101	0.115	99
TLA = -15.5 Mg + 21.4	0.041	0.227	100
TLA = -63.0 N + 35.7	0.346	< 0.01	94
JL			
TLA = -12.5 Na + 32.1	0.198	< 0.05	116
TLA = -2.50 K + 29.8	0.002	0.435	120
TLA = 7.55 Ca + 25.6	0.005	0.600	120
TLA = 15.5 Mg + 25.3	0.005	0.607	120
TLA = -115 N + 49.8	0.232	< 0.05	116

Although needle Na content was significantly correlated with TLA in both larch species ($P < 0.05$), the result of GLMM showed a species difference in TLA ($P < 0.001$). When the effects of Na contents on TLA were analyzed in each species, the significant relationship was observed only in JL ($R^2 = 0.20$, $P < 0.05$, AIC = 116) but not in DL ($R^2 = 0.02$, $P = 0.28$, AIC = 101).

DISUCISSION

I evaluated initial growth of Dahurian larch (DL) and Japanese larch (JL) seedlings treated with the simulated eO_3 and alkaline salt stress. In contrast to the present expectations, eO_3 did not suppress the total dry mass of both larch species. Moreover, eO_3 did not induce significant nutritional imbalance in needles even with salt stress. Elevated O_3 significantly increased the dry mass of JL while I did not observe any significant inhibitions of biometric and physiological parameters, except for TLA. In fact, the similar results indicated that JL can show hormetic responses of photosynthesis rates and dry mass to mild O_3 stress (Dong-Gyu et al., 2015, Sugai et al., 2018). Since leaf quantity as well as photosynthetic capacity are related to plant growth (Poorter 1989), the dry mass increment might be related to the TLA response (Fig. 3-2-1)

The best factor explaining variables of TLA was needle N contents. The results of negative correlation between TLA and N contents suggests that DL originally may not produce TLA regardless of any growth conditions as relatively higher N contents per needle area, while JL may be able to adjust producing TLA as relatively lower N contents. This result suggests that the N use efficiency in forming needles may vary between the two larches, and DL may have adaptive abilities for harsh conditions, such as low temperature and limited soil nutrient availability more than JL (Gower and Richards 1990). Koike et al. (2012) reported that the photosynthetic N use efficiency of DL was higher (over 20%) compared to JL. Instead of these higher abilities in a needle scale, DL may be inferior to adjust TLA along with abiotic environments (Abaimov 2010, Polezhaeva et al., 2010, Mamet et al., 2019).

In a previous study, one-month-old saplings of European larch (*Larix decidua* Mill) showed a 16% lower dry mass at 150 mM NaCl compared to controls (Plesa et al., 2018). While salt treatment showed no significant suppression in any initial growth, I observed significant biochemical responses in needles (i.e., several element contents; Table 3-2-2). As expected, DL showed a relatively lower degree of needle Na content under salt stress compared to JL. The increased degree based on mean values was up to 3.5 times, indicating that the capacity to accumulate Na into needles may be higher in JL. Furthermore, DL showed no change in K contents under salt stress as compared with JL. High Na concentration can have negative effects on physiological functions due to the inhibition of enzyme activities and K uptakes (Marschner 2012, Polle and Chen 2015). K has an outstanding role in plant-water relations, contributing to the osmotic potential of cells and tissues (Marschner 2012). Reductions of K contents under salt stress in JL, therefore, supported this competitive absorption with Na. However, the salt effect on needle K content was not significant in DL. Previous studies have also reported stable values of K of other *Larix* species (e.g., *Larix laricina* Du Roi; Renault et al., 2006, *L. decidua* Mill; Plesa et al, 2018). The K homeostasis can be accomplished by cation selectivity in uptake systems from the cytoplasm into vacuoles. Plesa et al. (2018) have pointed out that needle K content of *L. decidua* increased under salt treatment. Since I did not observe any increments of K contents across all treatments, future investigations should compare the specific mechanism differences of K homeostasis within the genus *Larix*.

I observed homeostasis of other mineral contents. Regression analysis showed negative correlations between needle Na and Ca, and between Na and Mg contents in both larches and each larch seedlings (Fig. 3-2-2), while significant salt effects were only observed in JL (Table 3-2-2). In particular, I found significant species differences regarding the relationship between needle Na and Ca contents, suggesting that the Na sensitivity to needle Ca contents was higher in JL than DL. Ca plays an important role in the cell membrane, cell wall stabilization, signaling functions, and the mitigation of salinity (Köster et al., 2019). These results supported the hypothesis that salt tolerance would be greater in DL, and that mineral homeostasis was related to other mineral elements apart from K. DL may obtain the adaptive capacity to salt stress as the original distribution of the species where the primary salinization is likely to occur cause to drought condition (Polezhaeva et al., 2010, Mamet et al., 2019). In contrast, JL is naturally distributed in central Japan. Species differences in adaptive traits, including salt tolerance, may be induced by the geographical isolation from other continental *Larix* species in the interglacial period (Polezhaeva et al., 2010)

While I hypothesized that the increment of N content via the synergy with K^+ uptake would be either species-specific responses or related to osmotic regulations, I did not observe significant changes in needle N content, except for the area-based value of JL (Table 3-2-2). However, I found higher Chl a/b under salt stress in DL, but not in JL. In tamarack saplings (*L. laricina* Du Roi), 60 mM NaCl reduced the total Chl and the Chl a/b (Renault et al., 2006). In *L. decidua*, 150 mM NaCl reduced the total Chl, while the Chl a/b did not change (Plesa et al., 2018). A high value of Chl a/b under salt treatment was previously reported in herbaceous plants, including sunflower (*Helianthus annuus* L., Liu and Shi 2010) and wheat (*Triticum aestivum*, Yang et al., 2008), while a lower Chl a/b was reported in poplar (*Populus alba* x *P. berolinensis*, Wang et al., 2013). Given the preferential reduction in Chl-b than Chl-a under salt stresses, it may act to protect the reaction center core more than the light harvesting capacity related to Chl-b. Future studies should continue to investigate N metabolism, with the consideration that this process may be related closely to Chl metabolic regulation (e.g., Yang et al., 2008).

Irrespective of the present hypothesis, I observed no clear combined effect of eO_3 and salt stress on physiological parameters in larch seedlings (Table 3-2-2). Therefore, even if I employ these larch species to manage soil salinization under eO_3, their initial growth may not be suppressed by eO_3 and salinity stress. Non-significant changes of needle element contents indicated that the element variables were maintained even under the combined effect. These results suggested that eO_3 may not inhibit the element homeostasis of larch species, especially in DL. This may be attributed to non-significant changes of the total dry mass in DL treated with single O_3 and the combined effect. It was reported that the stable P and iron contents in leaves implied homeostatic readjustment, contributing to preventing physiological inhibition of eO_3 (Agathokleous et al., 2018a). It is possible that the combined effect, and even single O_3 effect, were not detected due to the physiological status of seedlings, which were shown in F_v/F_m (Fig. 3-2-1). In all treatments, F_v/F_m showed almost the same value from 0.70 to 0.72, which were significantly lower than the standard normal value of health condition ranged between 0.81 and 0.83 (Schreiber et al., 1986).

Chapter 4: Interspecific difference in salt tolerance between Dahurian larch, Japanese larch and hybrid larch F_1

INTRODUCTION

Global salt affected land is estimated at approximately 1100 Mha (Wicke et al. 2011). Further increments of saline soil have been serious concerned under climate changes (Okur and Örçen 2020), which induces the change in precipitation and evaporation pattern, the rise of sea level, and the second salinization by over-irrigation. Soil salinization is one of worldwide issues in terms of the crop production management as well as the distribution of plant species (Polle and Chen 2015). Better understandings of the natural variability in salt tolerance have contribute to the ecological managements in environmental degradation (Bui 2013) as well as to estimate ecosystem functions under climate change (Chen et al. 2020, Zeng et al. 2020).

Impacts of salinity are mainly composed with both osmotic and ion toxic stresses of sodium (Na) ion, independently affecting plant developments and physiological activities (Lambers 2013). The various mechanisms to cope with salt stresses have been elucidated in crop and model plants over the years (Flowers 2004, Deinlein et al. 2014, Parihar et al. 2015, Munns and Gilliham 2015, van Zelm et al. 2020), for example, (i) the accumulation or exclusion of selective ions; (ii) the regulation of uptake and transport from root to shoots; (iii) ion compartmentalization; (iv) compatible solutes synthesis; and (v) changes in photosynthetic systems.

There are relatively few studies investigating the salt tolerance of woody species where the common purposes are associated with the conservation and environmental engineering from the secondary soil salinization (Polle and Chen 2015), sea level rises (Loucks 2010), deicing salts (Renault 2005), sand surface mining (Duan and Chang 2017).

Regarding ecological rehabilitation in saline soil, research interests in salt tolerances have been addressed in specific woody species at the representative saline soil regions (*Populus* sp, Chen and Polle 2010, *Bruguiera* sp, Kelleway et al. 2017). While massive studies have challenged to elucidate the highly salt-adaptive mechanisms of these model trees even at molecular levels (Chen and Polle 2010), the major species adopted for repairing degraded environments have hardly shown versatile tolerances (Polle et al. 2019), resulting in vulnerable ecosystems to climate change. For example, the plantation of willow (*Salix* sp.) and poplar has shown the high susceptibility to drought due to the high stomatal conductance (Borland et al. 2015, Polle et al. 2019). Further, the biased selection of developed planting species would lead to the biodiversity loss and the fragile ecosystem (Minhas et al. 2020). Thereby, it is needed to investigate the alternative tree species for optimal strategies in ecological rehabilitation (Polle and Chen 2015).

Larch (*Larix* sp.) is one of the most common boreal conifers in northern hemisphere (Gower and Richard 1990). The relationship between habitats of larches and saline soil from central to northeast Asia could imply the salt tolerance in larches. Indeed, it has been reported that Siberian larch (*L. sibirica*) has a relative high salt tolerance in woody species (Ogle and John 2010). One of representative *Larix* species in Asia is Dahurian larch (*L. gmelinii* complex). Dahurian larches have been selected as next-generation species for reforestation in northeast China (Zhang et al. 2000) where saline soil distributes. Hybrid larch F_1, crossed by a subspecies of Dahurian larch, *L. gmelinii* var. *japonica* and Japanese larch (*L. kaempferi*), has several superior traits, for example, the initial growth rate and the biotic resistance (Kurahashi 1988, Kita et al. 2009). However, little is known about the salt tolerance of larch species (Plesa et al. 2018) although larches are often planted in coastal forests (Pâques et al. 2013).

I investigated the morphophysiological and nutritional responses under experimental saline soil between three larch species; Dahurian larch, Japanese larch, and its hybrid larch F_1. The purpose of this study is to characterize salt tolerance of larch species. Larch species, which are not halophyte, would accumulate Na in needles whereas simultaneously other cations to maintain ion balances (Renault 2005, Plesa et al. 2018, Sugai et al. 2019), whereas the physiological significances of cation homeostasis are still under investigated (Rewald 2013). First, I assumed that the maintenance of cation homeostasis would mitigate the effect of Na on photosynthesis.

To verify this hypothesis, I evaluated both the relationship between Na and other cation concentration in needles and the relationship between photosynthetic rate and Na concentration in each species. Then, I compared the interspecific difference of both relationships for evaluating the salt tolerance at leaf-scale. In addition, I focused on the root morphological responses to salinity. Unlike herbaceous plants, woody roots generally show the secondary grow pattern along with their development. However, whether these plastic changes would be associated with salt tolerance remains to be elucidated (Rewald 2012). To quantify the degree of plastic development in both traits, I compared the root developmental difference in each root system of a seedling. I synthesized these results for the construction of novel phenotypes in the alternative plantation species for ecological rehabilitation.

MATERIAL AND METHODS

Experimental site and plant materials

This study conducted a pot experiment in a greenhouse covered with only the vinyl roof to avoid precipitation, located at Hokkaido University, Sapporo, the capital city of Hokkaido (43°07′N, 141°34′E, 15 m above sea level). The temperature in a greenhouse was monitored by a HOBO pendant data logger (UA-002-64, Onset Computer, Co., USA). The mean temperature (± SD) from May to September in a greenhouse were 17.51 ± 8.18 °C, 19.37 ± 6.02 °C, 23.32 ± 5.88 °C, 23.95 ± 5.51 °C, and 19.86 ± 6.80 °C, respectively. Three larch species of seedlings; *L. gmelinii* var. *japonica*, *L. kaempferi*, and its hybrid larch F_1 (*L. gmelinii* var. *japonica* x *L. kaempferi*) were grown for one year from seeds at a nursery at Hokkaido Research Organization, Forestry Research Institute, Bibai. On May 6, 2019, each larch seedling was individually planted in a 5 L pot (TOKAI polypot, 15 cm diameter and 12.5 cm height) before leaf formation, which contained mixed commercial soil to imitate immature volcanic ash soil (Kanuma soil and Akadama soil, volume ratio 1:1). Before starting treatments, I evaluated the Na adsorption capacity of this culture medium, where different amount levels of NaCl were added to a given weight to the same culture medium and the Na concentration in the soil solution was determined. Then, the adsorption rate was calculated as the ratio of the concentration of the extraction to the integrated value of the soil in relation to the amount of added NaCl. The calculated adsorption rate was almost the same between different NaCl levels, as approximately 60.2%. The After planting, adequate amounts of tap water irrigation were carried out regularly to prevent drought until the following experiments. I also applied 200 mL of commercial liquid fertilizer (HYPONEX; Japan, N = 72.4 mg L^{-1}, P = 284 mg L^{-1}, K = 94.2 mg L^{-1}) on a pot once a week until June to prevent soil desiccation and nutrient imbalances. All the prepared seedlings were divided into two groups for the following each experiment. The saline treatment design of each experiment was described as following.

Experiment 1

The saline treatment started on July 11, 2019, after two months from planting for all species once they had completely expanded needle leaves. To elucidate the salt tolerance of each larch species, the saline treatments were established as four levels of NaCl at different amounts; 20 mmol – S1, 40 mmol – S2, 80 mmol – S3, and Control. The target salt amount was achieved by loading 200 mL of each NaCl solution (25 mM – S1, 50 mM – S2, 100 mM – S3) on each pot once every two days over 20 days. Control was achieved by loading 200 mL of tap water with the same days. Three replications in each treatment and two seedlings with each replication and species were established for the first experiment (Total 72 seedlings, n = 3), where the initial size of height in each treatment was aligned by each species on June 10; 8.10 ± 0.05 cm at Control, 7.81 ± 0.22 cm at S1, 8.08 ± 0.21 cm at S2, 7.88 ± 0.20 cm at S3 for Dahurian larch; 15.07 ± 1.24 cm at Control, 14.89 ± 0.87 cm at S1, 14.83 ± 1.32 cm at S2, 14.66 ± 1.61 cm at S3 for Japanese larch;

and 13.83 ± 0.41 cm at Control, 14.03 ± 0.55 cm at S1, 13.91 ± 0.16 cm at S2, 13.37 ± 0.62 cm at S3 for hybrid larch F_1.

Experiment 2

The saline treatment started on August 11, 2019, after three months from planting. The saline treatments were established as two levels of the target concentration; 20 mM – S4, 70 mM – S5 and Control. The target salt concentration was achieved by loading 200 mL of the NaCl solution (20 mM – S4, 70 mM – S5) on each pot once every two days over 24 days. Control was achieved by the same method of the first experiment. Three replications in each treatment and three seedlings with each replication and species were established for the second experiment (Total 81 seedlings, n = 3) , where the initial size of height in each treatment was aligned by each species on August 9; 13.25 ± 1.56 cm at Control, 13.68 ± 1.85 cm at S4, 12.71 ± 1.33 cm at S5 for Dahurian larch; 19.66 ± 2.32 cm at Control, 20.39 ± 2.09 cm at S4, 19.76 ± 1.84 cm at S5 for Japanese larch; and 18.69 ± 2.39 cm at Control, 18.87 ± 2.30 cm at S4, 19.43 ± 2.33 cm at S5 for hybrid larch F_1.

Data collection

Growth

Height of all seedlings was measured on June 10 and July 30 for the first experiment, and on August 9 and September 7 for the second experiment. The calculation of RGR was based on the following equation:

$$RGR = \frac{Ln(S_2) - Ln(S_1)}{t_2 - t_1}$$

where the logarithm difference between initial (S_1) and final (S_2) size was divided by the time difference from the first (t1) to end (t2) of the measurement.

Leaf gas-exchange, LMA, and Chlorophyll fluorescence reactions

Leaf gas-exchange capacity was measured by an open gas-exchange system (LI-6400, Li-Cor Inc., NE, U.S.A.). The measurement was carried out inside the laboratory, where the temperature and relative humidity were kept as 25 °C and 50 ± 10 %. Measurements were conducted between 08:00 and 14:00, JST. For each seedling, we selected six fresh mature needles from the non-shaded position of a branch and attached in the leaf clip chamber of a LI-6400 to be flat. The net photosynthesis rate and stomatal conductance at 400 μmol CO_2 mol^{-1} (P_N, Gs) were determined as the photosynthetic capacity at steady growth condition. The condition inside chamber was kept for the photosynthetic photon flux as 1500 μmol m^{-2} s^{-1}, the water vapor deficit as 1.5 ± 0.5 kPa, and the leaf temperature as 25 ± 2 °C. The value was determined approximately 10 minutes after when the photosynthetic rate reached a steady state. P_N and Gs were measured in all 72 seedlings from July 31 to August 2nd. The measured 2 seedlings were randomly selected from each replication of treatment (Total 24 seedlings in each measurement day).

After each photosynthetic measurements, all the measured needles were sampled, immediately scanned, and were put into a dry oven at 75 °C for a week to determine the dry mass for calculating leaf mass per area (LMA, the ratio of dry mass to area) using Image-J software (U. S. National Institutes of Health, Bethesda, Maryland, USA; Schneider et al. 2012).

In the first experiment, chlorophyll fluorescence reactions were measured with a JUNIOR-PAM (pulse-amplitude modulation fluorometer, Walz, Effeltrich, Germany) from July 31 to August 2nd. Measurements were carried out in the same seedlings of gas-exchange measurements on each day. After the gas-exchange measurement, Seedlings were acclimated in dark conditions for 4 hours from 18:00. A mature green needle was selected, and a fixed distance was set between a needle and the light source by a leaf clip. The measuring light source was a blue LED with a maximum emission wavelength of 450 nm. The stable condition of minimum fluorescence yield (F_0) induced by too-weak modulated light of 0.5 μmol m^{-2} s^{-1} was checked, and the value was measured as soon as possible after setting. Subsequently, the maximum fluorescence yield (F_m) was measured by a saturating pulse light of 5,000 μmol m^{-2} s^{-1}. After measure the responses under the saturating pulse light, the actinic light of 185 μmol m^{-2} s^{-1} was irradiated for measurement of fluorescence quenching components. The steady state fluorescence (Fs) was then recorded within 2 min, and the maximum fluorescence of light adapted state (Fm’) was also determined after a second saturating pulse. The maximal photochemical quantum yield of PSII (F_v/F_m), the effective quantum yield of PSII photochemistry (Y(II)), and the relative electron transport rate (rETR) were calculated as the following equations based on Genty et al. (1989):

$$\frac{F_v}{F_m} = \frac{F_m - F_0}{F_m}$$

$$Y(II) = 1 - \frac{F_s}{F_m{}'}$$

$$rETR = 0.84 \times 0.5 \times Y(II) \times I$$

where *I* is the intensity of photosynthetically active radiation.

Needle and soils element analyses

Flesh mature needles for the element analysis were sampled from July 31 to August 2nd for the first experiment and September 7 for the second experiment. In the first experiment, needles were sampled from the shoots where the gas-exchange capacity was measured. To measure the nutrient status of the needles, approximately 50 mg of powder samples of needles were weighed and digested with 2 ml of 61% nitric acid (Kanto Chemical, Tokyo, Japan) at 110°C for approximately 2 hours. Then, 0.5 ml of hydrogen peroxide was added, and the sample was heated continuously at 110°C for 20 minutes. After cooling to room temperature, 10 ml of 2% nitric acid were added. Then, the concentration of Na in these samples was measured by ICP-MS (ELAN, DRC-e; Perkin Elmer, Waltham, MA, USA). The same element analysis was carried out in culture medium soils for the first experiment. Soil samples were obtained on the same time of root sampling, where three types of soils were sampled; 0 – 5 cm from the surface, 0 – 5 cm from surface the bottom of pot, and root zone, where the soil was sampled by the method of Ishizawa et al. (1957). In each pot, multiple soil samples were randomly obtained from within each determined range, and mixed. To measure the nutrient status of the soil, approximately 10 g of the soil and 25 ml ultrapure water were mixed and shaken for an hour. This sample was centrifuged at 2000 G for 20 minutes. Then, the supernatant fluid was obtained as the soil solution extracted water. To measure soil pH and conductivity, a portable pH meter (LAQUAtwin-PH-33B, HORIBA, Kyoto) and an electric conductivity meter (LAQUAtwin-EC-33B, HORIBA, Kyoto). To measure element contents, the solution was mixed with 61% nitric acid and adjusted for the concentration of 2% nitric acid. Finally, the concentration of Na, K, Ca, and Mg in these samples was measured by ICP-MS.

Dry mass and allocation

Aboveground were harvested in the end of experiment on August 3 for the first experiment, and September 7 for the second experiment. The harvested aboveground of each seedling was divided as following parts; stems, branches and needles. All separated organs were put into a dry oven at 75 °C for two weeks to determine the dry mass. the number of branches was individually counted in the first experiment.

The root system was excavated simultaneously. In the first experiment, the roots were carefully washed for eliminating soil and divided into two parts: fine roots (diameter < 2 mm) and other roots (diameter ≥ 2 mm) using by a digital caliper. Finally, the separated roots were dried in the oven at 75 °C for two weeks, and the dry weight was measured. Based on the value of each dry mass, the ratio of aboveground shoot dry mass to root dry mass (TR ratio) and the ratio of needle dry mass to aboveground shoot dry mass (LMR) were individually calculated.

Root analysis

In the second experiment, two seedlings of root system were randomly selected to analysis morphological parameters in each replication of all treatments (Total 54 root systems). To analysis anatomical traits, one seedling of root system was randomly selected in each replication. Further, the diversity of microbes in root zone was measured in the residual roots of anatomical samples.

To evaluate the morphological analysis, the sampled roots were covered with wet papers, immediately stored in a plastic bag, and transferred to a dark refrigerator (4 °C) in the laboratory until the following measurements. First, the remaining fine soil was carefully removed from roots by a brush. Next, a sampled root was divided into the main root and two types of lateral roots; root-branches under secondary growth, and root branches under primary growth. Then, the main root and five roots of each type were scanned using a double-lamp bed scanner with 800 dpi (GT-X 970, Epson, Japan). The acquired scan image was analyzed to determine total length, total surface area, and total volume of each fine root using by a root analyze software, WinRhizo 2013 Pro (Regent Instruments, Quebec, Canada). These values were used for calculating the following morphological traits values as a ration between the acquired values from the image analysis and the dry weight; specific root length – SRL (a ratio between total length and dry weight); specific root area – SRA (a ratio between total surface area and dry weight); root tissue density – RTD (a ratio between total volume and dry weight).

Regarding the anatomical analysis, both root-branches under the primary and second growth development were cut from whole-root-system sampled and washed, and immediately fixed in 2% glutaraldehyde. These root-branches were sectioned 25 μm thick mainly from Rs using a freezing microtome (Leica CM1950, Leica, Tokyo, Japan). All cross sections were stained with safranin–fast green and dehydrated in 50, 70, 90, 95, and 100% ethanol. Finally, the root sections were photographed under a light microscope (Zeiss AxioObserverZ1, Carl Zeiss, Oberkochen, Germany). The obtained image was analyzed by Image-J software for determining the average size of tracheotomy and the proportion of cell wall fraction (CWF) based on the previous methods (Scholz et al. 2013) with slight modification, which was calculated as following the equation:

$$CWF\ (\%) = \frac{CW_A}{S_A}$$

where the ratio of extracted cell wall area (CW_A) to total area of projected section (S_A).

Statistical analysis

I used ANOVA with Chi-squared test to evaluate the effect of salinity treatment on the measured traits in each species. The model was constructed by the general linear model with Gaussian distribution. The species difference in the relationship between the Na concentration in needles, other cations concentrations, and photosynthetic rate was analyzed by ANCOVA, where the individual data were used with linear model in each species. When the interaction between Na and species was significant ($P<0.05$), the regression analysis was performed in each species. Regarding the relationship between physiological traits and nutritional balance in needles, I firstly performed two types of the correlation analyses in each species for evaluating (i) the relationship between Pn and Na as the photosynthetic salt tolerance (PST), and (ii) the relationship between Na and other four cations as the ionic salt tolerance (IST). To calculate more accurate relationships of PST, and IST, the correlation analysis was performed for all individual responses to the treatments in each species. Finally, I verified the hypothesis that the cation homeostasis would be associated with the physiological functions in a scatter plot with PST and IST (Shema).

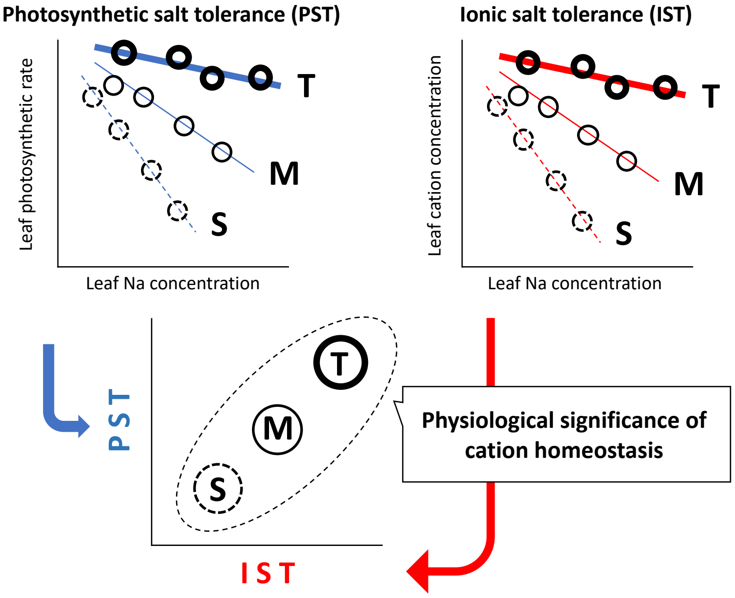

Shema. Analysis of salt tolerance in leaf scale.

Both relationships between leaf photosynthetic rate, leaf cation concentration, and leaf sodium (Na) concentration indicate the photosynthetic salt tolerance (PST) and the ionic salt tolerance (IST) in each species. Relationship between PST and IST mean the leaf salt tolerance, which has a physiological meaning in term of the functional contribution of cation homeostasis. T: Tolerance; M: moderate; S: sensitive.

Since the woody roots show the secondary growth, their specific root weight per morphological trait increases as they develop (Rewald 2012). The changes of specific root weight per morphological trait along with their developments can be interpreted as the combined consequence of the genetic regulation and the plastic responses to environment. To quantify the plastic developments in each morphological trait, I defined SRL and SRA as the carbon use efficiency to from root morphological traits. Based on these values, I calculated the ratio of carbon use efficiency in second growth development to that in primary growth development as the degree of specific root length development (DRL) and that of specific root area development (DRA) in each species. Regarding RTD, which was defined as the carbon cost to from root morphological traits, I calculated the ratio of carbon use efficiency in primary growth development to that in second growth development as the degree of specific root length development (DRD). All statistical analyses were conducted with R version 3.4.6, a free statistical software application (R core team 2017).

RESULTS

Salt treatment significantly reduced P_N, G_s, Fv/Fm, and increased needle Na concentration in all larch species (Table 4-1). Salt treatments significantly suppressed the total dry mass of HL ($P<0.01$) and JL ($P<0.001$). The maximum reduction rate was 20% in DL, 28% in HL, and 36% in JL, respectively (Fig. 4-1). Salinity stress also induced the reduction in LMR approximately 10% in all species and the reduction in HL and JL were significant ($P<0.05$). Besides, the root dry mass was suppressed by salinity stress only in JL ($P<0.001$).

Table 4-1. Summary of Chi-squared test results in the first experiment.

Responses to salinity treatments in Dahurian larch (DL), Japanese larch (JL), and hybrid larch F_1 (HL). Statistically significant levels were ***; $P < 0.001$, **; $P < 0.01$, *; $P < 0.05$, and n.s.; $P \geqq 0.05$.

	DL		HL		JL	
Traits	X^2	P value	X^2	P value	X^2	P value
Total dry mass (g)	1.279	n.s.	7.005	**	12.261	***
Aboveground (g)	2.097	n.s.	10.585	**	8.044	**
Needle (g)	2.358	n.s.	14.618	***	7.836	**
Branch (g)	0.783	n.s.	11.173	***	1.133	n.s.
Stem (g)	0.926	n.s.	0.189	n.s.	2.873	n.s.
Belowground (g)	0.317	n.s.	2.707	n.s.	11.926	***
Fine root (g)	0.531	n.s.	3.140	n.s.	7.527	**
TR ratio ($g\ g^{-1}$)	0.996	n.s.	3.983	*	0.111	*
LMR ($g\ g^{-1}$)	1.753	n.s.	6.594	*	3.966	*
P_N ($\mu mol\ m^{-2}\ s^{-1}$)	6.780	**	4.994	***	4.154	*
G_s ($mol\ m^{-2}\ s^{-1}$)	7.459	**	11.745	***	4.031	*
LMA ($g\ m^{-2}$)	1.136	n.s.	0.080	n.s.	0.023	n.s.
Y(II)	0.206	n.s.	5.047	*	0.65	n.s.
rETR ($\mu mol\ m^{-2}\ s^{-1}$)	0.205	n.s.	4.248	n.s.	0.643	*
F_v/F_m	0.002	***	0.082	**	5.477	***
Na ($mg\ g^{-1}$)	11.444	*	6.954	**	16.267	*
K ($mg\ g^{-1}$)	3.790	n.s.	9.129	n.s.	4.558	n.s.
Ca ($mg\ g^{-1}$)	0.050	n.s.	0.084	n.s.	1.094	n.s.
Mg ($mg\ g^{-1}$)	0.179	n.s.	1.422	n.s.	0.245	n.s.
Fe ($mg\ g^{-1}$)	0.114	n.s.	0.025	n.s.	0.259	n.s.

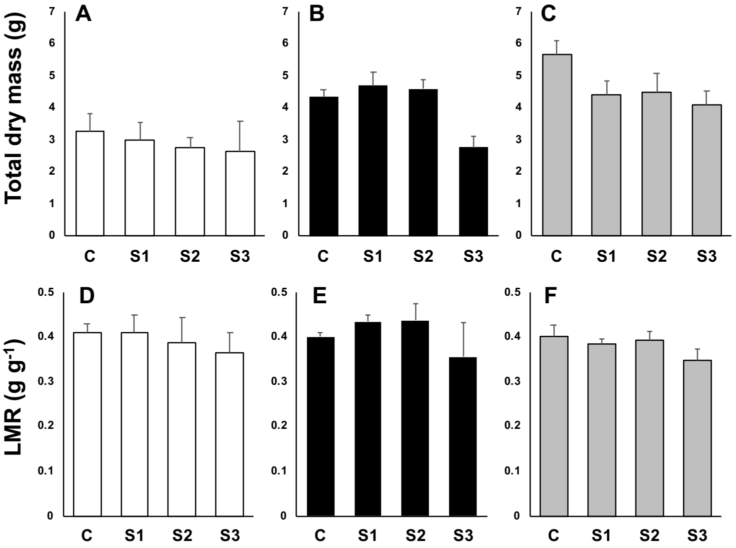

Fig. 4-1. Responses to total dry mass and LMR in the first experiment

Mean value of total dry mass (A-C) and LMR (D-F) in Dahurian larch (A, D; white), Japanese larch (B, E; black), and hybrid larch F_1 (C, F; gray) to control (C), 20 mmol Na (S1), 40 mmol Na (S2), and 80 mmol (S3). Error bar means standard error.

Results of ANCOVA showed that the regression coefficient between Na and K was 0.24 (Fig. 4-2A, $R = 0.19$, $P<0.01$) and between Na and P_N was –0.01 (Fig. 4-2E, $R = 0.25$, $P<0.001$). Besides, the relationship between Na and other cations – Ca and Mg concentration varied between larch species. In particular, HL showed the positive regression coefficient between Na and Ca ($R = 0.51$), and Mg ($R = 0.50$), which were opposite to other two species. The relationships between PST and IST were shown in each ratio of Na to other cations (Fig. 4-3). The highest negative PST was observed in JL, which was higher approximately 40% than the lowest PST of HL. Except for the ratio of Na to K (Fig. 4-3A), the scatter plot mapped the similar relationships between DL and JL since the ISTs of HL were the highest in three larches.

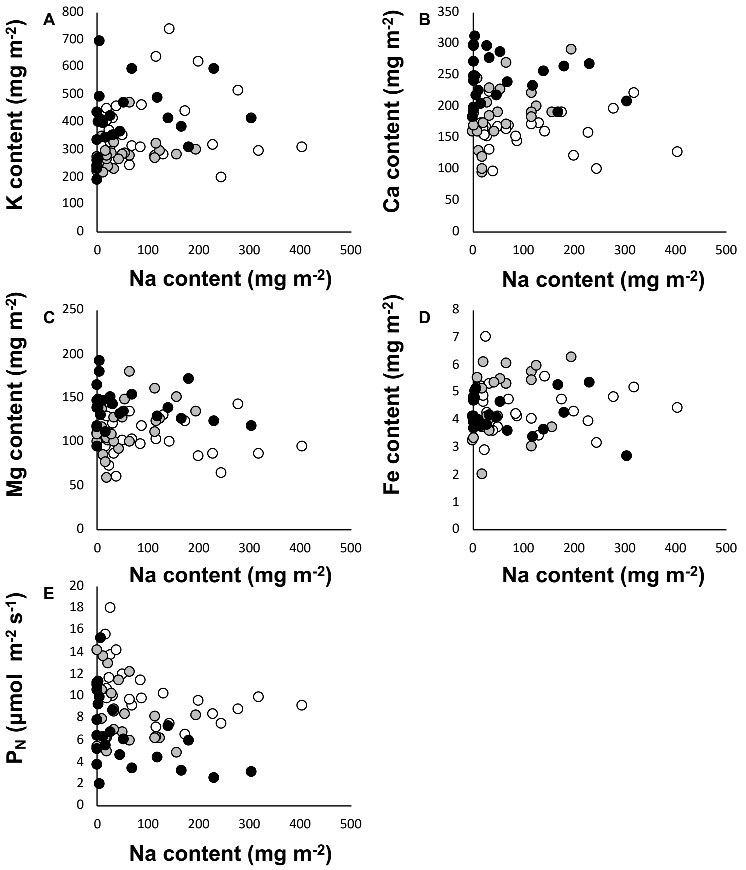

Fig. 4-2. Area-based relationship between needle Na contents, other cations, and photosynthesis in the first experiment.

Needle area-based relationship between Na contents and (i) K content (A), (ii) Ca content (B), Mg content (C), (iii) Fe content (D), and (iv) P_N in Dahurian larch (white), Japanese larch (black), and hybrid larch F_1 (gray). Each point was represented by an individual seedling (N=24 in each species, pooled within all the treatment).

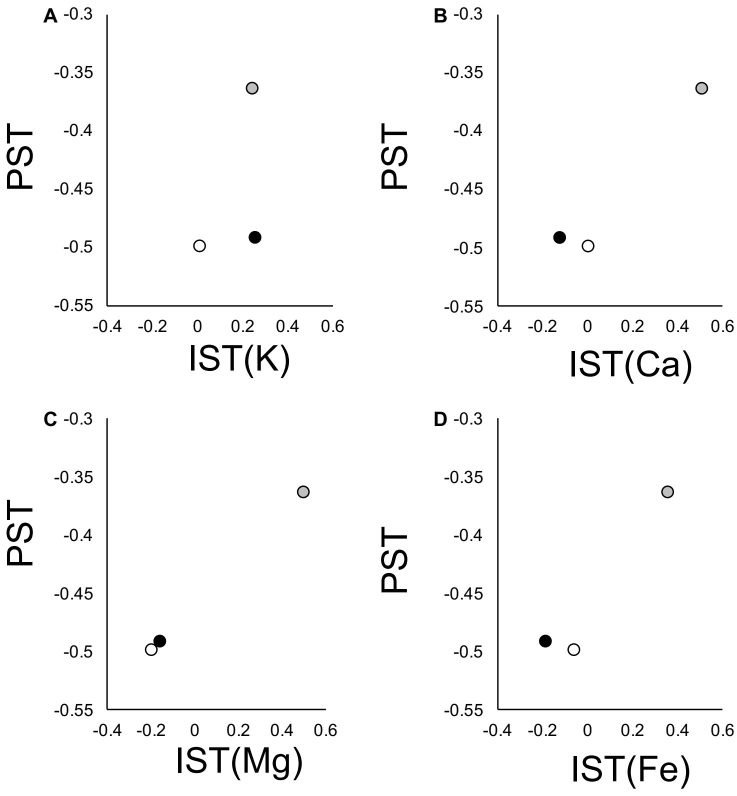

Fig. 4-3. Relationship between photosynthetic salt tolerance (PST) and ionic salt tolerance (IST).

Scatter plot showed the relationship between PST and IST of each cation (Na to K – A, Na to Ca – B, Na to Mg – C, Na to Fe – D) comparing three larch species; Dahurian larch (white), Japanese larch (black), and hybrid larch F_1 (gray). Each point represented the coefficient calculated by responses to all treatments in each species.

Salt treatments in the second experiment suppressed the total dry mass of JL (Table 4-2, P<0.001). The maximum reduction rate was 28% in JL whereas other species did not show the reduction in dry mass of both aboveground and belowground (Fig. 4-4). SRL and SRA were higher under primary growth development than those under secondary growth development and main roots. The opposite trend was obvious in RTD regardless of species difference (Table 4-3).

Table 4-2. Summary of Chi-squared test results in the second experiment.

Responses to salinity treatments in Dahurian larch (DL), Japanese larch (JL), and hybrid larch F_1 (HL). Statistically significant levels were ***; $P < 0.001$, **; $P < 0.01$, *; $P < 0.05$, and n.s.; $P \geqq 0.05$.

		DL		JL		HL	
Traits		X2	P value	X2	P value	X2	P value
Total dry mass (g)		0.353	n.s.	11.815	***	0.112	n.s.
Aboveground (g)		0.394	n.s.	8.803	**	0.522	n.s.
Belowground (g)		0.200	n.s.	13.495	***	0.014	n.s.
Na (mg g^{-1})		28.599	***	10.745	**	13.256	***
SRL (cm g^{-1})	1st	1.340	n.s.	0.923	n.s.	0.011	n.s.
	2nd	0.593	n.s.	0.914	n.s.	0.001	n.s.
	Main	0.151	n.s.	1.725	n.s.	0.274	n.s.
SRA (cm^2 g^{-1})	1st	0.063	n.s.	0.418	n.s.	3.284	n.s.
	2nd	1.045	n.s.	0.838	n.s.	0.035	n.s.
	Main	0.662	n.s.	0.391	n.s.	0.327	n.s.
RTD (g cm^3)	1st	0.423	n.s.	0.443	n.s.	1.487	n.s.
	2nd	0.849	n.s.	0.379	n.s.	0.017	n.s.
	Main	0.836	n.s.	1.051	n.s.	0.138	n.s.
DRL		0.059	n.s.	6.917	**	0.527	n.s.
DRA		0.265	n.s.	3.781	n.s.	0.162	n.s.
DRD		0.042	n.s.	0.007	n.s.	0.753	n.s.

Table 4-3. Results of root morphological analysis in the second experiment.

Mean value ± standard error of SRL, SRA, and RTD to control (C), 20 mmol Na (S4), and 70 mmol (S5) in Dahurian larch (DL), Japanese larch (JL), and hybrid larch F_1 (HL).

		DL			JL			HL		
Traits		C	S4	S5	C	S4	S5	C	S4	S5
SRL (cm g^{-1})	1st	17.37 ± 4.17	15.14 ± 4.10	26.74 ± 16.37	27.15 ± 6.05	31.7 ± 7.24	24.59 ± 1.14	24.39 ± 2.33	20.29 ± 1.16	17.74 ± 8.40
	2nd	1.79 ± 0.43	1.32 ± 0.32	1.93 ± 0.14	0.88 ± 0.08	1.43 ± 0.47	1.4 ± 0.58	0.81 ± 0.16	1.45 ± 0.23	1.03 ± 0.39
	Main	0.55 ± 0.16	0.58 ± 0.18	0.62 ± 0.27	0.48 ± 0.09	0.53 ± 0.09	0.39 ± 0.09	0.34 ± 0.11	0.38 ± 0.06	0.36 ± 0.03
SRA (cm^2 g^{-1})	1st	264.74 ± 20.28	268.95 ± 17.44	274.51 ± 66.71	282.14 ± 6.64	282.97 ± 12.20	271.62 ± 31.37	229.43 ± 21.33	212.96 ± 9.00	226.43 ± 8.16
	2nd	65.03 ± 9.08	61.62 ± 9.24	71.71 ± 6.95	49.8 ± 2.24	57.88 ± 7.73	58.12 ± 10.89	46.39 ± 2.48	52.12 ± 4.96	50.15 ± 7.72
	Main	29.1 ± 4.21	27.95 ± 4.83	32.95 ± 8.17	28.56 ± 3.90	31.95 ± 2.7	27.35 ± 3.89	25.16 ± 3.99	24.77 ± 2.83	24.62 ± 0.87
RTD (g cm^{-3})	1st	0.29 ± 0.01	0.32 ± 0.07	0.32 ± 0.04	0.28 ± 0.07	0.4 ± 0.10	0.36 ± 0.04	0.47 ± 0.07	0.54 ± 0.09	0.38 ± 0.14
	2nd	0.60 ± 0.27	0.48 ± 0.06	0.44 ± 0.03	0.49 ± 0.04	0.46 ± 0.03	0.5 ± 0.02	0.44 ± 0.03	0.59 ± 0.08	0.51 ± 0.09
	Main	0.84 ± 0.24	0.71 ± 0.15	0.66 ± 0.15	0.84 ± 0.13	0.58 ± 0.1	0.66 ± 0.03	0.63 ± 0.11	0.72 ± 0.06	0.78 ± 0.24

Besides, the root morphological traits were not significantly changed under salinity stresses in any species (Table 4-2). The maximum SRL under primary growth development was JL at S4, which was approximately two times of DL at the same salinity level. At control condition, DRL of JL was the highest in the species, which was approximately three times of DL (Fig. 4-5). The same trends were observed in DRA and DRD. Further, the salt stresses significantly reduced DRL of JL (Table 4-2, P<0.01) whereas other species did not show the significant changes at any treatments.

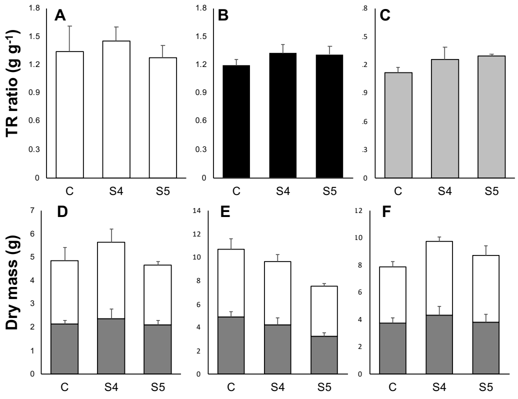

Fig. 4-4. Responses of TR ratio and dry mass in the second experiment

Mean value of TR ratio (A-C) and dry mass (D-F) of aboveground (above, white) and belowground (below, dark gray) in Dahurian larch (A, D; white), Japanese larch (B, E; black), and hybrid larch F₁ (C, F; gray) under the treatments of control (C), 20 mmol Na (S4), and 70 mmol (S5). Error bar means standard error.

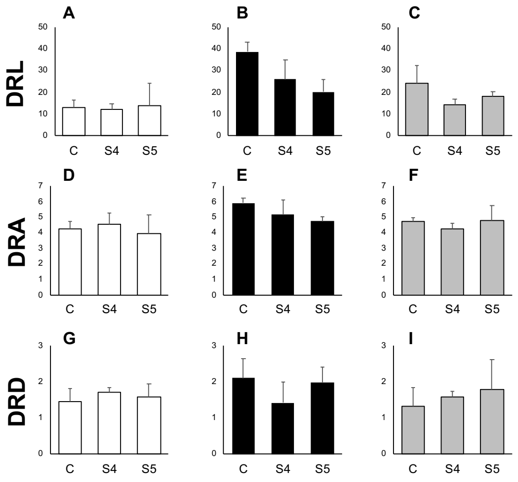

Fig. 4-5. The degree of root morphological development in the second experiment

Mean value of DRL (A-C), DRA (D-F), and DRD (G-I) in Dahurian larch (A, D; white), Japanese larch (B, E; black), and hybrid larch F₁ (C, F; gray) under the treatment of control (C), 20 mmol Na (S4), and 70 mmol (S5). Error bar means standard error.

DISCUSSION

The relationship between cation balances and photosynthesis

I compared the morpho-physiological traits between three larch species of seedlings. One of common nutritional responses to salinity impacts in glycophytes is known as to keep the low concentration of Na in leaves by specific strategies as like Na exclusion, block of absorption or transportation to leaves (van Zelm 2020). In this study, however, any negative regression coefficients were not observed. These results supported the previous study (Renalt 2005), suggesting that the blocking mechanisms would not be expected due to the linear increments of needle Na concentration (Plesa et al. 2018). In general, the Na accumulation induce the reduction of K concentration due to the same transport systems (Flowers et al. 1977, Munns and Tester 2008). Besides, it has reported that European larch (*L. decidua*) and tamarack (*L. laricina*) seedlings maintained or increased K concentration in needles under NaCl loading (Renault 2005, Plesa et al. 2018). The maintenance of K concentration under salt stresses has been reported in other plants, including conifer species (Shiop et al. 2015). Plesa et al. (2018) have suggested that salinity impacts would activate the K transport of European larch, which resulted in the increment proline probably for regulating osmotic conditions. Further, I found that both Ca and Mg concentrations were also not reduced under salt stresses in HL (Fig. 4-2). The mitigation effect of Ca on excess Na accumulation was generally reported (Kouchi and Kumazawa 1975, Marschner 2011). Although the physiological mechanisms to maintain needle Ca concentration, it would be related to salt tolerance of larch species. Besides, Mg has an essential role of several proteins synthesis as like chlorophyll, glycolytic pathway, and N metabolism. Previous study has reported that the activity of Mg transporter was correlated with one of Na influx transporters (Farooq et al. 2018), which might be a cue to understand the complex mechanisms of cation homeostasis.

I focused on the effects of cation balances on photosynthetic rate (Fig. 4-3). PST and IST of HL were the highest in three larches, meaning that the salt tolerance at leaf scale would be most superior in HL, which probably might be caused by the heterosis.

Heterosis is a specific phenomenon in hybrid F_1 where the superior phenotypic traits occur than the two parents (Lippman and Zamir 2007). Previously, several vigor traits of salt tolerance have been reported in crop (King et al. 1997, SarangaY et al. 1991) and tree species (Zeng et al. 2015). The superior phenotypic traits in hybrid plants under salt stresses are the growth increment (SarangaY et al. 1991), which could be induced by the developed antioxidative capacities. Focusing on larch species, the interspecific hybridization commonly occurs due to the continuous distribution (Pâques 1989, Polezhaeva et al. 2010), which has attracted numerous studies so far (Baltunis and Greenwood 1999, Marchal et al. 2017). Given that the paternal inheritance of chloroplast was observed in most *Larix* sp. (Szmidt et al. 1987), it would be expected that the photosynthetic traits would be similar between JL and HL (Koike et al. 1988, Harayama et al. 2013). Results of ANCOVA in this study have indicated that the interspecific difference would not be significant in the relationship between P_N and needle Na concentration (Fig. 4-2). These results partly supported previous study (Matyssek and Schulze 1987), reported that there would not be significant difference in relationship between photosynthetic capacity and needle N concentration between hybrid larch and its parents. Thereby, I consider that the superior salt tolerance at leaf scale could be induced by IST in hybrid larch F_1. Although I did not understand the physiological mechanisms of cation homeostasis, it is noteworthy that the beneficial consequence of maintained ion balance could be verified from biosynthesis of compatible solutes (e.g. proline) as well as physiological functions.

Root morphological developments

Root morphological traits are linked to the hydraulic conductivity, the root proliferation, and the absorption capacity under salt stresses (Rewald 2012). Here, I validated the interspecific difference in the degree of carbon use efficiency change in root development among JL, HL, and DL (Fig.4-5). Results indicated that the carbon use efficiency of root branched under secondary growth development was significantly reduced in JL, and its degree was higher than other larch species. This interspecific difference would partly support the previous studies (Qu et al. 2016), where the root morphological traits of JL seedlings just after germination was higher than those of HL under different soil temperature. In contrast, other two species seem to maintain the carbon use efficiency in root development between primary and secondary growth development.

These interspecific differences indicate that the capacity of root morphological development would high in Dahurian larch complex probably due to the adaptive strategies in belowground. Compared to JL, Dahurian larch generally distributes in flatland environment with relatively lower elevation (Gower and Richard 1990). It has reported that several conifers native to lower elevation ecotypes would show the relatively vigorous growth based on an enough growth season rather than those of higher elevation ecotypes (Körner 2003). Besides, the original habitats of JL are considered as the relatively higher elevation regions. Indeed, a rapidly root growth of JL has been considered as the characteristic of pioneer successional species (Asada and Sato 1981), which perhaps would be associated with the higher DRL of JL.

The increments of SRL and SRA under salinity would be expected as the compensation for suppressed root functions. This hypothesis has partly been supported by previous studies (Echeverria et al. 2008). It has reported that the secondary growth development would be associated with the root longevity without further elongation under salt stresses (Neves et al. 2010). While, the contrast results indicated that the high variability of morphological responses between root types and orders (Rewald et al. 2012). In this study, DRL of JL was significantly reduced by salt stresses, indicating that JL might acclimate salt stresses by changing the carbon use efficiency in root morphological developments. Although there were not significant changes (Table 4-2, $\chi^2 = 3.78$, $P = 0.05$), DRA of JL showed the same trends. These results would agree with the above hypothesis (Echeverria et al. 2008). While, the maintained the carbon use efficiency was also observed in other two larch species, which did not show the suppression of total dry mass under salt stresses.

It indicated that the high carbon efficiency of root morphological development would be related to the salt tolerance in larch species. I further considered the available factor of carbon efficiency changes in root development from the anatomical measurements although there were non-significant changes in CWF under salt stresses regardless of root types.

Chapter 5: General Discussion

Risk assessment toward sustainable forest management

Under rapid environmental changes enforcing the urgent shift from previous mono-cultural productions to a novel forest management with improved forest diversity, larch trees would have a potential as another species adding to world major afforestation species. Larch has several superior traits for forestry as like its fast growth at juvenile growth, high resistant to biotic and abiotic stresses, wood density, natural endurance based on heartwood (Asada and Sato 1981, Kita et al. 2009), resulting in commonly utilization and high expectation and in Europe, North America, and Asia (Asada and Sato 1981, Gower and Richards 1990, Pâques et al. 2013). Further, the development in tree breeding and processing for larch has gradually addressed the use of larch as alternative afforestation species (Ryu et al. 2009, Mason and Zhu 2014, Kita et al. 2018).

For confirming the sustainable productivity of managed forest, it is needed to evaluate the effects of rapidly changing environment since the performance of ecological functions are long term. Sustainable afforestation is closely correlated with ecological services, and it would be achieved with the risk assessment to changing environments (Keenan 2015, Kijowska-Oberc et al. 2020). Here, the eco-physiological insights are essential for better understanding of the adaptive strategies based on the biological knowledge between several scales, which provide quite important parameters at whole-plant level, i.e. growth responses, as a consequence of physiological reactions as well as the clearest indicator of yield.

I have compared the stress responses of a breeding-developed hybrid with those of their parents. Chronic exposure to O_3 induced non-linear responses in both larches, which showed stress at low and high O_3 exposures. Stress induced by low exposure to O_3 led to suppressed dry matter production in hybrid larch but did not lead to lower dry matter in Japanese larch, suggesting a restoration cost under O_3 stress was relatively high in hybrid larch and a potential difference in the biological plasticity between larches.

In addition, growth and physiological responses of Japanese larch and a hybrid larch

F_1 varied based on the combined effects of N loading as well as elevated O_3. Furthermore, N loading mitigated the negative effects of O_3 on the total dry mass of Japanese larch. Conversely, N loading increased O_3 sensitivity in hybrid larch F_1 to some extent. These results have several implications; (i) a productive efficiency under N loading was relatively higher in hybrid larch, which suggested the potential difference in plastic responses between larches and (ii) the growth sensitivities to O_3 stress were altered by N loading, meaning the response capacity to O_3 could be labile trait for larches. The reason why the O_3 sensitivity is a labile would be related to both the quality as environmental stresses for plants and the plant capacity as evolutionarily adaptive traits. The responses to anthropogenic pollutants might not be directly associated with developed adaptive traits.

Implication in ecophysiological study of larch

This study investigated the variability of growth responses in larch seedlings depending on environmental conditions and species difference. Understanding of why responses to manipulated condition are variable due to the presence of other contaminated factors and the interspecific difference would provide reasonable clues for how a given species adapt the specific environment and has a certain distribution as a result. Further, the variable response between hybrid and parent(s) is key component for understanding how the genetic diversity of a species is created and maintained. Both provided insights could further contribute to the normative guidelines; which species to plant where, and what traits to breed, for novel forest management under changing environment.

Although the ecological significance would not be fully understood in the responses to air pollutants, the distribution of woody species would be restricted by the adaptive strategies to soil salinity (Kozlowski 1997, Bui 2013, Chen and Polle 2010). I elucidated the salt tolerance of three larch species, suggesting that larch species might adapt to salt stresses by accumulating Na rather than blocking the adsorption or transport from root to shoots. Japanese larch had the relatively high susceptibility of salt stresses at a whole-plant level while hybrid larch F_1 would have the most superior tolerance at a leaf-level. Root morphological responses would be associated with salt tolerance of larch species. The changes of the carbon use efficiency in roots would be acclimation to salt stresses (Rewald 2012) as both types of avoidance and resistance to stresses. On the other hands, the carbon use efficiency of root developments was maintained in Dahurian larch and hybrid larch F_1. When considering the geographical relationship between saline soil and larch distribution in Northeast Asia, relatively high tolerance in Dahurian larch would be reasonable, which also showed the highest Na accumulation in needles. On the other hands, Japanese larch would not be expected as salt tolerance since it is the most southerly distributed with a predominantly mountainous environment.

Hybrid larch F_1 would have the superior salt tolerance rather than its parent larch seedlings at a leaf level. The vigor capacity of hybrid larch F_1 may indirectly represent the geological factor regulating larch distribution in Northeast Asia while hybrid larch F_1 was artificially developed and its crossbreeding seems not to naturally occur. However, if heterosis occurs in salt tolerance of larch species, salt tolerance might be novel factor which defines the southern limitation of larch species in Eurasian continent, where the saline soil is also distributed. Given that the hybridization commonly occurs between *Larix* taxa, these results might provide insights for better understanding of heterosis in the potential capacity to respond environments as well as for developing breeding technologies to adapt changing environment.

Future larch afforestation has a widely expectation in Northeast Asia whereas serious concerns about the impacts of changing environment still remain. I conclude that the risk of larch seedlings under elevated O_3 is potentially high whereas larch has also a high potential capacity for repairing degraded environments. With reforestation already underway, the decisions for sustainable reforestation under rapidly changing environment are quite complicated that more advanced knowledge is essential. I believe that results shown in this study will serve as a functional guideline of larch afforestation.

Summary

1) Interspecific differences of afforestation species were revealed in responses to elevated ground-level ozone (O_3) and nitrogen (N) loading. Japanese larch decreased photosynthetic capacity with decreasing needle N under elevated O_3 while Sakhalin fir would allocate N from aged needles to current ones.
2) Relatively higher O_3 sensitivity was observed in hybrid larch F_1 than in Japanese larch. I found “hormesis”; the non-linear responses to elevated O_3 in larch, where growth was suppressed by high O_3 concentration whereas it was contrarily increased under low O_3 concentration.
3) Based on the contrast responses to effects of O_3 and N loading, the risks assessment of O_3 in larches requires the selection of afforestation area in terms of soil N condition. Results also showed the vulnerability of O_3 sensitivities itself in larch which could be variable by N loading.
4) Simulation of soil salinization at northeast Asia demonstrated that the salt tolerance would vary between larch species while it might not be affected by O_3 exposure. Results indicated the interspecific differences in salt tolerance between larch species.
5) Needle sodium accumulation simultaneously occurred with other cations, suggesting that salt tolerance of larches would be associated with maintaining of cation homeostasis. Hybrid larch F_1 was superior than parents in the relationship between the cation balance and photosynthetic sensitivity to sodium, as a needle salt tolerance.
6) Changes in carbon use efficiency of roots, especially specific root length corresponded to variable salt tolerance between larch species, which would represent the different adaptive strategies of underground.
7) Results of comparison between hybrid larch and parent(s) in stress responses will help further our understanding in the conservation of genetic diversity as well as identification of traits to be bred, i.e. the the response capacity to environment.
8) Larch has superior potentials for novel forest management under changing environments, which would be achieved by the selection of afforestation area and the breeding in response capacity.

Acknowledgement

本研究の遂行ならびに論文執筆にあたり多大なご指導とご配慮いただきました、北海道大学農学部 植物栄養学研究室 准教授 渡部敏裕先生に心から感謝致します。本論文の御校閲、ならびに寛大な御支援をいただきました同研究室 教授 信濃卓郎、助教 丸山隼人先生、名誉教授 小池孝良先生、林産製造学研究室 教授 玉井裕先生に心から感謝致します。北海道総合研究機構 林業試験場 来田和人博士をはじめとする皆様には、研究材料の分譲のみならず、多くの御支援をいただきました。同試験場 石塚航博士には、いつも快く研究の相談に応じていただきました。本当にありがとうございました。実験の遂行にあたり、北海道大学北方圏フィールド科学センター札幌研究林の利用を許していただきました林長 佐藤冬樹教授、苗畑を管理していただきました故 市川一様、藤戸永志様、佐々木圭子様に心から感謝致します。本研究の遂行に際して、沢山の御支援をいただきました森林総合研究所 北尾光俊博士、南京信生工程大学 Agathokleous Evgenios 教授、南開大学 石福巨教授、北海道教育大学 出口哲久准教授、信州大学助教 牧田直樹先生、矢原ひかり様、北海道大学農学部作物学研究室 講師 柏木純一先生、同助教 中島大賢先生、環境科学院 杉本敦子教授、星野悠美様、平田聡之助教、樹木生物学研究室 佐野雄三教授、渡邊陽子博士、造林学研究室 澁谷正人教授、同講師 斎藤秀之先生に厚く御礼申し上げます。

多くの素晴らしい出会いに恵まれて、研究生活を送ることができました。特に、小池先生には初めて配属された造林学研究室から今日に至るまで、懇切丁寧に御指導いただきました。先生の飽くなき探究心には常に感化され、これまで研究に励むことができました。また博士課程では、渡部先生、信濃先生、丸山先生、森美紀様、今井希様に、研究以外の面でも御支援をいただきました。研究の世界に飛び込むことを後押ししていただいた小林真先生、内田義崇先生に深く感謝しています。林産製造学研究室、造林学研究室、植物栄養学研究室をはじめとする多くの皆様には、本当に沢山の御支援をいただきました。この場を借りて、心から御礼申し上げます。本当にありがとうございました。

最後になりますが、遠方から学生生活を見守り、支援していただきました両親に心から感謝致します。

2020年6月　菅井徹人

References

Abaimov, A. P. (2010). Geographical distribution and genetics of Siberian larch species. In *Permafrost ecosystems,* pp. 41-58. Springer, Dordrecht.

Abaimov, A. P., Zyryanova, O. A., Prokushkin, S. G., Koike, T., Matsuura, Y. (2000). Forest ecosystems of the cryolithic zone of Siberia: regional features, mechanisms of stability and pyrogenic changes. *Eurasian Journal of Forest Research*, *1*, 1-10.

Aber, J. D., Nadelhoffer, K. J., Steudler, P., Melillo, J. M. (1989). Nitrogen saturation in northern forest ecosystems. *BioScience*, *39*(6), 378-286.

Agathokleous, E. (2017). Perspectives for elucidating the ethylenediurea (EDU) mode of action for protection against O_3 phytotoxicity. *Ecotoxicology and Environmental Safety*, *142*, 530-537.

Agathokleous, E. (2018a). Environmental hormesis, a fundamental non-monotonic biological phenomenon with implications in ecotoxicology and environmental safety. *Ecotoxicology and Environmental Safety* 148, 1042-1053.

Agathokleous, E., Kitao, M., Qingnan, C., Saitanis, C. J., Paoletti, E., Manning, W. J., et al. (2018b). Effects of ozone (O_3) and ethylenediurea (EDU) on the ecological stoichiometry of a willow grown in a free-air exposure system. *Environmental Pollution*, *238*, 663-676.

Agathokleous, E., Saitanis, C. J., Koike, T. (2015). Tropospheric O_3, the nightmare of wild plants: a review study. *Journal of Agricultural Meteorology*, *71*(2), 142-152.

Agathokleous, E., Saitanis, C. J., Wang, X., Watanabe, M., Koike, T. (2016). A review study on past 40 years of research on effects of tropospheric O_3 on belowground structure, functioning, and processes of trees: a linkage with potential ecological implications. *Water, Air, & Soil Pollution*, *227*(1), 33.

Agathokleous, E., Vanderstock, A., Kita, K., Koike, T. (2017). Stem and crown growth of Japanese larch and its hybrid F_1 grown in two soils and exposed to two free-air O_3 regimes. *Environmental Science and Pollution Research*, *24*(7), 6634-6647.

Ainsworth, E. A., Lemonnier, P., Wedow, J. M. (2020). The influence of rising tropospheric carbon dioxide and ozone on plant productivity. *Plant Biology*, *22*, 5-11.

Ainsworth, E. A., Long, S. P. (2005). What have we learned from 15 years of free-air CO_2 enrichment (FACE)? A meta-analytic review of the responses of photosynthesis, canopy properties and plant production to rising CO_2. *New Phytologist*, *165*(2), 351-372.

Ainsworth, E. A., Yendrek, C. R., Sitch, S., Collins, W. J., Emberson, L. D. (2012). The effects of tropospheric ozone on net primary productivity and implications for climate change. *Annual Review of Plant Biology*, *63*, 637-661.

Aitken, S. N., Whitlock, M. C. (2013). Assisted gene flow to facilitate local adaptation to climate change. *Annual Review of Ecology, Evolution, and Systematics*, *44*, 367-388.

Akaike, H. (1974). A new look at the statistical model identification. *IEEE transactions on automatic control*, *19*(6), 716-723.

Akimoto, H. (2017). Overview of policy actions and observational data for $PM_{2.5}$ and O_3 in Japan: A study of urban air quality improvement in Asia. *JICA Research Institute*.

Akimoto, H., Mori, Y., Sasaki, K., Nakanishi, H., Ohizumi, T., Itano, Y. (2015). Analysis of monitoring data of ground-level ozone in Japan for long-term trend during 1990–2010: Causes of temporal and spatial variation. *Atmospheric Environment*, *102*, 302-310.

Alcántara, E., de la Guardia, M. D., Montilla, I., Romera, F. J. (2006). Interaction between ozone exposure and iron nutrition in two tobacco cultivars. *Journal of Plant Nutrition*, *29*(12), 2245-2255.

Alexeyev, V. A., Birdsey, R. A., Stakanov, V. D., Korotkov, I. A. (2000). Carbon storage in the Asian boreal forests of Russia. In *Fire, Climate Change, and Carbon Cycling in the Boreal Forest*, pp 239-257. Springer, New York, NY.

Allen, J. A., Chambers, J. L., Stine, M. (1994). Prospects for increasing the salt tolerance of forest trees: a review. *Tree Physiology*, *14*(7-8-9), 843-853.

Arnold, P. A., Kruuk, L. E., Nicotra, A. B. (2019). How to analyze plant phenotypic plasticity in response to a changing climate. *New Phytologist*, *222*(3), 1235-1241.

Asada, S., Sato, T. (1981). The afforestation of Japanese larch trees. Nobunkyo,Tokyo (in Japanese)

Azam, G., Grant, C. D., Nuberg, I. K., Murray, R. S., Misra, R. K. (2012). Establishing woody perennials on hostile soils in arid and semi-arid regions–A review. *Plant and Soil*, *360*(1-2), 55-76.

Babushkina, E. A., Vaganov, E. A., Grachev, A. M., Oreshkova, N. V., Belokopytova, L. V., Kostyakova, T. V., Krutovsky, K. V. (2016). The effect of individual genetic heterozygosity on general homeostasis, heterosis and resilience in Siberian larch (*Larix sibirica* Ledeb.) using dendrochronology and microsatellite loci genotyping. *Dendrochronologia*, *38*, 26-37.

Ball, M. C. (1988). Ecophysiology of mangroves. *Trees*, *2*(3), 129-142.

Baltunis, B. S., Greenwood, M. S. (1999). Variation in lateral shoot elongation patterns and hybrid vigor in full-sib families and interspecific hybrids of larch. *Tree Physiology*, *19*(2), 131-136.

Barnes, J. D., Balaguer, L., Manrique, E., Elvira, S., Davison, A. W. (1992). A reappraisal of the use of DMSO for the extraction and determination of chlorophylls a and b in lichens and higher plants. *Environmental and Experimental Botany*, *32*(2), 85-100.

Barnes, J. D., Pfirrmann, T., Steiner, K., Lütz, C., Busch, U., Küchenhoff, H., Payer, H. D. (1995). Effects of elevated CO_2, elevated O_3 and potassium deficiency on Norway spruce [*Picea abies* (L) Karst.]:

seasonal changes in photosynthesis and non-structural carbohydrate content. *Plant, Cell & Environment*, *18*(12), 1345-1457.

Batavia, C., Nelson, M. P. (2016). Conceptual ambiguities and practical challenges of ecological forestry: a critical review. *Journal of Forestry*, *114*(5), 572-581.

Bell, D. T. (1999). Australian trees for the rehabilitation of waterlogged and salinity-damaged landscapes. *Australian Journal of Botany*, *47*(5), 697-716.

Bernacchi, C. J., Singsaas, E. L., Pimentel, C., Portis Jr, A. R., Long, S. P. (2001). Improved temperature response functions for models of Rubisco-limited photosynthesis. *Plant, Cell & Environment*, *24*(2), 253-259.

Beyers, J. L., Riechers, G. H., Temple, P. J. (1992). Effects of long-term ozone exposure and drought on the photosynthetic capacity of ponderosa pine (*Pinus ponderosa* Laws.). *New Phytologist*, *122*(1), 81-90.

Binkley, D., Högberg, P. (2016). Tamm review: revisiting the influence of nitrogen deposition on Swedish forests. *Forest Ecology and Management*, *368*, 222-239.

Bleeker, A., Hicks, W. K., Dentener, F., Galloway, J., Erisman, J. W. (2011). N deposition as a threat to the World's protected areas under the Convention on Biological Diversity. *Environmental pollution*, *159*(10), 2280-2288.

Borland, A. M., Wullschleger, S. D., Weston, D. J., Hartwell, J., Tuskan, G. A., Yang, X., et al. (2015). Climate-resilient agroforestry: physiological responses to climate change and engineering of crassulacean acid metabolism (CAM) as a mitigation strategy. *Plant, Cell & Environment*, *38*(9), 1833-1849.

Bouwman, L., Goldewijk, K. K., Van Der Hoek, K. W., Beusen, A. H., Van Vuuren, D. P., Willems, J., et al. (2013). Exploring global changes in nitrogen and phosphorus cycles in agriculture induced by livestock production over the 1900–2050 period. *Proceedings of the National Academy of Sciences*, *110*(52), 20882-20887.

Box, G. E., Cox, D. R. (1964). An analysis of transformations. *Journal of the Royal Statistical Society: Series B (Methodological)*, *26*(2), 211-243.

Breed, M. F., Harrison, P. A., Blyth, C., Byrne, M., Gaget, V., Gellie, N. J., et al. (2019). The potential of genomics for restoring ecosystems and biodiversity. *Nature Reviews Genetics*, *20*(10), 615-628.

Brodribb, T. J., Powers, J., Cochard, H., Choat, B. (2020). Hanging by a thread? Forests and drought. *Science*, *368*(6488), 261-266.

Bui, E. N. (2013). Soil salinity: a neglected factor in plant ecology and biogeography. *Journal of Arid Environments*, *92*, 14-25.

Bussotti, F. (2008). Functional leaf traits, plant communities and acclimation processes in relation to oxidative stress in trees: a critical overview. *Global Change Biology*, *14*(11), 2727-2739.

Calabrese, E. J. (2013). Biphasic dose responses in biology, toxicology and medicine: accounting for their generalizability and quantitative features. *Environmental Pollution*, *182*, 452-460.

Calabrese, E. J. (2014). Hormesis: a fundamental concept in biology. *Microbial Cell*, *1*(5), 145.

Calabrese, E. J. (2015). Hormesis: principles and applications. *Homeopathy*, *104*(02), 69-82.

Calatayud, V., Marco, F., Cerveró, J., Sánchez-Peña, G., Sanz, M. J. (2010). Contrasting ozone sensitivity in related evergreen and deciduous shrubs. *Environmental Pollution*, *158*(12), 3580-3587.

Calzone, A., Podda, A., Lorenzini, G., Maserti, B. E., Carrari, E., Deleanu, E., et al. (2019). Cross-talk between physiological and biochemical adjustments by *Punica granatum* cv. Dente di cavallo mitigates the effects of salinity and ozone stress. *Science of The Total Environment*, *656*, 589-597.

Cao, J., Shang, H., Chen, Z., Tian, Y., Yu, H. (2016). Effects of elevated ozone on stoichiometry and nutrient pools of *Phoebe Bournei* (Hemsl.) Yang and *Phoebe Zhennan* S. Lee et FN Wei seedlings in subtropical China. *Forests*, *7*(4), 78.

Cedergreen, N., Streibig, J. C., Kudsk, P., Mathiassen, S. K., Duke, S. O. (2007). The occurrence of hormesis in plants and algae. *Dose-response*, *5*(2), 150-162.

Chappelka, A. H., Samuelson, L. J. (1998). Ambient ozone effects on forest trees of the eastern United States: a review. *New Phytologist*, *139*(1), 91-108.

Chatani, S., Amann, M., Goel, A., Hao, J., Klimont, Z., Kumar, A., et al. (2014). Photochemical roles of rapid economic growth and potential abatement strategies on tropospheric ozone over South and East Asia in 2030. *Atmospheric Chemistry and Physics*, *14*(17), 9279-9293.

Chazdon, R. L. (2008). Beyond deforestation: restoring forests and ecosystem services on degraded lands. *Science*, *320*(5882), 1458-1460.

Chen, C. L., van der Schoot, H., Dehghan, S., Alvim Kamei, C. L., Schwarz, K. U., Meyer, H., et al. (2017). Genetic diversity of salt tolerance in Miscanthus. *Frontiers in Plant Science*, *8*, 187.

Chen, G., Yue, D., Zhou, Y., Wang, D., Wang, H., Hui, C., Guo, J. (2020) Driving factors of community-level plant functional traits and species distributions in the desert-wetland ecosystem of Shule River, China. *Land Degradation & Development*.

Chen, S., Polle, A. (2010). Salinity tolerance of *Populus*. *Plant biology*, *12*(2), 317-333.

Chen, W., Tang, H., Zhao, H. (2015). Diurnal, weekly and monthly spatial variations of air pollutants and air quality of Beijing. *Atmospheric Environment*, *119*, 21-34.

Chen, Z., Wang, X., Feng, Z., Zheng, F., Duan, X., Yang, W. (2008). Effects of elevated ozone on growth and yield of field-grown rice in Yangtze River Delta, China. *Journal of Environmental Sciences*, *20*(3), 320-325.

Cho, K., Tiwari, S., Agrawal, S. B., Torres, N. L., Agrawal, M., Sarkar, A., et al. (2011). Tropospheric ozone and plants: absorption, responses, and consequences. In *Reviews of Environmental Contamination and Toxicology Volume 212,* pp. 61-111. Springer, New York, NY.

Cimato, A., Castelli, S., Tattini, M., Traversi, M. L. (2010). An ecophysiological analysis of salinity tolerance in olive. *Environmental and Experimental Botany*, *68*(2), 214-221.

Clausen, J. J., Kozlowski, T. T. (1970). Observations on growth of long shoots in *Larix laricina*. *Canadian Journal of Botany*, *48*(6), 1045-1048.

Crane Jr, J. L., Dickmann, D. I., Flore, J. A. (1983). Photosynthesis and transpiration by young *Larix kaempferi* trees: C_3 responses to light and temperature. *Physiologia Plantarum*, *59*(4), 635-640.

Davila, Y., Henze, D. K. (2018). The impact of future emission policies on tropospheric ozone using a parameterised approach. *Atmospheric Chemistry and Physics*, *18*(12).

Deinlein, U., Stephan, A. B., Horie, T., Luo, W., Xu, G., Schroeder, J. I. (2014). Plant salt-tolerance mechanisms. *Trends in Plant Science*, *19*(6), 371-379.

Dong-Gyu, K., Shi, C., Watanabe, M., Kita, K., Satoh, F., Koike, T. (2015). Growth of Japanese and hybrid larch seedlings grown under free-air O_3 fumigation—an initial assessment of the effects of adequate and excessive nitrogen. *Journal of Agricultural Meteorology*, *71*(3), 239-244.

Duan, M., Chang, S. X. (2017). Nitrogen fertilization improves the growth of lodgepole pine and white spruce seedlings under low salt stress through enhancing photosynthesis and plant nutrition. *Forest Ecology and Management*, *404*, 197-204.

Eamus, D., Barnes, J. D., Mortensen, L., Ro-Poulsen, H., Davison, A. W. (1990). Persistent stimulation of CO_2 assimilation and stomatal conductance by summer ozone fumigation in Norway spruce. *Environmental Pollution*, *63*(4), 365-379.

Echeverria, M., Scambato, A. A., Sannazzaro, A. I., Maiale, S., Ruiz, O. A., Menéndez, A. B. (2008). Phenotypic plasticity with respect to salt stress response by *Lotus glaber*: the role of its AM fungal and rhizobial symbionts. *Mycorrhiza*, *18*(6-7), 317-329.

Elser, J. J., Fagan, W. F., Kerkhoff, A. J., Swenson, N. G., Enquist, B. J. (2010). Biological stoichiometry of plant production: metabolism, scaling and ecological response to global change. *New Phytologist*, *186*(3), 593-608.

FAO (2015). WFP. 2015. *The state of food insecurity in the world*, 1-62.

FAOSTAT (2016). Agriculture Organization of the United Nations Statistics Division. http://faostat3. fao. org/home/E.

Fang, J., Guo, Z., Hu, H., Kato, T., Muraoka, H., Son, Y. (2014). Forest biomass carbon sinks in East Asia, with special reference to the relative contributions of forest expansion and forest growth. *Global Change Biology*, *20*(6), 2019-2030.

Farjon, A. (1990). *Pinaceae. Drawings and descriptions of the genera Abies, Cedrus, Pseudolarix, Keteleeria, Nothotsuga, Tsuga, Cathaya, Pseudotsuga, Larix and Picea*. Koeltz scientific books.

Farooq, S., Ahmad, S., Hussain, S., Hussain, M. (2018). Nutrient homeostasis and salt stress tolerance. In *Plant Nutrients and Abiotic Stress Tolerance,* pp. 391-413. Springer, Singapore.

Farquhar, G. D., von Caemmerer, S. V., Berry, J. A. (1980). A biochemical model of photosynthetic CO_2 assimilation in leaves of C_3 species. *Planta*, *149*(1), 78-90.

Farrell, R. C., Bell, D. T., Akilan, K., Marshall, J. K. (1996). Morphological and physiological comparisons of clonal lines of *Eucalyptus camaldulensis*. II. Responses to waterlogging/salinity and alkalinity. *Functional Plant Biology*, *23*(4), 509-518.

Feng, Z., Büker, P., Pleijel, H., Emberson, L., Karlsson, P. E., Uddling, J. (2018). A unifying explanation for variation in ozone sensitivity among woody plants. *Global Change Biology*, *24*(1), 78-84.

Feng, Z., Hu, E., Wang, X., Jiang, L., Liu, X. (2015). Ground-level O_3 pollution and its impacts on food crops in China: a review. *Environmental Pollution*, *199*, 42-48.

Feng, Z., Paoletti, E., Bytnerowicz, A., Harmens, H. (2015). Ozone and plants. *Environmental Pollution*, *202*, 215-216.

Feng, Z., Shang, B., Li, Z., Calatayud, V., Agathokleous, E. (2019). Ozone will remain a threat for plants independently of nitrogen load. *Functional Ecology*, *33*(10), 1854-1870.

Feng, Z., Yang, Y., Zhang, Y., Zhang, P., Li, Y. (2005). Grain-for-green policy and its impacts on grain supply in West China. *Land Use Policy*, *22*(4), 301-312.

Field, C. H., Mooney, H. A. (1986). Photosynthesis--nitrogen relationship in wild plants. In: *On the Economy of Plant Form and Function: Proceedings of the Sixth Maria Moors Cabot Symposium, Evolutionary Constraints on Primary Productivity, Adaptive Patterns of Energy Capture in Plants, Harvard Forest, August 1983*.

Fiore, A. M., Naik, V., Leibensperger, E. M. (2015). Air quality and climate connections. *Journal of the Air & Waste Management Association*, *65*(6), 645-685.

Flowers, M. D., Fiscus, E. L., Burkey, K. O., Booker, F. L., Dubois, J. J. B. (2007). Photosynthesis, chlorophyll fluorescence, and yield of snap bean (*Phaseolus vulgaris L.*) genotypes differing in sensitivity to ozone. *Environmental and Experimental Botany*, *61*(2), 190-198.

Flowers, T. J. (2004). Improving crop salt tolerance. *Journal of Experimental Botany*, *55*(396), 307-319.

Flowers, T. J., Troke, P. F., Yeo, A. R. (1977). The mechanism of salt tolerance in halophytes. *Annual Review of Plant Physiology*, *28*(1), 89-121.

Fowler, D., Amann, M., Anderson, R., Ashmore, M., Cox, P., Depledge, M., et al. (2008). *Ground-level ozone in the 21st century: future trends, impacts and policy implications* 15(8)

Fry, D. J., Phillips, I. D. J. (1976). Photosynthesis of Conifers in Relation to Annual Growth Cycles and Dry Matter Production: I. Some C_4 Characteristics in Photosynthesis of Japanese Larch (*Larix leptolepis*). *Physiologia Plantarum*, *37*(3), 185-190.

Fuhrer, J., Skärby, L., Ashmore, M. R. (1997). Critical levels for ozone effects on vegetation in Europe. *Environmental Pollution*, *97*(1-2), 91-106.

Fujita, S., Wang, X., Kita, K., Koike, T. (2018). Effects of nitrogen loading under low and high phosphorus conditions on above-and below-ground growth of hybrid larch F_1 seedlings. *iForest-Biogeosciences and Forestry*, *11*(1), 32.

Galloway, J. N., Dentener, F. J., Capone, D. G., Boyer, E. W., Howarth, R. W., Seitzinger, S. P., et al. (2004). Nitrogen cycles: past, present, and future. *Biogeochemistry*, *70*(2), 153-226.

Galvan-Ampudia, C. S., Julkowska, M. M., Darwish, E., Gandullo, J., Korver, R. A., Brunoud, G., et al. (2013). Halotropism is a response of plant roots to avoid a saline environment. *Current Biology*, *23*(20), 2044-2050.

Gaudel, A., Cooper, O. R., Ancellet, G., Barret, B., Boynard, A., Burrows, J. P., et al. (2018). Tropospheric Ozone Assessment Report: present-day distribution and trends of tropospheric ozone relevant to climate and global atmospheric chemistry model evaluation. *Elementa: Science of the Anthropocene*, *6*, 1-58.

Ge, Y., Li, J. D. (1990). A preliminary study on the effects of halophytes on salt accumulation and desalination in the soils of Songnen plain, Northeast China. *Acta Prataculturae Sinica*, *1*(1), 70-76.

Genty, B., Briantais, J. M., Baker, N. R. (1989). The relationship between the quantum yield of photosynthetic electron transport and quenching of chlorophyll fluorescence. *Biochimica et Biophysica Acta (BBA)-General Subjects*, *990*(1), 87-92.

George, J. P., Grabner, M., Karanitsch-Ackerl, S., Mayer, K., Weißenbacher, L., Schueler, S., Mäkelä, A. (2017). Genetic variation, phenotypic stability, and repeatability of drought response in European larch throughout 50 years in a common garden experiment. *Tree Physiology*, *37*(1), 33-46.

Gerosa, G., Marzuoli, R., Finco, A., Monga, R., Fusaro, I., Faoro, F. (2014). Contrasting effects of water salinity and ozone concentration on two cultivars of durum wheat (*Triticum durum* Desf.) in Mediterranean conditions. *Environmental Pollution*, *193*, 13-21.

Gielen, B., Löw, M., Deckmyn, G., Metzger, U., Franck, F., Heerdt, C., et al. (2007). Chronic ozone exposure affects leaf senescence of adult beech trees: a chlorophyll fluorescence approach. *Journal of Experimental Botany*, *58*(4), 785-795.

Glenn, E. P., Nagler, P. L. (2005). Comparative ecophysiology of *Tamarix ramosissima* and native trees in western US riparian zones. *Journal of Arid Environments*, *61*(3), 419-446.

Goto, S., Iijima, H., Ogawa, H., Ohya, K. (2011). Outbreeding depression caused by intraspecific hybridization between local and nonlocal genotypes in *Abies sachalinensis*. *Restoration Ecology*, *19*(2), 243-250.

Gower, S. T., Richards, J. H. (1990). Larches: deciduous conifers in an evergreen world. *BioScience*, *40*(11), 818-826.

Gowin, T., Lourtioux, A., Mousseau, M. (1980). Influence of constant growth temperature upon the productivity and gas exchange of seedlings of Scots pine and European larch. *Forest Science*, *26*(2), 301-309.

Grantz, D. A., Gunn, S., Vu, H. B. (2006). O_3 impacts on plant development: a meta-analysis of root/shoot allocation and growth. *Plant, Cell & Environment*, *29*(7), 1193-1209.

Grime, J. P. (1977). Evidence for the existence of three primary strategies in plants and its relevance to ecological and evolutionary theory. *The American Naturalist*, *111*(982), 1169-1194.

Grulke, N. E., Heath, R. L. (2020). Ozone effects on plants in natural ecosystems. *Plant Biology*, *22*, 12-37.

Guidi, L., Remorini, D., Cotrozzi, L., Giordani, T., Lorenzini, G., Massai, R., et al. (2017). The harsh life of an urban tree: the effect of a single pulse of ozone in salt-stressed *Quercus ilex* saplings. *Tree Physiology*, *37*(2), 246-260.

Gurjar, B. R., Ravindra, K., Nagpure, A. S. (2016). Air pollution trends over Indian megacities and their local-to-global implications. *Atmospheric Environment*, *142*, 475-495.

Güsewell, S. (2004). N: P ratios in terrestrial plants: variation and functional significance. *New Phytologist*, *164*(2), 243-266.

Hahn, W. A., Knoke, T. (2010). Sustainable development and sustainable forestry: analogies, differences, and the role of flexibility. *European Journal of Forest Research*, *129*(5), 787-801.

Halwatura, D., Lechner, A. M., Arnold, S. (2015). Drought severity–duration–frequency curves: a foundation for risk assessment and planning tool for ecosystem establishment in post-mining landscapes. *Hydrology and Earth System Sciences*, *19*(2), 1069-1091.

Harayama, H., Ohno, Y., Uemura, A., Kitaoka, S., Utsugi, H., Kita, K. (2013). Seasonal variations in photosynthetic properties in saplings of three *Larix* spp. *Boreal Forest Research* 61, 57-58. (in Japanese).

Hartmann, D. L., Tank, A. M. G. K., Rusticucci, M., Alexander, L. V., Brönnimann, S., Charabi, Y. A. R., et al. (2013). Observations: Atmosphere and surface: Climate Change 2013 the Physical Science

Basis: Working Group I Contribution to the Fifth Assessment Report of the Intergovernmental Panel on Climate Change. *Cambridge University Press*, 159.

Hatakeyama S. (2017) Aerosols. - In: Izuta T. (ed.): Air Pollution Impacts on Plants in East Asia, pp. 21-42. Springer, Tokyo

Hatakeyama, S. (2011). Investigations toward Elucidation of the Impacts of Long-Range-Transported Aerosols from East Asia on Plants and Human Health. *Earozoru Kenkyu*, *26*(2), 103-107. (in Japanese).

Hayes, F., Jones, M. L. M., Mills, G., Ashmore, M. (2007). Meta-analysis of the relative sensitivity of semi-natural vegetation species to ozone. *Environmental Pollution*, *146*(3), 754-762.

Hikosaka, K. (2004). Interspecific difference in the photosynthesis–nitrogen relationship: patterns, physiological causes, and ecological importance. *Journal of Plant Research*, *117*(6), 481-494.

Hoffmann, W. A., Poorter, H. (2002). Avoiding bias in calculations of relative growth rate. *Annals of Botany*, *90*(1), 37-42.

Hokkaido (2017) Policy of collecting park development in Hokkaido, http://www.pref.hokkaido.lg.jp/sr/srs/grp/hokkaidoseedplan.pdf. (Last accessed in 2020.06.01.)

Hopkins, W. G. (2000). A new view of statistics. Internet Society for Sport Science. http://newstats.org

Hoshika, Y., Paoletti, E., Agathokleous, E., Sugai, T., Koike, T. (2020). Developing ozone risk assessment for larch species. *Frontiers in Forests and Global Change*, *3*, 45.

Hoshika, Y., Katata, G., Deushi, M., Watanabe, M., Koike, T., Paoletti, E. (2015). Ozone-induced stomatal sluggishness changes carbon and water balance of temperate deciduous forests. *Scientific Reports*, *5*, 9871.

Hoshika, Y., Watanabe, M., Inada, N., Koike, T. (2013). Model-based analysis of avoidance of ozone stress by stomatal closure in Siebold's beech (*Fagus crenata*). *Annals of Botany*, *112*(6), 1149-1158.

Hu, E., Gao, F., Xin, Y., Jia, H., Li, K., Hu, J., Feng, Z. (2015). Concentration-and flux-based ozone dose–response relationships for five poplar clones grown in North China. *Environmental Pollution*, *207*, 21-30.

Högberg, P., Näsholm, T., Franklin, O., Högberg, M. N. (2017). Tamm Review: On the nature of the nitrogen limitation to plant growth in Fennoscandian boreal forests. *Forest Ecology and Management*, *403*, 161-185.

Hůnová, I., Kurfürst, P., Baláková, L. (2019). Areas under high ozone and nitrogen loads are spatially disjunct in Czech forests. *Science of The Total Environment*, *656*, 567-575.

IGBP Terrestrial Carbon Working Group. (1998). The terrestrial carbon cycle: implications for the Kyoto Protocol. *Science* 280: 1393–1394.

Isabel, N., Holliday, J. A., Aitken, S. N. (2020). Forest genomics: Advancing climate adaptation, forest health, productivity, and conservation. *Evolutionary Applications*, *13*(1), 3-10.

Isayenkov, S. V., Maathuis, F. J. (2019). Plant salinity stress: Many unanswered questions remain. *Frontiers in Plant Science*, *10*.

Ishizawa, S., Suzuki, T., Osamu, Sato, Toyoda, H. (1957). Studies on microbial population in the rhizosphere of higher plants with special reference to the method of study. *Soil Science and Plant Nutrition*, *3*(1), 85-94.

Ishizuka, W., Tabata, A., Ono, K., Fukuda, Y., Hara, T. (2017). Draft chloroplast genome of *Larix gmelinii* var. *japonica*: insight into intraspecific divergence. *Journal of Forest Research*, *22*(6), 393-398.

Izuta, T. (2017). *Air pollution impacts on plants in East Asia*. pp. 73-100, Springer, Tokyo

Jandl, R., Spathelf, P., Bolte, A., Prescott, C. E. (2019). Forest adaptation to climate change—is non-management an option?. *Annals of Forest Science*, *76*(2), 48.

Jansen, S., Geburek, T. (2016). Historic translocations of European larch (*Larix decidua* Mill.) genetic resources across Europe–A review from the 17th until the mid-20th century. *Forest Ecology and Management*, *379*, 114-123.

Japanese Ministry of the Environment (1996) Environmental Standards Relating to Air Pollution, https://www.env.go.jp/kijun/taiki.html

Kainulainen, P., Utriainen, J., Holopainen, J. K., Oksanen, J. A. R. I., Holopainen, T. (2000). Influence of elevated ozone and limited nitrogen availability on conifer seedlings in an open-air fumigation system: effects on growth, nutrient content, mycorrhiza, needle ultrastructure, starch and secondary compounds. *Global Change Biology*, *6*(3), 345-355.

Kalabokas, P. D., Thouret, V., Cammas, J. P., Volz-Thomas, A., Boulanger, D., Repapis, C. C. (2015). The geographical distribution of meteorological parameters associated with high and low summer ozone levels in the lower troposphere and the boundary layer over the eastern Mediterranean (Cairo case). *Tellus B: Chemical and Physical Meteorology*, *67*(1), 27853.

Keenan, R. J. (2015). Climate change impacts and adaptation in forest management: a review. *Annals of Forest Science*, *72*(2), 145-167.

Keenan, R. J., Reams, G. A., Achard, F., de Freitas, J. V., Grainger, A., Lindquist, E. (2015). Dynamics of global forest area: Results from the FAO Global Forest Resources Assessment 2015. *Forest Ecology and Management*, *352*, 9-20.

Keller, T., Matyssek, R. (1990). Limited compensation of ozone stress by potassium in Norway spruce. *Environmental Pollution*, *67*(1), 1-14.

Kelleway, J. J., Cavanaugh, K., Rogers, K., Feller, I. C., Ens, E., Doughty, C., Saintilan, N. (2017). Review of the ecosystem service implications of mangrove encroachment into salt marshes. *Global Change Biology*, *23*(10), 3967-3983.

Kijowska-Oberc, J., Staszak, A. M., Kamiński, J., Ratajczak, E. (2020). Adaptation of Forest Trees to Rapidly Changing Climate. *Forests*, *11*(2), 123.

Killingbeck T. (2004) Nutrient resorption, Plant Cell Death Processes, Elsevier, pp. 215-226,

King, I. P., Law, C. N., Cant, K. A., Orford, S. E., Reader, S. M., Miller, T. E. (1997). Tritipyrum, a potential new salt-tolerant cereal. *Plant Breeding*, *116*(2), 127-132.

Kinose, Y., Fukamachi, Y., Okabe, S., Hiroshima, H., Watanabe, M., Izuta, T. (2017). Nutrient supply to soil offsets the ozone-induced growth reduction in *Fagus crenata* seedlings. *Trees*, *31*(1), 259-272.

Kita, K., Fujimoto, T., Uchiyama, K., Kuromaru, M., Akutsu, H. (2009). Estimated amount of carbon accumulation of hybrid larch in three 31-year-old progeny test plantations. *Journal of Wood Science*, *55*(6), 425-434.

Kita, K, Sugai, T., Fujita, S., Koike, T. (2018). Breeding effort on hybrid larch F_1 and its responses to environmental stresses. Forest Genetics and Breeding, 7: 107-114. [in Japanese]

Kitao, M., Utsugi, H., Kuramoto, S., Tabuchi, R., Fujimoto, K., Lihpai, S. (2003). Light-dependent photosynthetic characteristics indicated by chlorophyll fluorescence in five mangrove species native to Pohnpei Island, Micronesia. *Physiologia Plantarum*, *117*(3), 376-382.

Kitao, M., Yasuda, Y., Komatsu, M., Kitaoka, S., Yazaki, K., Tobita, H., et al. (2017). Flux-Based O_3 Risk Assessment for Japanese Temperate Forests. In *Air Pollution Impacts on Plants in East Asia*, pp. 125-133. Springer, Tokyo.

Kitao, M., Yasuda, Y., Kominami, Y., Yamanoi, K., Komatsu, M., Miyama, T., et al. (2016). Increased phytotoxic O_3 dose accelerates autumn senescence in an O_3 -sensitive beech forest even under the present-level O_3. *Scientific Reports*, *6*(1), 1-9.

Kitaoka, S., Koike, T. (2004). Invasion of broad-leaf tree species into a larch plantation: seasonal light environment, photosynthesis and nitrogen allocation. *Physiologia Plantarum*, *121*(4), 604-611.

Kitaoka, S., Koike, T. (2005). Seasonal and yearly variations in light use and nitrogen use by seedlings of four deciduous broad-leaved tree species invading larch plantations. *Tree Physiology*, *25*(4), 467-475.

Koike T., Watanabe M., Hoshika Y. *et al*. (2013) Effects of ozone on forest ecosystems in East and Southeast Asia. In: Matyssek, R., Clarke, N., Cudlín, P., et al. (ed.). Climate change, air pollution and global challenges: understanding and perspectives from forest research. In *Developments in environmental science*, pp371-390. Elsevier.

Koike, T., Mao, Q., Inada, N., Kawaguchi, K., Hoshika, Y., Kita, K., Watanabe, M. (2012). Growth and photosynthetic responses of cuttings of a hybrid larch (*Larix gmelinii* var. *japonica* x *L. kaempferi*) to elevated ozone and/or carbon dioxide. *Asian Journal of Atmospheric Environment*, *6*(2), 104-110.

Koike, T., Nagasaka, K., Koono, K. (1988). Photosynthetic characteristics in larch and its hybrids in summer. *Transactions of the Meeting in Hokkaido Branch of the Japanese Forest Society*, *36*, 57-59. (in Japanese)

Kouchi, H., Kumazawa, K. (1975). Anatomical responses of root tips to boron deficiency I. Effects of boron deficiency on elongation of root tips and their morphological characteristics. *Soil Science and Plant Nutrition*, *21*(1), 21-28.

Kozlowski, T. T. (1997). Responses of woody plants to flooding and salinity. *Tree Physiology*, *17*(7), 490-490.

Krause, G. H., Virgo, A., Winter, K. (1995). High susceptibility to photoinhibition of young leaves of tropical forest trees. *Planta*, *197*(4), 583-591.

Kurahashi, A. (1988). Improvement of larches by species hybridization. *Bulletin of the Tokyo University Forests*, (79), 1-94. [in Japanese]

Kurinobu, S. (2005). Forest tree breeding for Japanese larch. *Eurasian Journal of Forest Research*, *8*(2), 127-134.

Körner, C. (2003). *Alpine plant life: functional plant ecology of high mountain ecosystems; with 47 tables*. Springer Science & Business Media.

Köster, P., Wallrad, L., Edel, K. H., Faisal, M., Alatar, A. A., Kudla, J. (2019). The battle of two ions: Ca^{2+} signaling against Na^{+} stress. *Plant Biology*, *21*, 39-48.

Küppers, M. (1989). Ecological significance of above-ground architectural patterns in woody plants: a question of cost-benefit relationships. *Trends in Ecology & Evolution*, *4*(12), 375-379.

Lambers, H., Chapin III, F. S., Pons, T. L. (2013). *Plant physiological ecology*. Springer Science & Business Media.

Larcher, W. (1969). Effect of environmental and physiological variables on the carbon dioxide gas exchange of trees. *Photosynthetica 3,* 167-198.

Larcher, W. (2003). Physiological Plant Ecology: The environment of plants. 2, Carbon utilization and dry matter production. *Plants under stress*. Springer.

Lee, D. K., Kang, H. S., Park, Y. D. (2004). Natural restoration of deforested woodlots in South Korea. *Forest Ecology and Management*, *201*(1), 23-32.

Lee, J. B., Cha, J. S., Hong, S. C., Choi, J. Y., Myoung, J. S., Park, R. J., et al. (2015). Projections of summertime ozone concentration over East Asia under multiple IPCC SRES emission scenarios. *Atmospheric Environment*, *106*, 335-346.

Li, H., Li, Z., Shen, Z. J., Luo, M. R., Liu, Y. L., Wei, M. Y., et al. (2020). Physiological and proteomic responses of mangrove plant *Avicennia marina* seedlings to simulated periodical inundation. *Plat and Soil*. (in press)

Li, J., Guo, Q., Zhang, J., Korpelainen, H., Li, C. (2016). Effects of nitrogen and phosphorus supply on growth and physiological traits of two *Larix* species. *Environmental and Experimental Botany*, *130*, 206-215.

Li, J., Pu, L., Han, M., Zhu, M., Zhang, R., Xiang, Y. (2014). Soil salinization research in China: advances and prospects. *Journal of Geographical Sciences*, *24*(5), 943-960.

Li, P., Calatayud, V., Gao, F., Uddling, J., Feng, Z. (2016). Differences in ozone sensitivity among woody species are related to leaf morphology and antioxidant levels. *Tree Physiology*, *36*(9), 1105-1116.

Li, P., Feng, Z., Catalayud, V., Yuan, X., Xu, Y., Paoletti, E. (2017). A meta-analysis on growth, physiological, and biochemical responses of woody species to ground-level ozone highlights the role of plant functional types. *Plant, Cell & Environment*, *40*(10), 2369-2380.

Liancourt, P., Callaway, R. M., Michalet, R. (2005). Stress tolerance and competitive-response ability determine the outcome of biotic interactions. *Ecology*, *86*(6), 1611-1618.

Lippman, Z. B., Zamir, D. (2007). Heterosis: revisiting the magic. *Trends in Genetics*, *23*(2), 60-66.

Litalien, A., Zeeb, B. (2020). Curing the earth: A review of anthropogenic soil salinization and plant-based strategies for sustainable mitigation. *Science of the Total Environment*, *698*, 134235.

Liu, J., Shi, D. C. (2010). Photosynthesis, chlorophyll fluorescence, inorganic ion and organic acid accumulations of sunflower in responses to salt and salt-alkaline mixed stress. *Photosynthetica*, *48*(1), 127-134.

Liu, X., Duan, L., Mo, J., Du, E., Shen, J., Lu, X., et al. (2011). Nitrogen deposition and its ecological impact in China: an overview. *Environmental Pollution*, *159*(10), 2251-2264.

Liu, X., Zhang, Y., Han, W., Tang, A., Shen, J., Cui, Z., et al. (2013). Enhanced nitrogen deposition over China. *Nature*, *494*(7438), 459-462.

Long, S. P., Bernacchi, C. J. (2003). Gas exchange measurements, what can they tell us about the underlying limitations to photosynthesis? Procedures and sources of error. *Journal of Experimental Botany*, *54*(392), 2393-2401.

Loucks, C., Barber-Meyer, S., Hossain, M. A. A., Barlow, A., Chowdhury, R. M. (2010). Sea level rise and tigers: predicted impacts to Bangladesh’s Sundarbans mangroves. *Climatic Change*, *98*(1-2), 291.

Luo, Y., Guo, W., Yuan, Y., Liu, J., Du, N., Wang, R. (2014). Increased nitrogen deposition alleviated the competitive effects of the introduced invasive plant *Robinia pseudoacacia* on the native tree *Quercus acutissima*. *Plant and Soil*, *385*(1-2), 63-75.

Ma, Z., Fu, C. (2006). Some evidence of drying trend over northern China from 1951 to 2004. *Chinese*

Science Bulletin, *51*(23), 2913-2925.

Mamet, S. D., Brown, C. D., Trant, A. J., Laroque, C. P. (2019). Shifting global *Larix* distributions: Northern expansion and southern retraction as species respond to changing climate. *Journal of Biogeography*, *46*(1), 30-44.

Manderscheid, R., Jäger, H. J., Kress, L. W. (1992). Effects of ozone on foliar nitrogen metabolism of *Pinus taeda* L. and implications for carbohydrate metabolism. *New Phytologist*, *121*(4), 623-633.

Manninen, S., Huttunen, S., Vanhatalo, M., Pakonen, T., Hämäläinen, A. (2009). Inter-and intra-specific responses to elevated ozone and chamber climate in northern birches. *Environmental Pollution*, *157*(5), 1679-1688.

Manning, W. J. (1989). Effects of ozone and ozone-acidic precipitation interaction on forest trees in North America. In *Studies in Environmental Science*, pp. 239-249. Elsevier.

Mao, P., Zhang, Y., Cao, B., Guo, L., Shao, H., Cao, Z., et al. (2016). Effects of salt stress on eco-physiological characteristics in *Robinia pseudoacacia* based on salt-soil rhizosphere. *Science of the Total Environment*, *568*, 118-123.

Mao, Q., Watanabe, M., Koike, T. (2010). Growth characteristics of two promising tree species for afforestation, birch and larch in the northeastern part of Asia. *Eurasian Journal of Forest Research*, *13*(2), 69-76.

Marchal, A., Muñoz, F., Millier, F., Sánchez, L., Pâques, L. E. (2017). Hybrid larch heterosis: for which traits and under which genetic control? *Tree Genetics & Genomes*, *13*(5), 92.

Marchi, E., Chung, W., Visser, R., Abbas, D., Nordfjell, T., Mederski, P. S., et al. (2018). Sustainable Forest Operations (SFO): A new paradigm in a changing world and climate. *Science of the Total Environment*, *634*, 1385-1397.

Marchner, H. (2011). Introduction to the mineral nutrition of plants. *Handbook Plant Physiology*, *154*, 31-38.

Marschner, H. (1995). Adaptation of plants to adverse chemical soil conditions. *Mineral nutrition of higher plants*. Marschner's mineral nutrition of higher plants-Third edition, Academic Press, pp.455-472

Mason, W. L., Zhu, J. J. (2014). Silviculture of planted forests managed for multi-functional objectives: lessons from Chinese and British experiences. In *Challenges and Opportunities for the World's Forests in the 21st Century* pp. 37-54. Springer, Dordrecht.

Matsuda, K., Shibuya, M., Koike, T. (2002). Maintenance and rehabilitation of the mixed conifer-broadleaf forests in Hokkaido, northern Japan. *Eurasian Journal of Forest Research*, *5*(2), 119-130.

Matyssek, R. (1986). Carbon, water and nitrogen relations in evergreen and deciduous conifers. *Tree Physiology*, *2*(1-2-3), 177-187.

Matyssek, R., Agerer, R., Ernst, D., Munch, J. C., Osswald, W., Pretzsch, H., et al. (2005). The plant's capacity in regulating resource demand. *Plant Biology*, *7*(06), 560-580.

Matyssek, R., Bytnerowicz, A., Karlsson, P. E., Paoletti, E., Sanz, M., Schaub, M., Wieser, G. (2007). Promoting the O_3 flux concept for European forest trees. *Environmental Pollution*, *146*(3), 587-607.

Matyssek, R., Maurer, S., Gunthardt-Goerg, M. S., Landolt, W., Saurer, M., Polle, A. (1997). Nutrition determines the "strategy" of *Betula pendula* for coping with ozone stress. *Phyton 37(*3*),* 157-168.

Matyssek, R., Sandermann, H. (2003). Impact of ozone on trees: an ecophysiological perspective. In *Progress in botany*, pp. 349-404. Springer, Berlin, Heidelberg.

Matyssek, R., Sandermann, H., Wieser, G., Booker, F., Cieslik, S., Musselman, R., Ernst, D. (2008). The challenge of making ozone risk assessment for forest trees more mechanistic. *Environmental Pollution*, *156*(3), 567-582.

Matyssek, R., Schulze, E. D. (1987). Heterosis in hybrid larch *(Larix decidua* x *leptolepis*). *Trees*, *1*(4), 219-224.

Matyssek, R., Wieser, G., Calfapietra, C., De Vries, W., Dizengremel, P., Ernst, D., et al. (2012). Forests under climate change and air pollution: gaps in understanding and future directions for research. *Environmental Pollution*, *160*, 57-65.

Matyssek, R., Wieser, G., Nunn, A. J., Kozovits, A. R., Reiter, I. M., Heerdt, C., et al. (2004). Comparison between AOT40 and ozone uptake in forest trees of different species, age and site conditions. *Atmospheric Environment*, *38*(15), 2271-2281.

Maurer, S., Matyssek, R., GuÈnthardt-Goerg, M. S., Landolt, W., Einig, W. (1997). Nutrition and the ozone sensitivity of birch (*Betula pendula*). *Trees*, *12*(1), 1-10.

Millard, P., Proe, M. F. (1992). Storage and internal cycling of nitrogen in relation to seasonal growth of Sitka spruce. *Tree Physiology*, *10*(1), 33-43.

Mills, G., Harmens, H., Wagg, S., Sharps, K., Hayes, F., Fowler, D., et al. (2016). Ozone impacts on vegetation in a nitrogen enriched and changing climate. *Environmental Pollution*, *208*, 898-908.

Mills, G., Sharps, K., Simpson, D., Pleijel, H., Broberg, M., Uddling, J., et al. (2018). Ozone pollution will compromise efforts to increase global wheat production. *Global Change Biology*, *24*(8), 3560-3574.

Minhas, P. S., Yadav, R. K., Bali, A. (2020). Perspectives on reviving waterlogged and saline soils through plantation forestry. *Agricultural Water Management*, *232*, 106063.

Miura, K. (1997) Soil environment analysis methods. Japanese Society. *Soil Science and Plant Nutrion.*1-427

Mortensen, L. M. (1994). The influence of carbon dioxide or ozone concentration on growth and assimilate partitioning in seedlings of nine conifers. *Acta Agriculturae Scandinavica B-Plant Soil*

Sciences, *44*(3), 157-163.

Munns, R., Gilliham, M. (2015). Salinity tolerance of crops–what is the cost? *New Phytologist*, *208*(3), 668-673.

Munns, R., Tester, M. (2008). Mechanisms of salinity tolerance. *Annual Review of Plant Biology*, *59*, 651-681.

Myneni, R. B., Dong, J., Tucker, C. J., Kaufmann, R. K., Kauppi, P. E., Liski, J., et al. (2001). A large carbon sink in the woody biomass of Northern forests. *Proceedings of the National Academy of Sciences*, *98*(26), 14784-14789.

Nagamitsu, T., Nagasaka, K., Yoshimaru, H., Tsumura, Y. (2014). Provenance tests for survival and growth of 50-year-old Japanese larch (*Larix kaempferi*) trees related to climatic conditions in central Japan. *Tree Genetics & Genomes*, *10*(1), 87-99.

Nagashima, T., Ohara, T., Sudo, K., Akimoto, H. (2010). The relative importance of various source regions on East Asian surface ozone. *Atmospheric Chemistry & Physics Discussions*, *10*(4).

Nagashima, T., Sudo, K., Akimoto, H., Kurokawa, J., Ohara, T. (2017). Long-term change in the source contribution to surface ozone over Japan. *Atmospheric Chemistry and Physics*, *17*(13), 8231.

Nakaji, T., Izuta, T. (2001). Effects of ozone and/or excess soil nitrogen on growth, needle gas exchange rates and Rubisco contents of *Pinus densiflora* seedlings. *Water, Air, and Soil Pollution*, *130*(1-4), 971-976.

Nelson, H. W., Williamson, T. B., Macaulay, C., Mahony, C. (2016). Assessing the potential for forest management practitioner participation in climate change adaptation. *Forest Ecology and Management*, *360*, 388-399.

Neves, G. Y. S., Marchiosi, R., Ferrarese, M. L. L., Siqueira-Soares, R. C., Ferrarese-Filho, O. (2010). Root growth inhibition and lignification induced by salt stress in soybean. *Journal of Agronomy and Crop Science*, *196*(6), 467-473.

Nicotra, A. B., Atkin, O. K., Bonser, S. P., Davidson, A. M., Finnegan, E. J., Mathesius, U., et al. (2010). Plant phenotypic plasticity in a changing climate. *Trends in Plant Science*, *15*(12), 684-692.

Niinemets, U. (1999). Components of leaf dry mass per area—thickness and density—alter photosynthetic capacity in reverse directions in woody plants. *New Phytologist*, *144*, 35-47.

Niinemets, Ü., Valladares, F. (2006). Tolerance to shade, drought, and waterlogging of temperate Northern Hemisphere trees and shrubs. *Ecological Monographs*, *76*(4), 521-547.

Niknam, S. R., McComb, J. (2000). Salt tolerance screening of selected Australian woody species—a review. *Forest Ecology and Management*, *139*(1-3), 1-19.

Noguchi M., Kayama M., Yoshida T., Koike T. (2003) Photosynthetic traits of seedlings of Sakhalin fir grown under selective cutting in a fir forest. *Transactions of the Meeting in Hokkaido Branch of the Japanese Forest Society 51*: 36-38. [in Japanese]

Ogle, D., John, S. T. (2010). Plants for saline to sodic soil conditions. USDA. *Natural Resources Conservation Service. Boise, Idaho. Technical Note*, (9A), p10150.

Okur, B., Örçen, N. (2020). Soil salinization and climate change. In *Climate Change and Soil Interactions*, pp. 331-350. Elsevier.

Osawa, A., Zyryanova, O. A., Matsuura, Y., Kajimoto, T., Wein, R. W. (2010). Permafrost ecosystems. *Ecological Studies*, *209*. Sprinver Verlag, Heidelberg, Berline

Paoletti, E. (2006). Impact of ozone on Mediterranean forests: a review. *Environmental Pollution*, *144*(2), 463-474.

Paoletti, E., Bytnerowicz, A., Andersen, C., Augustaitis, A., Ferretti, M., Grulke, N., et al. (2007). Impacts of air pollution and climate change on forest ecosystems—emerging research needs. *The Scientific World Journal*, *7*, 1-8.

Paoletti, E., Grulke, N. E. (2010). Ozone exposure and stomatal sluggishness in different plant physiognomic classes. *Environmental Pollution*, *158*(8), 2664-2671.

Paoletti, E., Manning, W. J. (2007). Toward a biologically significant and usable standard for ozone that will also protect plants. *Environmental Pollution*, *150*(1), 85-95.

Paoletti, E., Ranieri, A., Lauteri, M. (2008). Moving toward effective ozone flux assessment. *Environmental Pollution*, *156*(1), 16-19.

Parida, A. K., Jha, B. (2010). Salt tolerance mechanisms in mangroves: a review. *Trees*, *24*(2), 199-217.

Parihar, P., Singh, S., Singh, R., Singh, V. P., Prasad, S. M. (2015). Effect of salinity stress on plants and its tolerance strategies: a review. *Environmental Science and Pollution Research*, *22*(6), 4056-4075.

Pell, E. J., Schlagnhaufer, C. D., Arteca, R. N. (1997). Ozone-induced oxidative stress: mechanisms of action and reaction. *Physiologia Plantarum*, *100*(2), 264-273.

Pell, E. J., Sinn, J. P., Johansen, C. V. (1995). Nitrogen supply as a limiting factor determining the sensitivity of *Populus tremuloides* Michx. to ozone stress. *New Phytologist*, *130*(3), 437-446.

Pell, E. J., Temple, P. J., Friend, A. L., Mooney, H. A., Winner, W. E. (1994). Compensation as a plant response to ozone and associated stresses: an analysis of ROPIS experiments. *Journal of Environmental Quality*, *23*(3), 429-436.

Peng, W., Pukkala, T., Jin, X., Li, F. (2018). Optimal management of larch (*Larix olgensis* A. Henry) plantations in Northeast China when timber production and carbon stock are considered. *Annals of Forest Science*, *75*(2), 63.

Peterson, A. G. (1999). Reconciling the apparent difference between mass-and area-based expressions of the photosynthesis-nitrogen relationship. *Oecologia*, *118*(2), 144-150.

Plesa, I. M., González-Orenga, S., Al Hassan, M., Sestras, A. F., Vicente, O., Prohens, J., et al. (2018). Effects of drought and salinity on European Larch (Larix decidua Mill.) seedlings. *Forests*, *9*(6), 320.

Polezhaeva, M. A., Lascoux, M., Semerikov, V. L. (2010). Cytoplasmic DNA variation and biogeography of *Larix* Mill. in Northeast Asia. *Molecular Ecology*, *19*(6), 1239-1252.

Polle, A., Chen, S. (2015). On the salty side of life: molecular, physiological and anatomical adaptation and acclimation of trees to extreme habitats. *Plant, Cell & Environment*, *38*(9), 1794-1816.

Polle, A., Chen, S. L., Eckert, C., Harfouche, A. (2019). Engineering drought resistance in forest trees. *Frontiers in Plant Science*, *9*, 1875.

Poorter, H. (1989). Interspecific variation in relative growth rate: on ecological causes and physiological consequences. *Causes and consequences of variation in growth rate and productivity of higher plants*, *24*, 45-68.

Powell, G. R. (1988). Shoot elongation, leaf demography and bud formation in relation to branch position on *Larix laricina* saplings. *Trees*, *2*(3), 150-164.

Pâques, L. E. (1989). A critical review of larch hybridization and its incidence on breeding strategies. *Annales des Sciences Forestières*, 46(2), 141-153

Pâques, L. E., Foffová, E., Heinze, B., Lelu-Walter, M. A., Liesebach, M., Philippe, G. (2013). Larches (*Larix* sp.). In *Forest tree breeding in Europe,* pp. 13-122. Springer, Dordrecht.

Qu, L. (2016). Ecophysiological study on the natural regeneration of the two larch species with special references to soil environment in larch forests. *Eurasian Journal of Forest Research*, *19*(1), 1-51.

Reich, P. B., Oleksyn, J. (2004). Global patterns of plant leaf N and P in relation to temperature and latitude. *Proceedings of the National Academy of Sciences*, *101*(30), 11001-11006.

Reich, P. B., Walters, M. B., Ellsworth, D. S. (1992). Leaf life-span in relation to leaf, plant, and stand characteristics among diverse ecosystems. *Ecological Monographs*, *62*(3), 365-392.

Reich, P. B., Walters, M. B., Kloeppel, B. D., Ellsworth, D. S. (1995). Different photosynthesis-nitrogen relations in deciduous hardwood and evergreen coniferous tree species. *Oecologia*, *104*(1), 24-30.

Reilly, J., Paltsev, S., Felzer, B., Wang, X., Kicklighter, D., Melillo, J., et al. (2007). Global economic effects of changes in crops, pasture, and forests due to changing climate, carbon dioxide, and ozone. *Energy Policy*, *35*(11), 5370-5383.

Ren, G., Young, S. S., Wang, L., Wang, W., Long, Y., Wu, R., et al. (2015). Effectiveness of China's national forest protection program and nature reserves. *Conservation Biology*, *29*(5), 1368-1377.

Renault, S. (2005). Tamarack response to salinity: effects of sodium chloride on growth and ion, pigment, and soluble carbohydrate levels. *Canadian Journal of Forest Research*, *35*(12), 2806-2812.

Resco de Dios, V., Mereed, T. E., Ferrio, J. P., Tissue, D. T., Voltas, J. (2016). Intraspecific variation in juvenile tree growth under elevated CO_2 alone and with O_3: a meta-analysis. *Tree Physiology*, *36*(6), 682-693.

Rewald, B., Shelef, O., Ephrath, J. E., Rachmilevitch, S. (2013). Adaptive plasticity of salt-stressed root systems. In *Ecophysiology and responses of plants under salt stress,* pp. 169-201. Springer, New York, NY.

Richards, J. H., Teeri, J. A. (1982). Re-evaluation of proposed C_4 photosynthetic characteristics in the genus *Larix*. *Physiologia Plantarum*, *55*(2), 117-120.

Ryu, K., Watanabe, M., Shibata, H., Takagi, K., Nomura, M., Koike, T. (2009). Ecophysiological responses of the larch species in northern Japan to environmental changes as a basis for afforestation. *Landscape and Ecological Engineering*, *5*(2), 99-106.

Saitanis, C. J., Agathokleous, E. (2019). Stress response and population dynamics: Is Allee effect hormesis? *Science of The Total Environment*, *682*, 623-628.

Sakai, Y. (2012). Approach for Salt-Affected Soil Amelioration by Desulfurization of By-Products in China and Its Future Perspectives. *Bulletin of the Society of Sea Water Science, Japan*, *66*, 66-73.

Saranga, Y., Zamir, D., Marani, A., Rudich, J. (1991). Breeding tomatoes for salt tolerance: field evaluation of Lycopersicon germplasm for yield and dry-matter production. *Journal of the American Society for Horticultural Science*, *116*(6), 1067-1071.

Schiop, S. T., Al Hassan, M., Sestras, A. F., Boscaiu, M., Sestras, R. E., Vicente, O. (2015). Identification of Salt Stress Biomarkers in Romanian Carpathian Populations of *Picea abies* (L.) Karst. *PloS One*, *10*(8).

Schneider, C. A., Rasband, W. S., Eliceiri, K. W. (2012). NIH Image to ImageJ: 25 years of image analysis. *Nature Methods*, *9*(7), 671-675.

Scholz, A., Klepsch, M., Karimi, Z., Jansen, S. (2013). How to quantify conduits in wood? *Frontiers in Plant Science*, *4*, 56.

Schreiber, U., Schliwa, U., Bilger, W. (1986). Continuous recording of photochemical and non-photochemical chlorophyll fluorescence quenching with a new type of modulation fluorometer. *Photosynthesis Research*, *10*(1-2), 51-62.

Semerikov, V. L., Iroshnikov, A. I., Lascoux, M. (2007). Mitochondrial DNA variation pattern and postglacial history of the Siberian Larch (*Larix sibirica* Ledeb.). *Russian Journal of Ecology*, *38*(3), 147-154.

Setia, R., Gottschalk, P., Smith, P., Marschner, P., Baldock, J., Setia, D., Smith, J. (2013). Soil salinity decreases global soil organic carbon stocks. *Science of The Total Environment*, *465*, 267-272.

Sha, Z., Oka, N., Watanabe, T., Tampubolon, B. D., Okazaki, K., Osaki, M., Shinano, T. (2012). Ionome of soybean seed affected by previous cropping with mycorrhizal plant and manure application. *Journal of Agricultural and Food Chemistry*, *60*(38), 9543-9552.

Shang, B., Feng, Z., Li, P., Calatayud, V. (2018). Elevated ozone affects C, N and P ecological stoichiometry and nutrient resorption of two poplar clones. *Environmental Pollution*, *234*, 136-144.

Shang, B., Xu, Y., Dai, L., Yuan, X., Feng, Z. (2019). Elevated ozone reduced leaf nitrogen allocation to photosynthesis in poplar. *Science of the Total Environment*, *657*, 169-178.

Sharkey, T. D. (1985). Photosynthesis in intact leaves of C_3 plants: physics, physiology and rate limitations. *The Botanical Review*, *51*(1), 53-105.

Shi, C., Eguchi, N., Meng, F., Watanabe, T., Satoh, F., Koike, T. (2016). Retranslocation of foliar nutrients of deciduous tree seedlings in different soil condition under free-air O_3 enrichment. *iForest-Biogeosciences and Forestry*, *9*(5), 835.

Shi, C., Watanabe, T., Koike, T. (2017). Leaf stoichiometry of deciduous tree species in different soils exposed to free-air O_3 enrichment over two growing seasons. *Environmental and Experimental Botany*, *138*, 148-163.

Shi, F., Sasa, K., Koike, T. (2010). Characteristics of larch forests in Daxingan mountains, Northeast China. In *Permafrost ecosystems* (pp. 367-383). Springer, Dordrecht.

Shinano, T., Lei, T. T., Kawamukai, T., Inoue, M. T., Koike, T., Tadano, T. (1996). Dimethylsulfoxide method for the extraction of chlorophylls a and b from the leaves of wheat, field bean, dwarf bamboo, and oak. *Photosynthetica*, *32*(3), 409-415.

Shiraishi, S., Isoda, K., Watanabe, A., Kawasaki, H. (1996). DNA systematical study on the *Larix* relicted at Mt. Manokami, the Zao Mountains. *Journal of the Japanese Forestry Society*, *78*(2), 175-182. [in Japanese]

Sicard, P., Augustaitis, A., Belyazid, S., Calfapietra, C., de Marco, A., Fenn, M., et al. (2016). Global topics and novel approaches in the study of air pollution, climate change and forest ecosystems. *Environmental Pollution*, *213*, 977-987.

Sicard, P., Dalstein-Richier, L. (2015). Health and vitality assessment of two common pine species in the context of climate change in southern Europe. *Environmental Research*, *137*, 235-245.

Sicard, P., De Marco, A., Dalstein-Richier, L., Tagliaferro, F., Renou, C., Paoletti, E. (2016). An epidemiological assessment of stomatal ozone flux-based critical levels for visible ozone injury in Southern European forests. *Science of the Total Environment*, *541*, 729-741.

Singh, K., Pandey, V. C., Singh, B., Singh, R. R. (2012). Ecological restoration of degraded sodic lands through afforestation and cropping. *Ecological Engineering*, *43*, 70-80.

Small, E. (1972). Photosynthetic rates in relation to nitrogen recycling as an adaptation to nutrient deficiency in peat bog plants. *Canadian Journal of Botany*, *50*(11), 2227-2233.

Sugai, T., Kam, D. G., Agathokleous, E., Watanabe, M., Kita, K., Koike, T. (2018). Growth and photosynthetic response of two larches exposed to O_3 mixing ratios ranging from preindustrial to near future. *Photosynthetica*, *56*(3), 901-910.

Sugai, T., Watanabe, T., Kita, K., Koike, T. (2019). Nitrogen loading increases the ozone sensitivity of larch seedlings with higher sensitivity to nitrogen loading. *Science of the Total Environment*, *663*, 587-595.

Sugai, T., Wang, Y., W., Watanabe, T., Satoh, F., Qu, L., Koike, T. (2019). Salt Stress Reduced the Seedling Growth of Two Larch Species Under Elevated Ozone. *Frontier in Forest Global Change*, *2*, 53.

Sun, Y., Zhang, X., Zwiers, F. W., Song, L., Wan, H., Hu, T., et al. (2014). Rapid increase in the risk of extreme summer heat in Eastern China. *Nature Climate Change*, *4*(12), 1082-1085.

Szmidt, A. E., Aldén, T., Hällgren, J. E. (1987). Paternal inheritance of chloroplast DNA in *Larix*. *Plant Molecular Biology*, *9*(1), 59-64.

Takashima, T., Hikosaka, K., Hirose, T. (2004). Photosynthesis or persistence: nitrogen allocation in leaves of evergreen and deciduous Quercus species. *Plant, Cell & Environment*, *27*(8), 1047-1054.

Takemoto, B. K., Bytnerowicz, A., Fenn, M. E. (2001). Current and future effects of ozone and atmospheric nitrogen deposition on California’s mixed conifer forests. *Forest Ecology and Management*, *144*(1-3), 159-173.

Team, R. C. (2017). R: A language and environment for statistical computing.

Temple, P. J., Riechers, G. H. (1995). Nitrogen allocation in ponderosa pine seedlings exposed to interacting ozone and drought stresses. *New Phytologist*, *130*(1), 97-104.

Thom, D., Rammer, W., Seidl, R. (2017). Disturbances catalyze the adaptation of forest ecosystems to changing climate conditions. *Global Change Biology*, *23*(1), 269-282.

Tian, D., Du, E., Jiang, L., Ma, S., Zeng, W., Zou, A., et al. (2018). Responses of forest ecosystems to increasing N deposition in China: A critical review. *Environmental Pollution*, *243*, 75-86.

Uddling, J., Karlsson, P. E., Glorvigen, A., Selldén, G. (2006). Ozone impairs autumnal resorption of nitrogen from birch (*Betula pendula*) leaves, causing an increase in whole-tree nitrogen loss through litter fall. *Tree Physiology*, *26*(1), 113-120.

United Nations. (2019). World population prospects 2019.

Utriainen, J., Holopainen, T. (2001). Nitrogen availability modifies the ozone responses of Scots pine seedlings exposed in an open-field system. *Tree Physiology*, *21*(16), 1205-1213.

Vainonen, J. P., Kangasjärvi, J. (2015). Plant signaling in acute ozone exposure. *Plant, Cell & Environment*, *38*(2), 240-252.

Vazquez-Ybarra, J. A., Pena-Valdivia, C. B., Trejo, C., Villegas-Bastida, A., Benedicto-Valdez, S., Sanchez-Garcia, P. (2015). Promoting growth of lettuce plants (*Lactuca sativa* L.) with sublethal ozone doses applied to culture medium. *Revista Fitotecnia Mexicana*, *38*(4), 405-413.

Verstraeten, W. W., Neu, J. L., Williams, J. E., Bowman, K. W., Worden, J. R., Boersma, K. F. (2015). Rapid increases in tropospheric ozone production and export from China. *Nature Geoscience*, *8*(9), 690-695.

Vitousek, P. M., Hättenschwiler, S., Olander, L., Allison, S. (2002). Nitrogen and nature. *AMBIO: A Journal of the Human Environment*, *31*(2), 97-101.

Wallin, G., Karlsson, P. E., Selldén, G., Ottosson, S., Medin, E. L., Pleijel, H., Skärby, L. (2002). Impact of four years exposure to different levels of ozone, phosphorus and drought on chlorophyll, mineral nutrients, and stem volume of Norway spruce, *Picea abies*. *Physiologia Plantarum*, *114*(2), 192-206.

Wang, C., Gower, S. T., Wang, Y., Zhao, H., Yan, P., Bond-Lamberty, B. P. (2001). The influence of fire on carbon distribution and net primary production of boreal *Larix gmelinii* forests in north-eastern China. *Global Change Biology*, *7*(6), 719-730.

Wang, H. M., Wang, W. J., Wang, H. Z., Wang, Y., Xu, H. N., Zu, Y. G. (2013). Effect of inland salt-alkaline stress on C4 enzymes, pigments, antioxidant enzymes, and photosynthesis in leaf, bark, and branch chlorenchyma of poplars. *Photosynthetica*, *51*(1), 115-126.

Wang, L., Seki, K., Miyazaki, T., Ishihama, Y. (2009). The causes of soil alkalinization in the Songnen Plain of Northeast China. *Paddy and Water Environment*, *7*(3), 259-270.

Wang, X., Agathokleous, E., Qu, L., Fujita, S., Watanabe, M., Tamai, Y., et al. (2018). Effects of simulated nitrogen deposition on ectomycorrhizae community structure in hybrid larch and its parents grown in volcanic ash soil: The role of phosphorous. *Science of the Total Environment*, *618*, 905-915.

Wang, X., Agathokleous, E., Qu, L., Watanabe, M., Koike, T. (2016). Effects of CO_2 and O_3 on the interaction between root of woody plants and ectomycorrhizae. *Journal of Agricultural Meteorology*, *72*(2), 95-105.

Wang, X., Qu, L., Mao, Q., Watanabe, M., Hoshika, Y., Koyama, A., et al. (2015). Ectomycorrhizal colonization and growth of the hybrid larch F_1 under elevated CO_2 and O_3. *Environmental Pollution*, *197*, 116-126.

Wang, X., Qu, L., Mao, Q., Watanabe, M., Hoshika, Y., Koyama, A., et al. (2015). Ectomycorrhizal colonization and growth of the hybrid larch F_1 under elevated CO_2 and O_3. *Environmental Pollution*, *197*, 116-126.Watanabe, M., Hoshika, Y., Koike, T., Izuta, T. (2017). Combined effects of ozone and other environmental factors on Japanese trees. In *Air Pollution Impacts on Plants in East Asia*, pp. 101-110. Springer, Tokyo.

Watanabe, M., Yamaguchi, M., Iwasaki, M., Matsuo, N., Naba, J., Tabe, C., et al. (2006). Effects of ozone and/or nitrogen load on the growth of *Larix kaempferi*, *Pinus densiflora* and *Cryptomeria japonica* seedlings. *Journal of Japan Society for Atmospheric Environment*, *41*(6), 320-334.

Weigt, R. B., Häberle, K. H., Millard, P., Metzger, U., Ritter, W., Blaschke, H., et al. (2012). Ground-level ozone differentially affects nitrogen acquisition and allocation in mature European beech (*Fagus sylvatica*) and Norway spruce (*Picea abies*) trees. *Tree Physiology*, *32*(10), 1259-1273.

West-Eberhard, M. J. (2003). *Developmental plasticity and evolution*. Oxford University Press.

Whitehead, F. H., Myerscough, P. J. (1962). Growth analysis of plants. The ratio of mean relative growth rate to mean relative rate of leaf area increase. *New Phytologist*, *61*(3), 314-321.

Wicke, B., Smeets, E., Dornburg, V., Vashev, B., Gaiser, T., Turkenburg, W., Faaij, A. (2011). The global technical and economic potential of bioenergy from salt-affected soils. *Energy & Environmental Science*, *4*(8), 2669-2681.

Wieser, G., Havranek, W. M. (1996). Evaluation of ozone impact on mature spruce and larch in the field. *Journal of Plant Physiology*, *148*(1-2), 189-194.

Wieser, G., Hecke, K., Tausz, M., Matyssek, R. (2013). Foliage type specific susceptibility to ozone in *Picea abies*, *Pinus cembra* and *Larix decidua* at treeline: a synthesis. *Environmental and Experimental Botany*, *90*, 4-11.

Wittig, V. E., Ainsworth, E. A., Naidu, S. L., Karnosky, D. F., Long, S. P. (2009). Quantifying the impact of current and future tropospheric ozone on tree biomass, growth, physiology and biochemistry: a quantitative meta-analysis. *Global Change Biology*, *15*(2), 396-424.

Wright, I. J., Reich, P. B., Westoby, M., Ackerly, D. D., Baruch, Z., Bongers, F., et al. (2004). The worldwide leaf economics spectrum. *Nature*, *428*(6985), 821-827.

Wungrampha, S., Joshi, R., Singla-Pareek, S. L., Pareek, A. (2018). Photosynthesis and salinity: are these mutually exclusive? *Photosynthetica*, *56*(1), 366-381.

Xu, J. (2011). China's new forests aren't as green as they seem. *Nature*, *477*(7365), 371-371.

Xu, J., Wilkes, A. (2004). Biodiversity impact analysis in northwest Yunnan, southwest China. *Biodiversity & Conservation*, *13*(5), 959-983.

Yamaguchi, M., Otani, Y., Li, P., Nagao, H., Lenggoro, I. W., Ishida, A., et al. (2014). Effects of long-term exposure to ammonium sulfate particles on growth and gas exchange rates of *Fagus crenata*, *Castanopsis sieboldii*, *Larix kaempferi* and *Cryptomeria japonica* seedlings. *Atmospheric Environment*, *97*, 493-500.

Yamaguchi, M., Watanabe, M., Iwasaki, M., Tabe, C., Matsumura, H., Kohno, Y., Izuta, T. (2007). Growth and photosynthetic responses of *Fagus crenata* seedlings to O_3 under different nitrogen loads. *Trees*, *21*(6), 707-718.

Yamaguchi, M., Watanabe, M., Matsumura, H., Kohno, Y., Izuta, T. (2011). Experimental studies on the effects of ozone on growth and photosynthetic activity of Japanese forest tree species. *Asian Journal of Atmospheric Environment*, *5*(2), 65-78.

Yamaguchi, M., Watanabe, M., Matsumura, H., Kohno, Y., Izuta, T. (2010). Effects of ozone on nitrogen metabolism in the leaves of *Fagus crenata* seedlings under different soil nitrogen loads. *Trees*, *24*(1), 175-184.

Yamaji, K., Ohara, T., Uno, I., Kurokawa, J. I., Pochanart, P., Akimoto, H. (2008). Future prediction of surface ozone over east Asia using models-3 community multiscale air quality modeling system and regional emission inventory in Asia. *Journal of Geophysical Research: Atmospheres*, *113*(D8).

Yamaji, K., Ohara, T., Uno, I., Tanimoto, H., Kurokawa, J. I., Akimoto, H. (2006). Analysis of the seasonal variation of ozone in the boundary layer in East Asia using the Community Multi-scale Air Quality model: what controls surface ozone levels over Japan? *Atmospheric Environment*, *40*(10), 1856-1868.

Yendrek, C. R., Leisner, C. P., Ainsworth, E. A. (2013). Chronic ozone exacerbates the reduction in photosynthesis and acceleration of senescence caused by limited N availability in *Nicotiana sylvestris*. *Global Change Biology*, *19*(10), 3155-3166.

Yoshida, T. (2010). Toward ecological forestry, In Influence on Forests, Kaiseisha-Press, Otsu,199-211 [in Japanese]

Yu, D., Zhou, L., Zhou, W., Ding, H., Wang, Q., Wang, Y., et al. (2011). Forest management in Northeast China: history, problems, and challenges. *Environmental Management*, *48*(6), 1122-1135.

Yue, S., Munir, I. U., Hyder, S., Nassani, A. A., Abro, M. M. Q., Zaman, K. (2020). Sustainable food production, forest biodiversity and mineral pricing: Interconnected global issues. *Resources Policy*, *65*, 101583.

Zeng, F. S., Li, L. L., Liang, N. S., Wang, X., Li, X., Zhan, Y. G. (2015). Salt tolerance and alterations in cytosine methylation in the interspecific hybrids of *Fraxinus velutina* and *Fraxinus mandshurica*. *Euphytica*, *205*(3), 721-737.

Zeng, Y., Zhao, C., Shi, F., Schneider, M., Lv, G., Li, Y. (2020). Impact of groundwater depth and soil salinity on riparian plant diversity and distribution in an arid area of china. *Scientific Reports*, *10*(1), 1-10.

Zhang, H., Li, W., Adams, H. D., Wang, A., Wu, J., Jin, C., et al. (2018). Responses of woody plant functional traits to nitrogen addition: a meta-analysis of leaf economics, gas exchange, and hydraulic traits. *Frontiers in Plant Science*, *9*, 683.

Zhang, P., Shao, G., Zhao, G., Le Master, D. C., Parker, G. R., Dunning, J. B., Li, Q. (2000). China's forest policy for the 21st century. *Science*, *288*(5474), 2135-2136.

Zhang, P., Wen, Y., Wang, L., Zhang, H., Wang, G. G., Wu, T. (2020). Leaf Structural Carbohydrate Decreased for *Pinus thunbergii* along Coast–Inland Gradients. *Forests*, *11*(4), 449.

Zhang, W., Feng, Z., Wang, X., Niu, J. (2012). Responses of native broadleaved woody species to elevated ozone in subtropical China. *Environmental Pollution*, *163*, 149-157.

Zhao, C., Zhang, H., Song, C., Zhu, J. K., Shabala, S. (2020). Mechanisms of plant responses and adaptation to soil salinity. *The Innovation*, *1*(1), 100017.

van Zelm, E., Zhang, Y., Testerink, C. (2020). Salt tolerance mechanisms of plants. *Annual Review of Plant Biology*, *71*.

SUPPLEMENTSL DATA

Table S4-1. Summary of soil condition in the first experiment.

Mean values ± standard error in Dahurian larch (DL), Japanese larch (JL), and hybrid larch F_1 (HL) to control (C), 20 mmol Na (S1), 40 mmol Na (S2), and 80 mmol (S3). S: surface soil layer; R: root-zone; B: bottom soil layer.

		S	R	B	S	R	B
			pH			EC (mS m^{-2})	
DL	C	6.668 ± 0.329	6.820 ± 0.141	7.025 ± 0.227	0.578 ± 0.215	0.380 ± 0.04	0.408 ± 0.032
	S	6.545 ± 0.141	6.440 ± 0.262	6.825 ± 0.145	0.744 ± 0.221	0.545 ± 0.177	0.338 ± 0.130
	SS	6.520 ± 0.079	6.353 ± 0.323	6.633 ± 0.155	0.598 ± 0.305	0.229 ± 0.026	0.281 ± 0.051
	SSS	6.430 ± 0.154	6.325 ± 0.299	6.695 ± 0.278	1.115 ± 0.397	0.331 ± 0.067	0.333 ± 0.057
JL	C	6.665 ± 0.188	6.913 ± 0.097	7.045 ± 0.122	0.469 ± 0.249	0.350 ± 0.057	0.426 ± 0.049
	S	6.565 ± 0.245	6.305 ± 0.145	6.475 ± 0.245	0.545 ± 0.285	0.598 ± 0.016	0.35 ± 0.251
	SS	6.553 ± 0.036	6.363 ± 0.329	6.575 ± 0.123	0.885 ± 0.178	0.241 ± 0.046	0.255 ± 0.030
	SSS	6.430 ± 0.154	6.325 ± 0.299	6.695 ± 0.278	1.085 ± 0.301	0.331 ± 0.067	0.333 ± 0.057
HL	C	6.598 ± 0.322	6.778 ± 0.121	6.950 ± 0.214	0.338 ± 0.159	0.336 ± 0.033	0.456 ± 0.018
	S	6.488 ± 0.191	6.285 ± 0.128	6.608 ± 0.224	0.456 ± 0.223	0.539 ± 0.103	0.336 ± 0.165
	SS	6.520 ± 0.079	6.353 ± 0.323	6.633 ± 0.155	0.774 ± 0.182	0.229 ± 0.026	0.281 ± 0.051
	SSS	6.458 ± 0.261	6.320 ± 0.107	6.395 ± 0.21	1.095 ± 0.456	0.460 ± 0.139	0.346 ± 0.196
			Na (mg g^{-1})			K (mg g^{-1})	
DL	C	0.176 ± 0.082	0.133 ± 0.015	0.078 ± 0.047	0.019 ± 0.009	0.006 ± 0.001	0.005 ± 0.005
	S	2.153 ± 1.001	0.688 ± 0.221	1.485 ± 0.759	0.036 ± 0.016	0.016 ± 0.006	0.026 ± 0.016
	SS	5.319 ± 0.795	1.122 ± 0.132	1.23 ± 0.233	0.062 ± 0.011	0.022 ± 0.003	0.016 ± 0.001
	SSS	8.794 ± 1.013	1.603 ± 0.101	1.772 ± 0.342	0.079 ± 0.012	0.017 ± 0.001	0.019 ± 0.005
JL	C	0.156 ± 0.05	0.122 ± 0.034	0.196 ± 0.047	0.016 ± 0.007	0.005 ± 0.001	0.013 ± 0.011
	S	2.701 ± 0.228	0.886 ± 0.011	0.647 ± 0.198	0.037 ± 0.004	0.007 ± 0.001	0.011 ± 0.002
	SS	6.591 ± 3.380	1.353 ± 0.354	1.332 ± 0.243	0.096 ± 0.008	0.012 ± 0.001	0.011 ± 0.001
	SSS	9.262 ± 3.284	1.601 ± 0.078	1.922 ± 0.070	0.103 ± 0.003	0.018 ± 0.003	0.017 ± 0.004
HL	C	0.169 ± 0.064	0.131 ± 0.018	0.338 ± 0.225	0.022 ± 0.004	0.007 ± 0.004	0.008 ± 0.002
	S	3.365 ± 3.058	0.670 ± 0.148	1.045 ± 0.731	0.036 ± 0.034	0.011 ± 0.004	0.025 ± 0.016
	SS	6.932 ± 1.054	1.369 ± 0.165	2.219 ± 1.256	0.088 ± 0.020	0.015 ± 0.003	0.033 ± 0.024
	SSS	9.299 ± 0.974	1.634 ± 0.149	1.684 ± 0.139	0.090 ± 0.008	0.016 ± 0.001	0.019 ± 0.009
			Ca (mg g^{-1})			Mg (mg g^{-1})	
DL	C	0.085 ± 0.037	0.059 ± 0.012	0.077 ± 0.009	0.026 ± 0.012	0.014 ± 0.003	0.022 ± 0.003
	S	0.255 ± 0.116	0.092 ± 0.011	0.186 ± 0.117	0.074 ± 0.033	0.024 ± 0.004	0.054 ± 0.036
	SS	0.429 ± 0.099	0.106 ± 0.003	0.096 ± 0.007	0.129 ± 0.035	0.027 ± 0.002	0.025 ± 0.002
	SSS	0.533 ± 0.030	0.118 ± 0.015	0.131 ± 0.046	0.152 ± 0.012	0.03 ± 0.005	0.035 ± 0.014
JL	C	0.080 ± 0.011	0.067 ± 0.001	0.127 ± 0.054	0.024 ± 0.002	0.016 ± 0.003	0.034 ± 0.017
	S	0.291 ± 0.030	0.108 ± 0.001	0.087 ± 0.003	0.080 ± 0.010	0.023 ± 0.001	0.022 ± 0.001
	SS	0.636 ± 0.114	0.144 ± 0.050	0.129 ± 0.030	0.203 ± 0.049	0.037 ± 0.012	0.037 ± 0.008
	SSS	0.609 ± 0.016	0.175 ± 0.037	0.141 ± 0.005	0.191 ± 0.007	0.047 ± 0.011	0.039 ± 0.001
HL	C	0.089 ± 0.022	0.055 ± 0.004	0.065 ± 0.009	0.027 ± 0.008	0.013 ± 0.003	0.017 ± 0.002
	S	0.233 ± 0.198	0.093 ± 0.020	0.165 ± 0.091	0.069 ± 0.06	0.022 ± 0.005	0.045 ± 0.026
	SS	0.572 ± 0.086	0.132 ± 0.022	0.278 ± 0.176	0.176 ± 0.032	0.034 ± 0.005	0.080 ± 0.054
	SSS	0.604 ± 0.028	0.125 ± 0.015	0.129 ± 0.024	0.185 ± 0.011	0.032 ± 0.003	0.037 ± 0.007

Table S4-2. Summary of traits responses to salt stresses

Mean values ± standard error in Dahurian larch (DL), Japanese larch (JL), and hybrid larch F_1 (HL) to control (C), 20 mmol Na (S1), 40 mmol Na (S2), 80 mmol (S3), and 20 mmol Na (S4), and 70 mmol (S5).

First experiment

	DL				JL				HL			
Traits	C	S1	S2	S3	C	S1	S2	S3	C	S1	S2	S3
RGR (ln cm)	0.017 ± 0.002	0.019 ± 0.004	0.02 ± 0.003	0.017 ± 0.002	0.008 ± 0.001	0.008 ± 0.001	0.008 ± 0.001	0.008 ± 0.001	0.012 ± 0.002	0.009 ± 0.004	0.009 ± 0.001	0.01 ± 0.001
Growth (cm)	9.82 ± 1.32	10.53 ± 2.93	11.67 ± 2.48	8.47 ± 1.72	7.10 ± 0.91	6.58 ± 0.26	6.08 ± 0.02	6.63 ± 1.35	9.67 ± 1.95	7.52 ± 2.8	7.30 ± 1.14	7.20 ± 0.69
Aboveground (g)	2.04 ± 0.29	1.87 ± 0.36	1.72 ± 0.31	1.55 ± 0.55	2.64 ± 0.18	2.97 ± 0.19	2.92 ± 0.32	2.56 ± 0.33	3.48 ± 0.30	2.73 ± 0.24	2.73 ± 0.28	2.40 ± 0.28
Needle (g)	1.34 ± 0.18	1.21 ± 0.24	1.08 ± 0.26	0.97 ± 0.39	1.74 ± 0.10	2.03 ± 0.15	2.01 ± 0.24	1.70 ± 0.27	2.27 ± 0.19	1.69 ± 0.18	1.76 ± 0.15	1.45 ± 0.09
Branch (g)	0.35 ± 0.04	0.30 ± 0.05	0.36 ± 0.03	0.28 ± 0.09	0.33 ± 0.08	0.38 ± 0.03	0.37 ± 0.03	0.33 ± 0.05	0.60 ± 0.07	0.44 ± 0.03	0.42 ± 0.04	0.38 ± 0.06
Stem (g)	0.35 ± 0.08	0.36 ± 0.11	0.29 ± 0.03	0.30 ± 0.08	0.57 ± 0.03	0.56 ± 0.05	0.53 ± 0.05	0.53 ± 0.05	0.61 ± 0.06	0.60 ± 0.08	0.54 ± 0.11	0.58 ± 0.13
Fine root (g)	0.59 ± 0.07	0.53 ± 0.15	0.50 ± 0.05	0.50 ± 0.21	0.98 ± 0.04	1.06 ± 0.20	1.00 ± 0.13	0.76 ± 0.08	1.15 ± 0.09	0.78 ± 0.06	0.91 ± 0.28	0.77 ± 0.09
TR ratio (g g^{-1})	1.66 ± 0.15	1.76 ± 0.33	1.68 ± 0.31	1.48 ± 0.18	1.55 ± 0.05	1.75 ± 0.14	1.80 ± 0.4	1.92 ± 0.15	1.63 ± 0.21	1.64 ± 0.07	1.58 ± 0.14	1.41 ± 0.02
LMR (g g^{-1})	0.41 ± 0.02	0.41 ± 0.04	0.39 ± 0.06	0.36 ± 0.04	0.40 ± 0.01	0.43 ± 0.01	0.44 ± 0.04	0.43 ± 0.01	0.40 ± 0.03	0.38 ± 0.01	0.39 ± 0.02	0.35 ± 0.03
P_N (μmol m^{-2} s^{-1})	12.92 ± 2.04	10.88 ± 1.13	8.58 ± 1.09	8.32 ± 0.51	8.26 ± 0.64	8.67 ± 2.17	4.84 ± 1.08	4.82 ± 1.59	9.24 ± 1.41	10.15 ± 2.38	8.50 ± 0.32	5.71 ± 0.22
G_s (mol m^{-2} s^{-1})	0.21 ± 0.03	0.17 ± 0.03	0.12 ± 0.01	0.12 ± 0.01	0.16 ± 0.01	0.14 ± 0.04	0.08 ± 0.02	0.09 ± 0.03	0.14 ± 0.01	0.15 ± 0.03	0.11 ± 0.01	0.07 ± 0.01
LMA (g m^{-2})	77.19 ± 6.70	77.43 ± 9.95	67.07 ± 2.81	70.04 ± 2.39	69.64 ± 1.81	80.76 ± 4.16	77.36 ± 8.04	73.54 ± 4.38	75.29 ± 3.31	74.68 ± 3.45	76.37 ± 1.43	73.21 ± 9.28
Y(II)	0.44 ± 0.02	0.40 ± 0.01	0.43 ± 0.02	0.44 ± 0.03	0.40 ± 0.01	0.43 ± 0.01	0.39 ± 0.02	0.43 ± 0.02	0.45 ± 0.02	0.43 ± 0.02	0.41 ± 0.01	0.40 ± 0.03
rETR (μmol m^{-2} s^{-1})	52.9 ± 2.11	48.4 ± 0.46	51.68 ± 2.26	53.02 ± 3.86	48.17 ± 0.69	50.9 ± 1.39	46.33 ± 2.62	51.63 ± 2.86	53.72 ± 1.85	51.55 ± 2.09	50.1 ± 2.08	47.45 ± 3.44
F_v/F_m	0.80 ± 0.01	0.79 ± 0.03	0.83 ± 0.02	0.8 ± 0.04	0.81 ± 0.02	0.80 ± 0.01	0.76 ± 0.00	0.73 ± 0.06	0.82 ± 0.01	0.81 ± 0.02	0.84 ± 0.00	0.82 ± 0.01
Na (mg g^{-1})	0.33 ± 0.03	0.64 ± 0.10	3.04 ± 1.00	2.98 ± 1.17	0.04 ± 0.00	0.19 ± 0.19	0.70 ± 0.43	2.39 ± 1.25	0.28 ± 0.17	0.36 ± 0.22	1.16 ± 0.6	1.13 ± 0.29
K (mg g^{-1})	4.66 ± 0.56	5.76 ± 1.01	5.99 ± 0.43	6.21 ± 0.89	3.91 ± 0.40	5.28 ± 1.08	5.77 ± 1.23	6.06 ± 1.05	3.64 ± 0.29	3.87 ± 0.61	4.21 ± 0.59	4.96 ± 0.51
Ca (mg g^{-1})	2.25 ± 0.11	1.93 ± 0.18	2.45 ± 0.40	2.18 ± 0.25	3.58 ± 0.15	3.06 ± 0.23	3.19 ± 0.14	3.24 ± 0.14	2.51 ± 0.28	2.26 ± 0.20	2.75 ± 0.38	2.31 ± 0.37
Mg (mg g^{-1})	1.60 ± 0.11	1.21 ± 0.23	1.57 ± 0.32	1.38 ± 0.06	1.85 ± 0.05	1.81 ± 0.22	1.96 ± 0.24	1.75 ± 0.07	1.52 ± 0.08	1.48 ± 0.15	1.45 ± 0.12	1.67 ± 0.20
Fe (mg g^{-1})	0.07 ± 0.01	0.05 ± 0.01	0.06 ± 0.00	0.06 ± 0.00	0.06 ± 0.00	0.05 ± 0.01	0.05 ± 0.00	0.06 ± 0.02	0.06 ± 0.01	0.06 ± 0.01	0.07 ± 0.01	0.06 ± 0.01

Second experiment

	DL			HL			JL		
Traits	C	S4	S5	C	S4	S5	C	S4	S5
RGR (ln cm day^{-1})	0.016 ± 0.003	0.018 ± 0.002	0.015 ± 0.001	0.009 ± 0.001	0.009 ± 0.001	0.009 ± 0.001	0.007 ± 0.002	0.006 ± 0.001	0.004 ± 0.001
Growth (cm)	10.30 ± 2.12	12.83 ± 0.6	9.68 ± 0.76	7.76 ± 0.54	8.27 ± 0.71	8.58 ± 1.52	6.33 ± 1.8	5.93 ± 1.09	3.90 ± 0.95
Aboveground (g)	2.7 ± 0.55	3.28 ± 0.57	2.57 ± 0.01	4.16 ± 0.36	5.37 ± 0.36	4.88 ± 0.72	5.83 ± 0.86	5.47 ± 0.56	4.23 ± 0.24
Belowground (g)	2.15 ± 0.15	2.37 ± 0.43	2.09 ± 0.21	3.72 ± 0.41	4.35 ± 0.63	3.81 ± 0.6	4.9 ± 0.43	4.2 ± 0.61	3.28 ± 0.28
TR ratio (g g^{-1})	1.34 ± 0.27	1.45 ± 0.15	1.27 ± 0.13	1.12 ± 0.05	1.25 ± 0.13	1.29 ± 0.02	1.19 ± 0.06	1.32 ± 0.09	1.31 ± 0.09
Na (mg g^{-1})	0.91 ± 0.13	1.22 ± 0.09	1.57 ± 0.12	0.48 ± 0.19	0.87 ± 0.08	1.09 ± 0.13	0.38 ± 0.22	0.75 ± 0.22	1.13 ± 0.24
K (mg g^{-1})	7.12 ± 0.18	7.72 ± 0.56	6.51 ± 0.44	5.97 ± 0.65	5.78 ± 0.6	6.22 ± 0.38	6.15 ± 1.12	7.15 ± 0.32	7.74 ± 0.98
Ca (mg g^{-1})	2.53 ± 0.22	2.28 ± 0.13	2.3 ± 0.01	2.14 ± 0.26	2.26 ± 0.08	2.13 ± 0.1	2.65 ± 0.17	2.41 ± 0.13	2.76 ± 0.26
Mg (mg g^{-1})	1.42 ± 0.16	1.44 ± 0.07	1.25 ± 0.02	1.41 ± 0.16	1.54 ± 0.18	1.36 ± 0.03	1.72 ± 0.1	1.47 ± 0.07	1.75 ± 0.15
Fe (mg g^{-1})	0.09 ± 0.01	0.1 ± 0.01	0.08 ± 0.01	0.08 ± 0.01	0.11 ± 0.01	0.09 ± 0.01	0.09 ± 0.02	0.08 ± 0	0.07 ± 0

Table. S4-3. Results of root anatomical analysis in the second experiment.

Mean value ± standard error in Dahurian larch (DL), Japanese larch (JL), and hybrid larch F_1 (HL) to control (C), 20 mmol (S4), and 70 mmol (S5). Detected total OUT number was 643. Biological replication was three in each treatment (N=9 in each species).

		Mean size of tracheotomy (μm^2)		CWF (%)		Count cell number	
Sp	Treatment	1st	2nd	1st	2nd	1st	2nd
DL	C	227.83 ± 20.95	213.44 ± 38.15	50.02 ± 0.85	49.71 ± 4.41	3734.5 ± 1488.5	29247.33 ± 6087.84
	S4	248.71 ± 47.75	360.48 ± 76.65	46.33 ± 4.91	42.41 ± 0.45	3405 ± 2332	8475.67 ± 4814.5
	S5	222.01 ± 3.51	416.83 ± 39.2	52.68 ± 6.93	44.38 ± 4.14	1226.5 ± 29.5	5289.67 ± 1825.44
JL	C	325.61 ± 50.28	351.35 ± 60.5	43.93 ± 1.61	45.07 ± 4.81	4005.67 ± 1450.25	16902 ± 6895.41
	S4	284.08 ± 119.55	497.08 ± 51.5	47.44 ± 6.08	42.65 ± 3.61	1461.33 ± 670.29	3750.33 ± 961.91
	S5	285.31 ± 69.17	352.83 ± 165.3	46.48 ± 2.66	43.93 ± 4.25	2165.33 ± 681.81	17945.33 ± 8842.41
HL	C	157.14 ± 4.85	255.78 ± 93.48	52.74 ± 8.38	48.51 ± 4.71	3990.67 ± 1671.95	21531.67 ± 8532.72
	S4	238.18 ± 29.32	429.02 ± 207.72	49.07 ± 0.94	45.24 ± 3.29	3184 ± 1559.21	8182.67 ± 7648.58
	S5	259.43 ± 29.6	265.48 ± 60.76	45.97 ± 2.24	44.19 ± 2.83	3666.33 ± 1849.84	30861 ± 9284.28

Analysis of ECM fungal community the second experiment

To evaluate the fungal communities within root zone, the residual roots after sampling for anatomical analysis were immediately stored in a plastic bag and transferred to deep freezer (–80 °C) in the laboratory until the following measurements. The sampled roots were completely grinded within liquid nitrogen. The template DNA was extracted from the powder samples using by DNeasy Plant Mini Kit (QIAGEN, Tokyo, Japan). The 5.8S rRNA gene and internal transcribed spacer regions were amplified via PCR using a primer set of gITS7 (ACACTCTTTCCCTACACGACGCTCTTCCGATCT-NNNNN- GTGARTCATCGARTCTTTG) and ITS4 (GTGACTGGAGTTCAGACGTGTGCTCTTCCGATCT-NNNNN-TCCTCCGCTTATTGATATGC). The 1st PCR was conducted using 20 μl assays: 2.0 μl of extraction buffer, 1.6μl of dNTPs, 1.0 μl of the first primer (gITS7_MIX), 1.0 μl of the second primer (ITS4_MIX), 1.0 μl of template DNA, 0.2 μl of Ex-taq, and 13.2 μl of Mill-Q water. The PCR thermal profile consisted of an initial denaturation and enzyme activation step of 94 °C for 2 min, followed by 30 cycles of 94 °C for 30 s, 50 °C for 30 s and 72 °C for 60 s, and finally 72 °C for 5 min. To confirm the PCR amplification, 5 μl of PCR solution was separated by 2% agarose gel stained with SYBR Green I, which was projected by a CCD projection (FAS-III, TOYOBO, Tokyo, JPN). Subsequent analyses were commissioned to a custom pipeline produced by Fasmac Inc. (Atsugi, Japan). The validated PCR solution was mixed with AMPure XP and the first PCR product was purified. After the measurement of concentration in the first PCR product by the Synergy H1 and QuantiFluor dsDNA system, the second PCR was conducted for making the library, where the library quality was confirmed by the Fragment Analyzer and dsDNA 915 Reagenet Kit. Then, paired-end 2 x 300 bp sequenching of the barcoded amplicons was performed on a MiSwq machine (Illumina Inc, San Diego, USA). Only the read sequences whose beginning of the read sequence obtained using fastq_barcode_splilter of the Fastx toolkit (ver. 0.0.14) matches perfectly with the primer sequence used were extracted. The primer sequences from the extracted reads were removed with fastx_trimer in the Fastx toolkit. After that, sequences with a quality value of less than 20 were removed using sickle (ver. 1.33), and sequences with a length of less than 40 bases and their paired sequences were discarded. Using the paired-end read binding script FLASH (ver. 1.2.11), reads were bound under the conditions of 320 nucleotides in the post-binding sequence length, 280 nucleotides in the read binding length, and a minimum overlap of 10 nucleotides. The leads that could not be bound were extracted, and 50 bases on the 3' side of both chains were deleted and recombined. The same work was done two more times. The sequences obtained through a total of four binding operations were integrated, and subsequent analyses were performed. The dada2 plugin for Qiime2 (ver. 2020.2) removed the chimeric and noise sequences and outputted representative sequences and OTU tables. Using the feature-classifier plugin, we compared the 97% OTU of UNITE (ver. 8.2) with the obtained representative sequence and phylogenetic estimation. The obtained datasets of Miseq were scandalized based on the number of OTC counts to relative abundance values, where the OTUs were filtered at the threshold of 0.01% of the total abundance. To evaluate the microbial community richness, the number of OTUs was used for calculating the Shannon-Weaver index (H') as the following equation:

$$H' = -\sum_{i=1}^{S} \frac{N_i}{N_t} \times Ln(\frac{N_i}{N_t})$$

Where N_i was the number of reads in each OUT; N_t was the sum of OTUs. For avoiding Ni = 0 during the calculation of logarithm, 1 was added for all N_i data. The calculation was conducted by the package of vegan (CRAN 2019). The relative abundance of microbial community was calculated at the order level. As the principal component analysis, I adopted non-metric multidimensional scaling (NMDS) to visualize the microbial community richness.

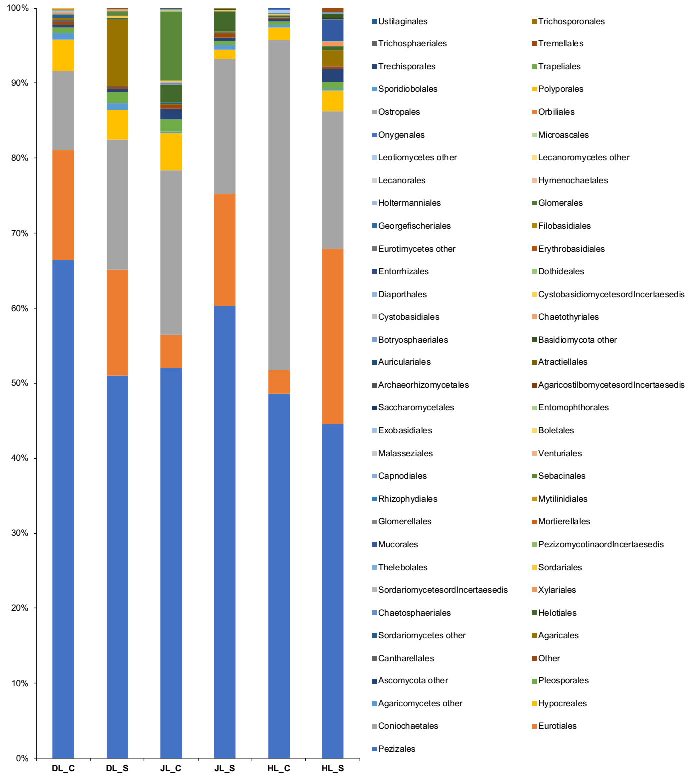

Fig. S4-1. Dominance of fungal community at genus-level in the second experiment. Results were Dahurian larch (DL), Japanese larch (JL), and hybrid larch F$_1$ (HL) to control (C) and 70 mmol (S). Total genus number was 66 including anonymous (other).

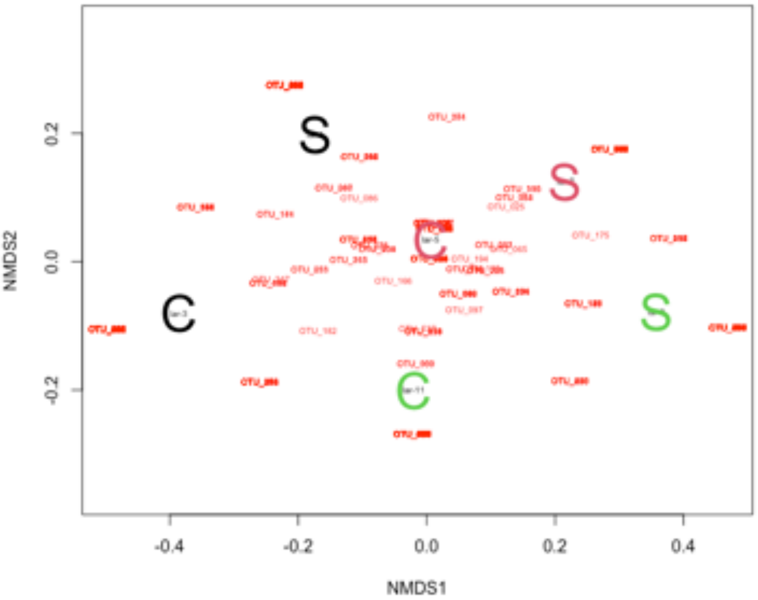

Fig. S4-2. Results of NMDS analysis in the second experiment.

Results of microorganism structure in Dahurian larch (black), Japanese larch (green), and hybrid larch F_1 (red) to control (C) and 70 mmol (S). Detected total OUT number was 643. Analysis and figure constriction were performed by the Vegan package. Biological replication was one in each treatment (N=6).